SLAC – PUB – 4248
January 1987
(T/E)

Heavy Quark Spectroscopy and Decay*

RAFE H. SCHINDLER
Stanford Linear Accelerator Center
Stanford University, Stanford, California 94305

1. INTRODUCTION

The understanding of $q\bar{q}$ systems containing heavy, charmed, and bottom quarks has progressed rapidly in recent years, through steady improvements in experimental techniques for production and detection of their decays. These lectures are meant to be an experimentalist's review of the subject. In the first of two lectures, the existing data on the spectroscopy of the bound $c\bar{c}$ and $b\bar{b}$ systems will be discussed. Emphasis is placed on comparisons with the theoretical models described in greater detail in the lectures of F. Gilman, published in these proceedings. The second lecture covers the rapidly changing subject of the decays of heavy mesons ($c\bar{q}$ and $b\bar{q}$), and their excited states. Additional theoretical material is available in the article of I.I.Y.Bigi, published in these proceedings. The topics of CP violation and mixing are covered in the lectures of B.Winstein. In combination, the spectroscopy and decays of heavy quarks are shown to provide interesting insights into both the strong and electroweak interactions of the heavy quarks.

Two Lectures Presented at the XIVth SLAC Summer Institute on Particle Physics, Stanford, California, July 28 - August 8 1986.

* Work supported by the Department of Energy, contract DE – AC03 – 76SF00515.

2. THE SPECTROSCOPY OF CHARM AND BEAUTY[1]

The bound systems of two heavy charmed or bottom quarks below the threshold for production of the corresponding mesons provide a unique laboratory from which to test the flavor independence of the strong interactions, and our ability to work from the relativistic $c\bar{c}$ system into the nonrelativistic $b\bar{b}$ and $t\bar{t}$ systems. The general properties of these system, and the hitherto unobserved third generation toponium system are summarized in Table I. The properties of these systems will be shown to be determinable through detailed measurements of the level splittings, the fine and hyperfine structure, the transition rates, and the decays. In the first sections, the general structure of the two systems is reviewed.

Table I. Bound Systems of Heavy Quarks

	CHARMONIUM	BOTTOMONIUM	TOPONIUM
q mass	1.5 GeV	4.5 GeV	?
q charge	$\frac{2}{3}$	$-\frac{1}{3}$	$\frac{2}{3}$
$< \beta^2 >$	.15-.25	$< .1$	?
$\sqrt{< r^2 >}$	.4 f_m	.2 f_m	$M_\theta > 80$ GeV $< .05$
# Bound States	8	22	10 s—wave, 200 total

2.1 Charmonium

In Fig. 1 a typical level scheme for a $c\bar{c}$ bound system is shown. The details of the level structure are determined by the assumed form of the interquark potential. Figure 1 is based for example on the QCD inspired Cornell Model:[2]

$$V(r) = -\frac{4}{3}\frac{\alpha_s'}{r} + \lambda r \,. \tag{1}$$

Here the $\frac{1}{r}$ term represents the strong Coulombic-like potential that binds the system. Unlike the electromagnetic interactions in the hydrogen atom, the coupling α_s should diminish with the effective q^2 or quark masses, thus exhibiting the strong interaction property of asymptotic freedom. The second term represents an ansatz for the long range part of the potential, exhibiting the second property of the strong interaction, that of confinement. No explicit flavor dependence is

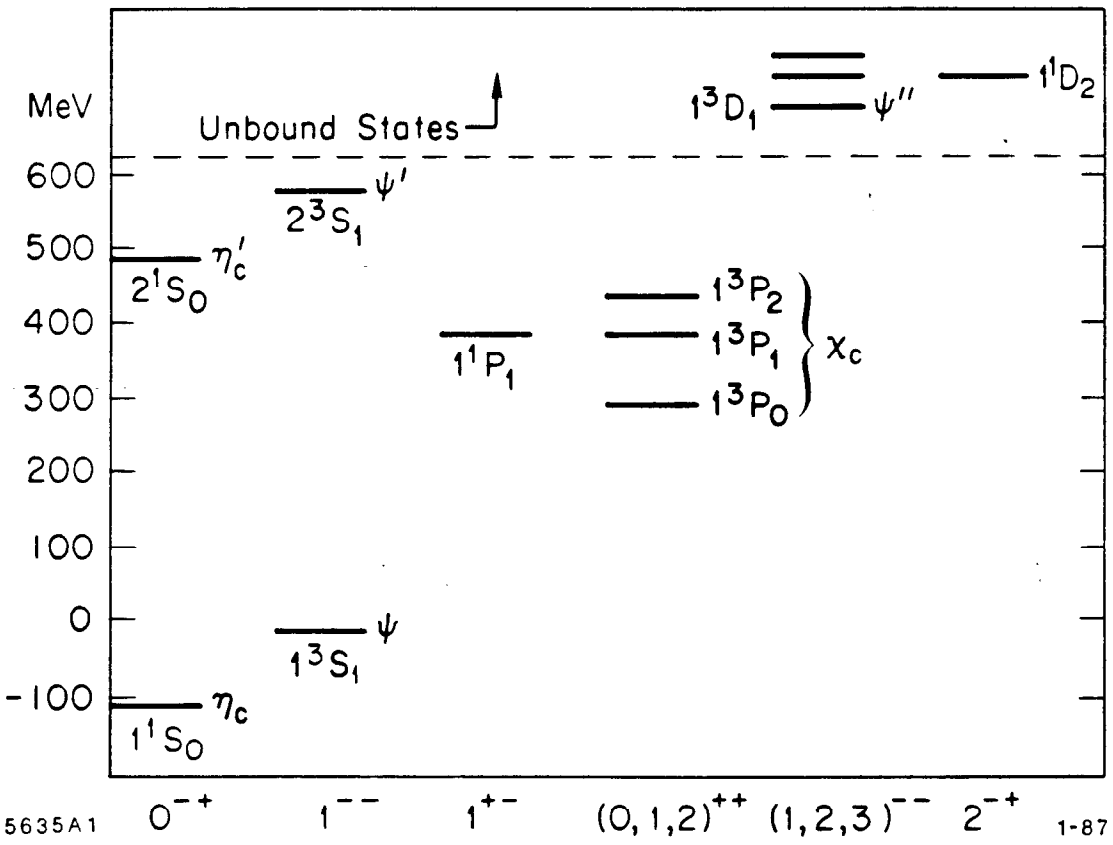

FIG. 1. The lowest lying states of charmonium.

exhibited in this potential. Under these assumptions, two narrow S-wave states are expected below the open charm threshold. The splitting of these ^{3}S states is determined by the strength and form of the spin independent $\frac{1}{r}$ part of the potential. Nonrelativistic models should reliably predict these splittings. The addition of the confinement term to the potential shifts the center of gravity (COG) of the otherwise degenerate P-wave states below that of the 2^3S state.

The detailed features of the level structure are analogous to the hydrogen atom. There is both fine and hyperfine structure which must be introduced by relativistic terms accounting for spin and orbital angular momentum of the quarks. The theoretical constraints on these parts of the potential are described in detail elsewhere in these proceedings.[3] The three ^3P_J states are themselves degenerate in the absence of a spin-orbit $(L \cdot S)$ interaction. The spin-spin $(S \cdot S)$ interaction breaks the degeneracy of the $^1S_0$ and the $^3S_1$ states. The $^1P_1$ remains degenerate at the COG of the ^3P_J states if the form the potential is short range. Tensor forces can contribute to the fine structure, and also mix states of the same J but different L, such as the 2^3S_1 and the 1^3D_1.

The possible transitions and decays of the charmonium states are shown in Fig. 2 . The M1 (magnetic) dipole transitions follow the selection rules: $L_i = L_f$ and $P_i = P_f$, while the E1 (electric)dipole transitions require $L_i = L_f \pm 1$, $P_i = -P_f$, and $|J_i - 1| \leq J_f \leq J_i + 1$, where P is the parity of the state. While the $^3S_1$ and $^3D_1$ states are directly produced in e^+e^- collisions and are connected by $\pi\pi$ and η strong interaction transitions, the $^1S_0$ and ^3P_J states can only be produced through the electromagnetic cascades from higher mass charmonium states. The $^1P_0$ state cannot be excited in e^+e^-, nor be reached through hadronic decays of the 2^3S_1 because of the limited phase space. It can be produced however in $p\bar{p}$ formation experiments. All the states have significant hadronic widths, which in principle can be used to determine their quantum numbers and spectroscopic assignment.

2.2 Bottomonium

The level structure of the bound $b\bar{b}$ system can be extrapolated reliably from Eq. (1), under the assumption of flavor independence, once the parameters of the potential are established from the charmonium system. Such an extrapolation is shown in Fig. 3 . The general features are determined by the addition of a third narrow $^3S_1$ bound state below threshold for open B meson production.

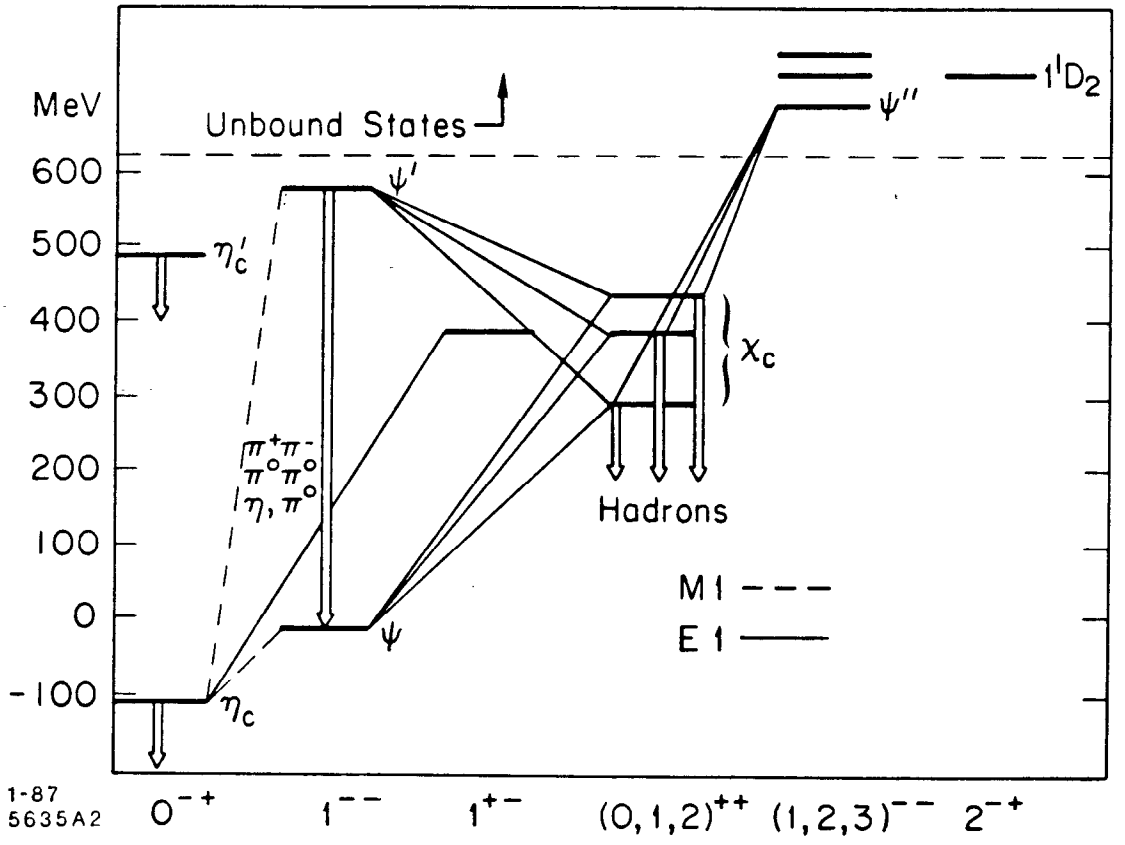

FIG. 2. The transitions and decays of charmonium states.

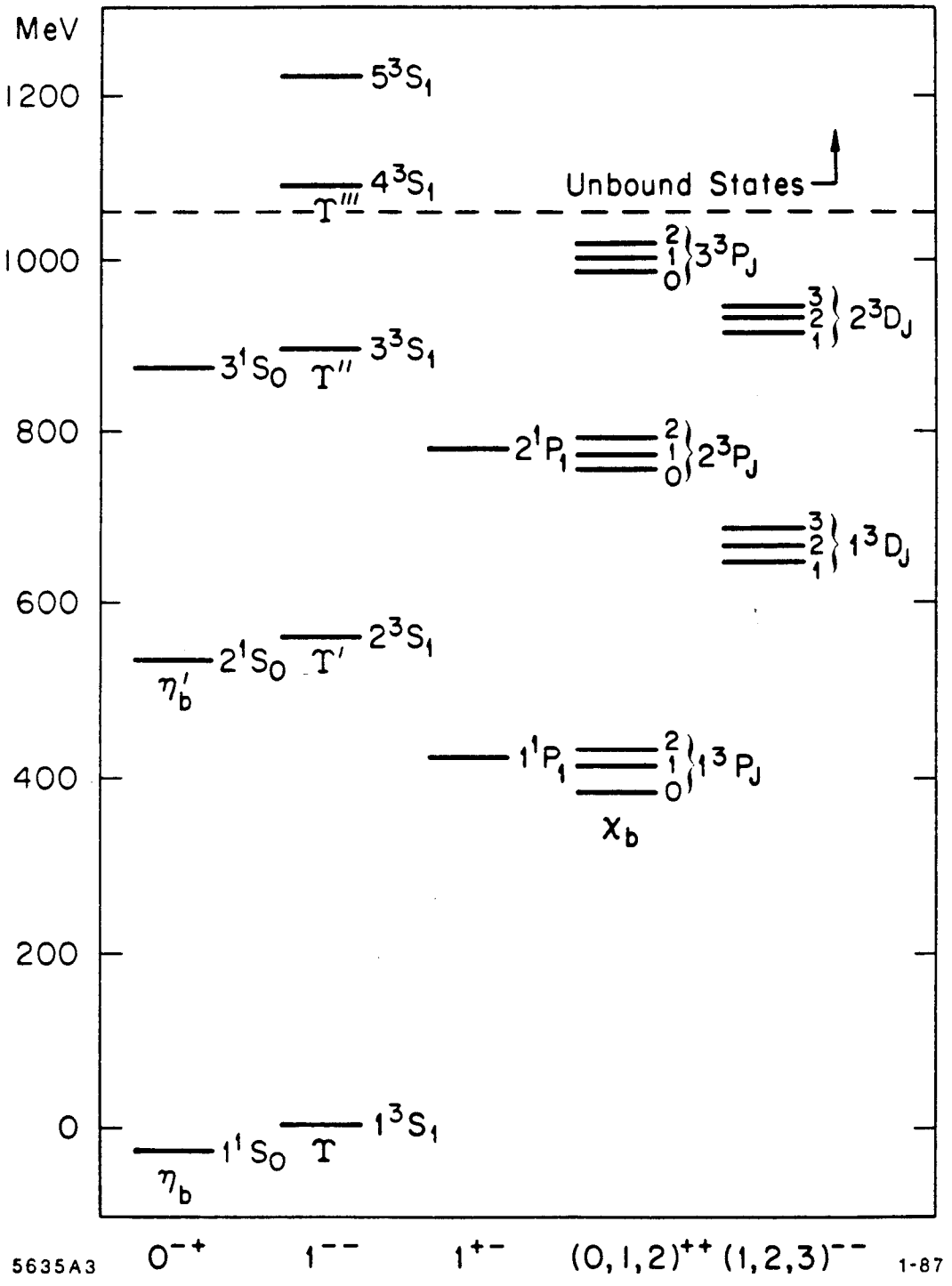

FIG. 3. The bound $b\bar{b}$ system.

This in turn implies a richer and more complicated spectroscopy, owing to the presence of additional P-wave multiplets, a third $^1S_0$ state, and the D-wave states *below* open beauty threshold. The fine and hyperfine splittings are smaller than the corresponding ones in the charmonium system, posing a more difficult experimental challenge.

The radiative transitions are shown in Fig. 4 . There are now several levels of cascades through the ^3P_J states, and weaker ones through the ^3D_J states. The hadronic transitions are considerably more complicated, as can be seen in Fig. 5 . Both two-π and three-π transitions are now energetically allowed. One interesting difference from charmonium is the accessibility of the 1^1P_1 state through a hadronic $\pi\pi$ transition from the 3^3S_1 state. The subsequent decay should have a large radiative width into the 1^1S_0 state.

2.3 Experimental Determination of Resonance Parameters

The most precise determinations of the masses and widths for $c\bar{c}$ and $b\bar{b}$ states comes from e^+e^- production. In e^+e^- storage rings the energy spread is small and the center of mass energy can typically be moved in few tenths of an MeV steps Thus the possibility of measuring an excitation curve exists:

$$\sigma(e^+e^- \rightarrow \psi \rightarrow f) = \frac{2\pi^2(2J+1)}{M_\psi^2} \frac{\Gamma_{ee}\Gamma_f}{(E - M_\psi)^2 + \Gamma_{tot}^2/4} . \qquad (2)$$

Here Γ_f can be the partial width to hadrons (Γ_{had}), electron pairs (Γ_{ee}) or muon pairs ($\Gamma_{\mu\mu}$). The observed data is corrected by convoluting (2) with the machine energy spread, and the effects of radiative corrections.

One way of extracting Γ_{ee}, Γ_{had}, and $\Gamma_{\mu\mu}$ is simply to fit to the excitation curve into each of the three final states. The more common technique uses the fact that the area (A) under (2) for hadronic final states is given by:

$$A = \frac{6\pi^2}{M_\psi^2} \frac{\Gamma_{ee}\Gamma_{had}}{\Gamma_{tot}} C_{rad} .$$

The radiative corrections (C_{rad}) are incorporated into the lineshape. Under the

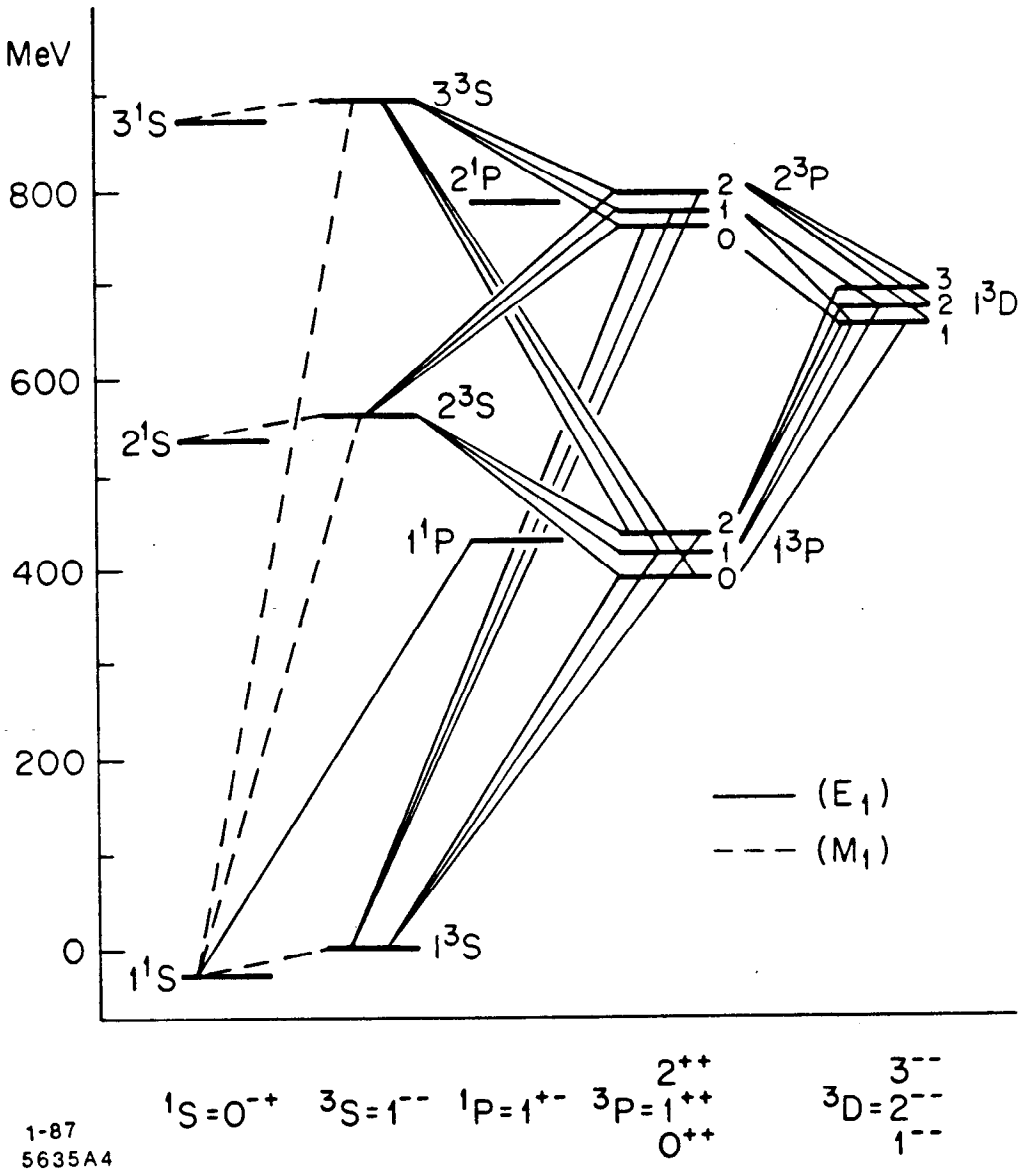

FIG. 4. Radiative transitions in the $b\bar{b}$ system.

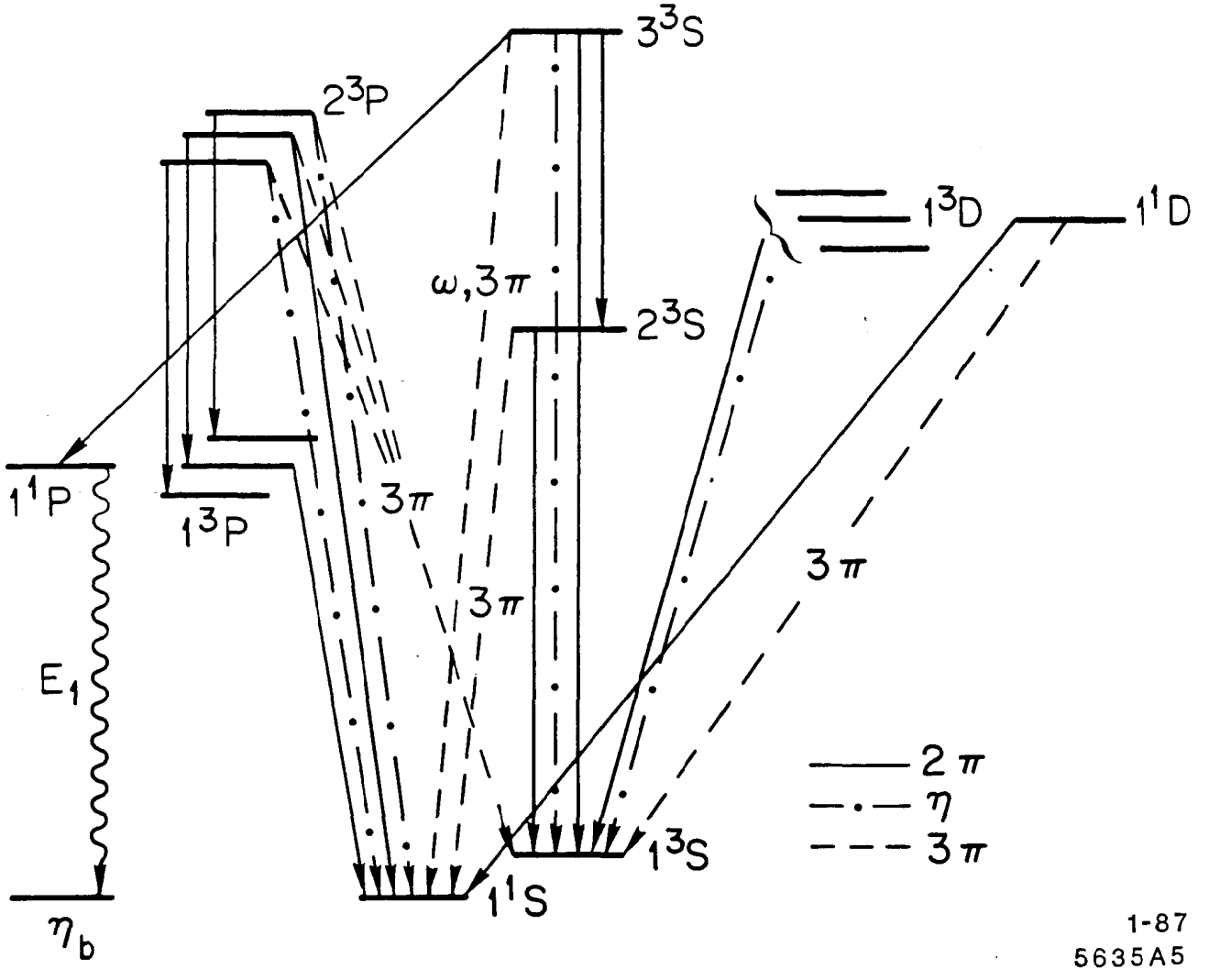

FIG. 5. Hadronic transitions in the $b\bar{b}$ system.

assumption of lepton universality, ($\Gamma_{\mu\mu}$=Γ_{ee}=$\Gamma_{\tau\tau}$) and assuming:

$$\frac{\Gamma_{had}}{\Gamma_{tot}} = 1 - NB_{\mu\mu},$$

then

$$\Gamma_{ee} = \frac{A\,M_{\psi}^2}{6\pi^2}\frac{1}{(1 - NB_{\mu\mu})}.$$

Here, N=2 for charmonium and N=3 for bottomonium. Hence measuring $B_{\mu\mu}$ and the integral of the hadronic cross section, gives Γ_{ee}. The total width (Γ_{tot}) is $\Gamma_{ee}/B_{\mu\mu}$, and Γ_{had}= Γ_{tot} - N Γ_{ee}.

To find $B_{\mu\mu}$, it is only necessary to measure the ratio of μ-pairs to hadrons on the resonance. Then:

$$B_{\mu\mu} = \frac{1}{\frac{\Gamma_{had}}{\Gamma_{\mu\mu}} + N}$$

since $\Gamma_{tot} = \Gamma_{had} +$ N $\Gamma_{\mu\mu}$.

2.3.1 S-wave and D-wave bound states of $c\bar{c}$ and $b\bar{b}$.

Below open charm threshold, the S-wave states (the ψ and ψ') appear as narrow states ($\Gamma \sim$ 100 KeV) in the hadronic cross section. Once above threshold for charmed meson production, the structure of the cross section becomes considerably more complex. The $^3D_1$ state (the ψ'') lies just above D-meson threshold and has a width of $\sim$ 25 MeV, typical of a strongly decaying meson of that mass. It appears to decay largely to charmed meson pairs.[4] Above the ψ'' however, the cross section becomes complex in structure,[5] (see for example Fig. 6), owing to the thresholds that open for the production of new charmed meson final states ($D\bar{D}, D\bar{D}^*$, $D^*\bar{D}^*$, $D_s\bar{D}_s, D_s\bar{D}_s^*$...etc.). Figure 6 also shows the prediction of the position from two potential models,[6][7] for the 3^3S_1 and 4^3S_1 states. The structures in the cross section in the 4 GeV region are roughly reproduced by the coupled-channel model shown in Fig. 7 .

The cross section data near 10 GeV show a similar structure[8] (see Fig. 8). The three lowest lying $b\bar{b}$ bound states (the $^3S_1$ states) are narrow, and are followed by a broader state just above threshold for open B production. This fourth state (the Υ''') decays predominantly to B_u and B_d mesons. A little higher in energy,

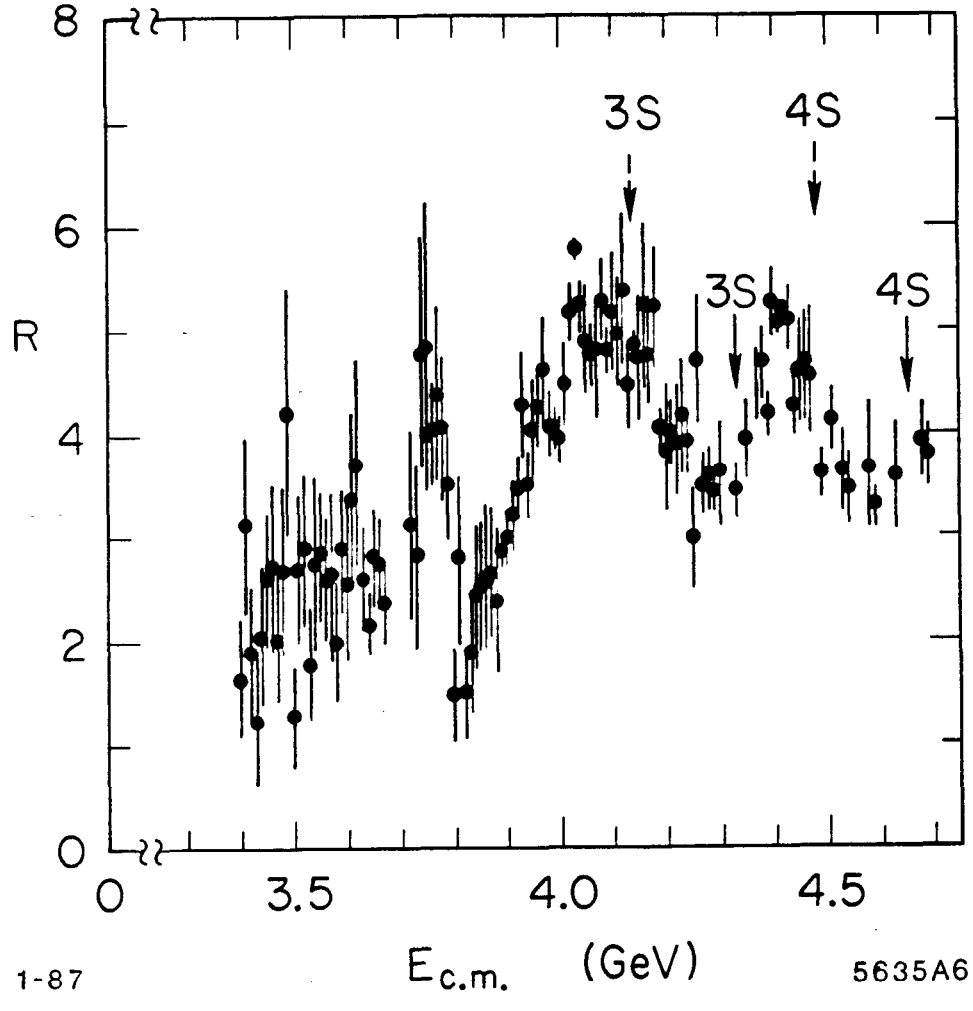

FIG. 6. The e^+e^- cross section divided by $\sigma_{\mu\mu}$, the point cross section, in the regime above charm threshold.[5] The solid arrows indicate the positions of the 3S and 4S states from Eichen *et al.*, while the dashed arrows are the same from Buchmuller and Tye.

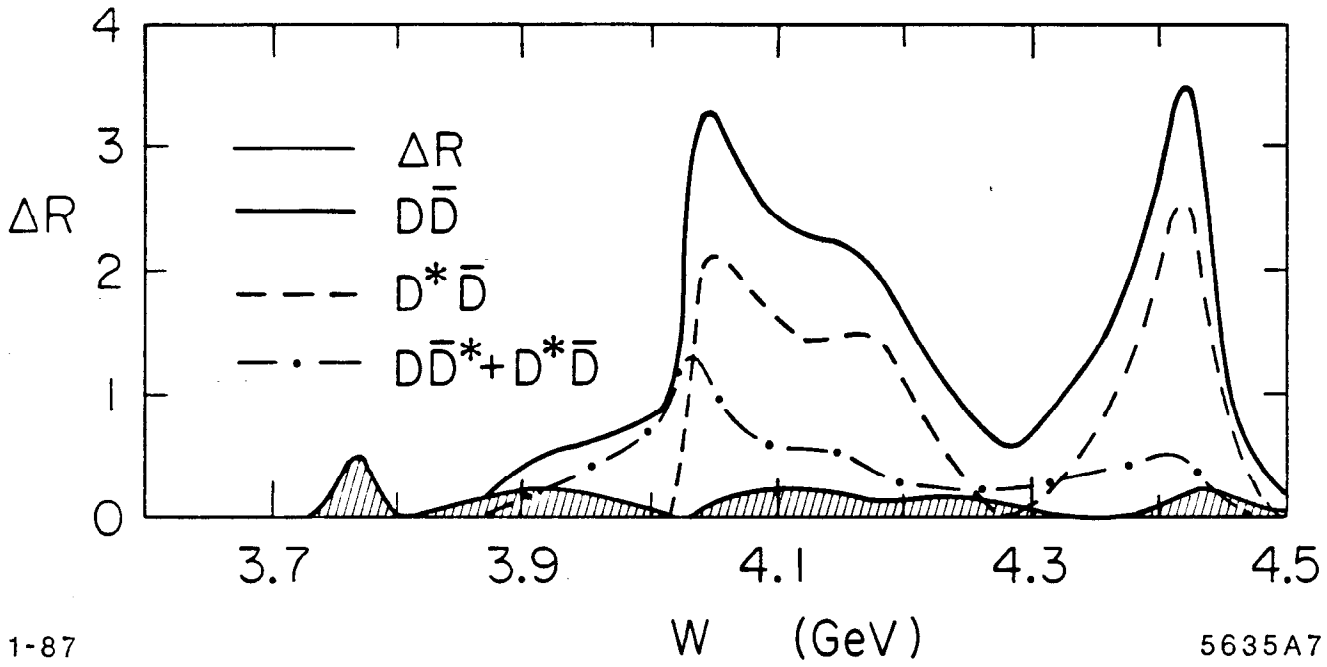

FIG. 7. Coupled channel model of Ref. [6].

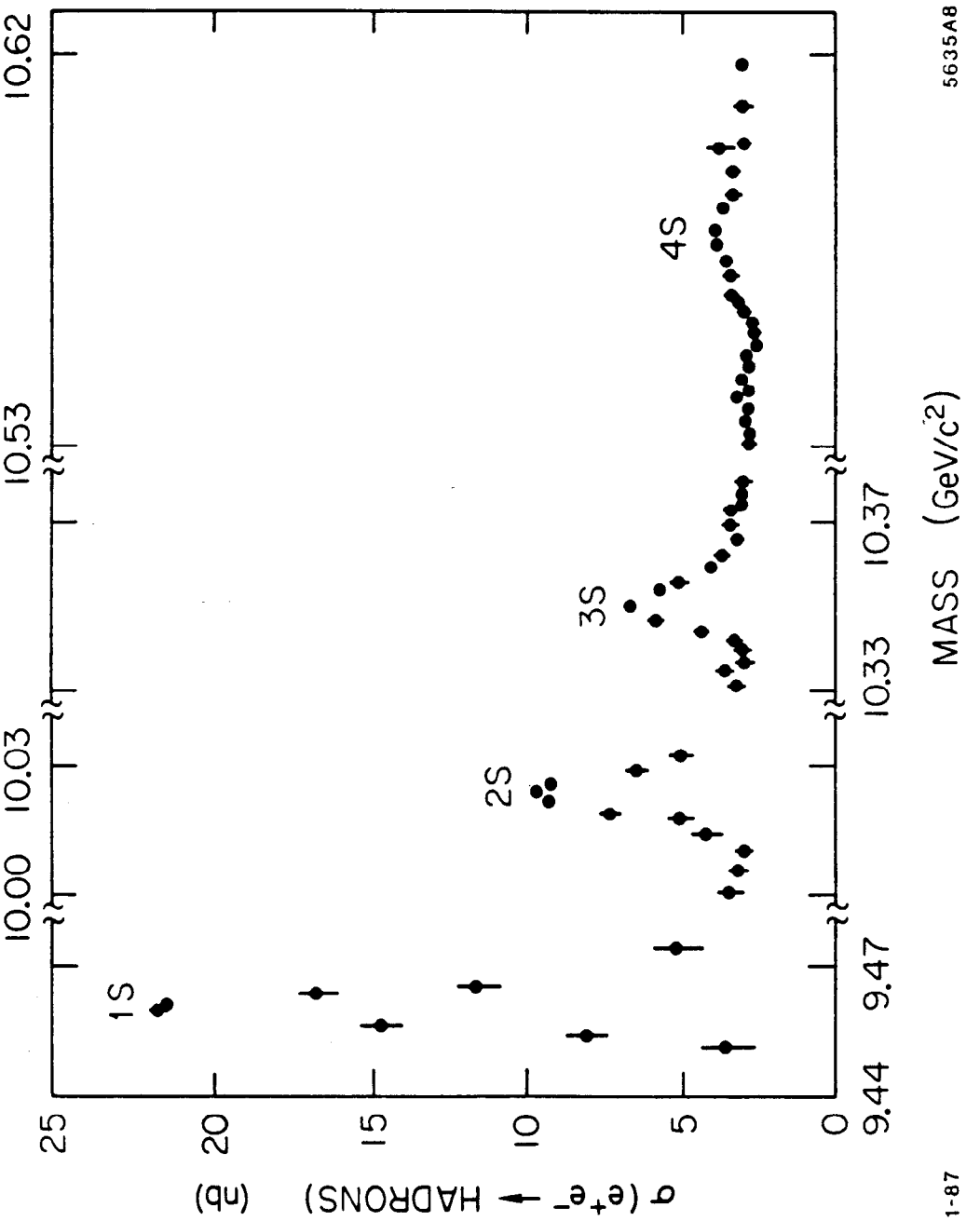

FIG. 8. Data from Ref. 8 of the Υ region.

the structure of the cross section becomes complex again.[9] This region is shown in detail in Fig. 9 . There is evidence for at least two additional resonances, which correspond well in position with the potential model calculations for the next two $^3S_1$ states, the $\Upsilon(5S)$ and $\Upsilon(6S)$. Structure above the 4^3S_1 state is also complicated by the opening of $B\bar{B}^*, B^*\bar{B}^*$, and B_s thresholds. The $\Upsilon(7S)$ is expected to have a mass of ~ 11.2 GeV.

Table II summarizes the current data on the $c\bar{c}$ S-wave states, while Table III summarizes the $b\bar{b}$ data. In charmonium, even the most naive calculation, namely the relative leptonic widths of the ψ and ψ' is difficult, owing to mixing of the ψ' with the nearby ψ''. In the coupled channel model of Eichten *et al.*, the mass and Γ_{ee} for the ψ are fixed and $\Gamma_{ee}(\psi')$ calculated to be 2.3 KeV, compared with the observed value of 2.1 KeV. This is basically a measure of how well the model computes the square of the radial wave function (R_0) at the origin. It is seen to be good to about 10%.

Table II. Comparison of $^3S_1$ State Charmonium Parameters[10]

	Γ_{ee}(KeV)	B_{ee}(%)	$\Gamma_{\mu\mu}$(KeV)	$B_{\mu\mu}$(%)	Γ_{had} (KeV)	Γ_{tot}(KeV)	Mass (MeV)
1S	$4.75 \pm .51$	6.9 ± 0.9	$4.85 \pm .51$	$6.9 \pm .9$	57.3 ± 10.9	63 ± 8.3	3096.93 ± 0.09
2S	$2.05 \pm .21$	0.88 ± 0.13		0.77 ± 0.17	224 ± 56	228 ± 56	3686.00 ± 0.10
3S	0.75 ± 0.15 0.77 ± 0.23				dominant dominant	52 ± 10 MeV 78 ± 20 MeV	4028 ± 2 4160 ± 20
4S	0.5 ± 0.1				dominant	43 ± 15 MeV	4415 ± 6

Table III. $^3S_1$ Bottomonium States[10] [11] [12]

	Γ_{ee} (KeV)	B_{ee} (%)	$B_{\mu\mu}$(%)	Γ_{tot} (KeV)	Mass
1S	1.224 ± 0.050	2.82 ± 0.31	2.78 ± 0.22 2.4 ± 0.2[11]	43.1 ± 3.1	9460.0 ± 0.19
2S	0.537 ± 0.033		1.8 ± 0.44	30 ± 7.3	10233.7 ± 0.34
3S	0.402 ± 0.031		0.3 ± 1.5 1.5 ± 0.4 [12]	12.0 26 ± 7[12]	10355.5 ± 0.5
4S	0.19 ± 0.04 CLEO 0.28 ± 0.04 CUSB			20.0 ± 4.5 25.0 ± 2.5 MeV	10577.5 ± 4.0
5S	0.22 ± 0.09 CLEO 0.37 ± 0.07 CUSB			110.4 ± 13 MeV	10865 ± 8
6S	0.095 ± 0.05 CLEO 0.156 ± 0.04 CUSB			79 ± 16 MeV	11019 ± 9

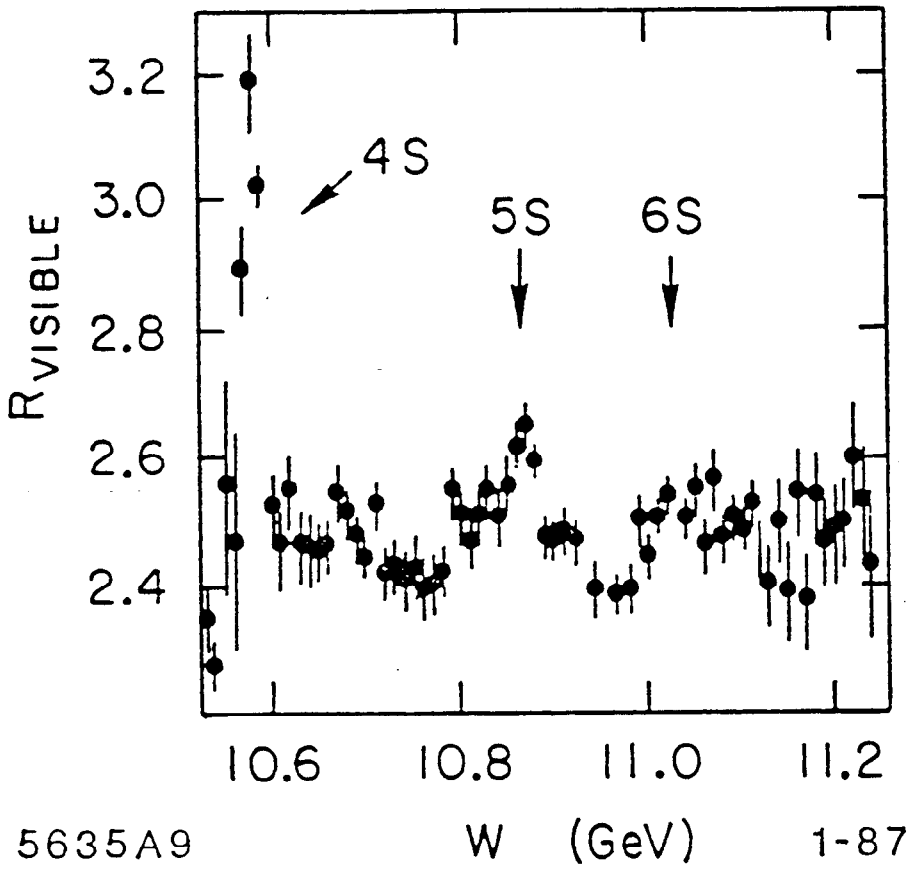

FIG. 9. The region above open beauty threshold from D. Lovelock *et al.*, Ref. 9.

In the $b\bar{b}$ system, the parameters of the potential derived from the $c\bar{c}$ system should provide a good description of the level splittings if the potential is truly flavor independent. From the model of Eichten *et al.*, the 2S-1S splitting is predicted to about 5%. If the model is adjusted to make it correct, then the 3S-1S is good to about 1% and the 4S-1S is good to about 4%. Recall that these splittings depend principally on the short range part of the potential. The leptonic widths of the 2S and 3S are calculated to within 10%, if the parameters for the 1S are used. Published measurements of the 4S are poorer, with large discrepancies between experiments.

2.4 The P-Wave States

2.4.1 $^1P_1$ and ^3P_J states of $c\bar{c}$.

These states have quantum numbers $J^{PC} = 1^{+-}$ and 1^{++}, and hence are not directly excitable in e^+e^- collisions. They must be studied through the electromagnetic transitions from higher S-wave states, as was shown in Figures 2 and 4. Three experimental approaches are employed for studying these states. They are the inclusive photon spectrum, reconstruction of the full cascade, or reconstruction of the first radiative transition with the subsequent hadronic decay of the P-wave state. These are pictured in Fig. 10 . The inclusive spectrum, combined with the exclusive full cascade measurement, determines the branching ratio for the P-wave states into $\gamma\psi$. In conjunction with the hadronic P-wave decays, the hadronic branching fractions are determinable. In the $c\bar{c}$ system, the primary photon has an energy of 130 to 270 MeV, while the level splittings are typically 50 MeV. In the $b\bar{b}$ system, the primary photon is 100 to 160 MeV, and the splittings only about 25 MeV. Typical glass detectors (NaI, BGO, Pb-glass) have resolutions of about 5 MeV at 100 MeV, while the use of e^+e^- pair gamma conversions improves the resolution to 1 to 2 MeV but at a cost of about one order of magnitude in detection efficiency.

The inclusive photon spectrum from the Crystal Ball detector[13] is shown in Fig. 11 . The fourth line is the merged Doppler shifted lines from the recoiling P-wave state. The typical resolution obtainable from hadronic decays of the P-wave states is shown in Fig. 12 .

The measurement of the natural widths of the P-wave mesons in the $c\bar{c}$ system can in principle be extracted from the gamma ray lineshape in the $\psi' \rightarrow \gamma\psi$

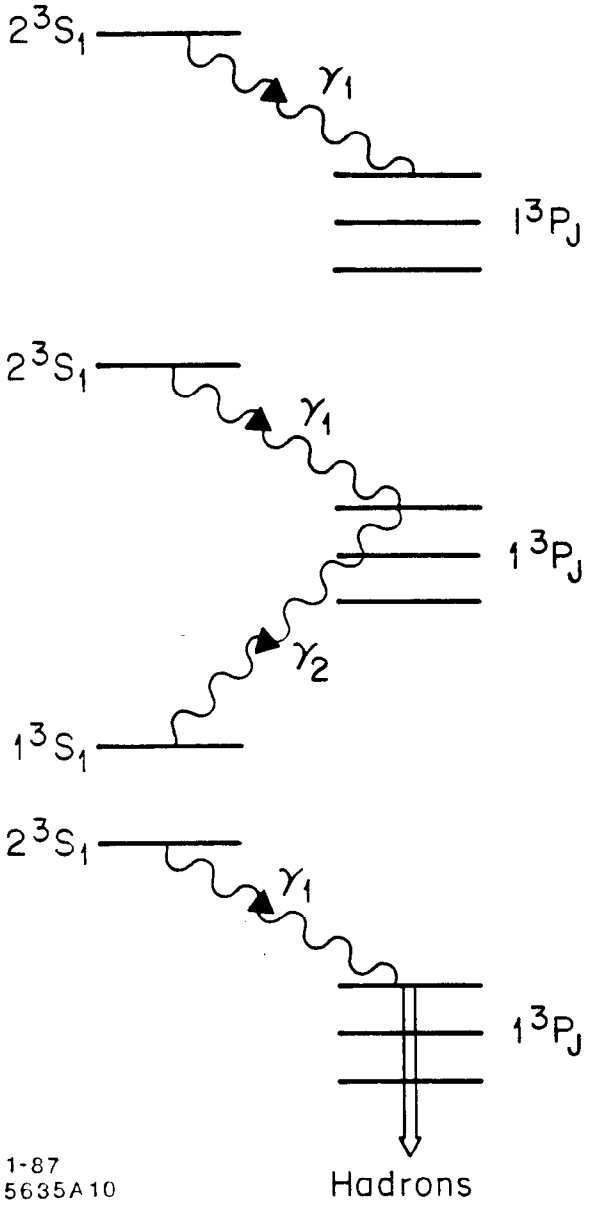

FIG. 10. Three approaches to observing P-wave states.

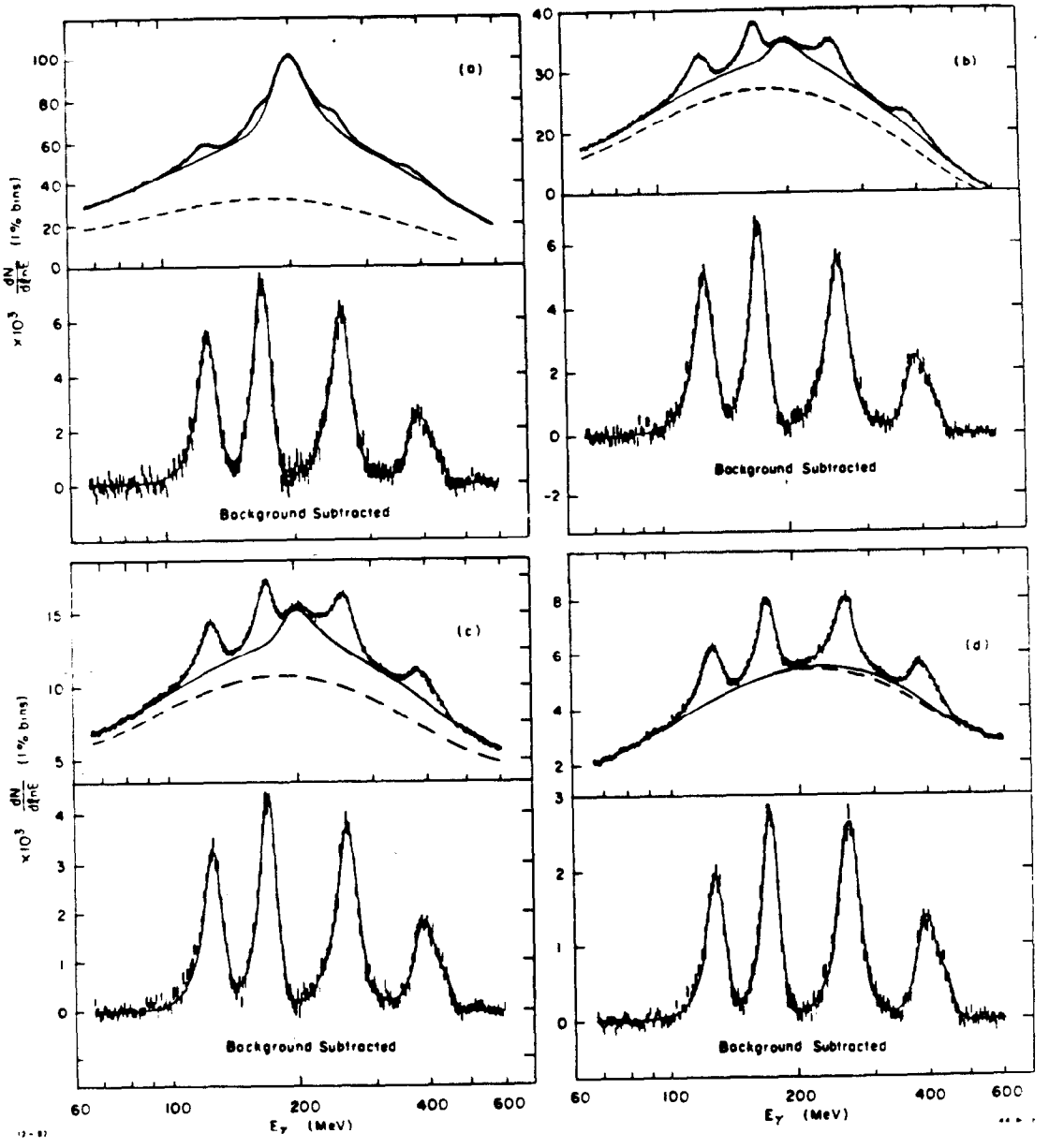

FIG. 11. Crystal Ball inclusive photon spectrum.[13]

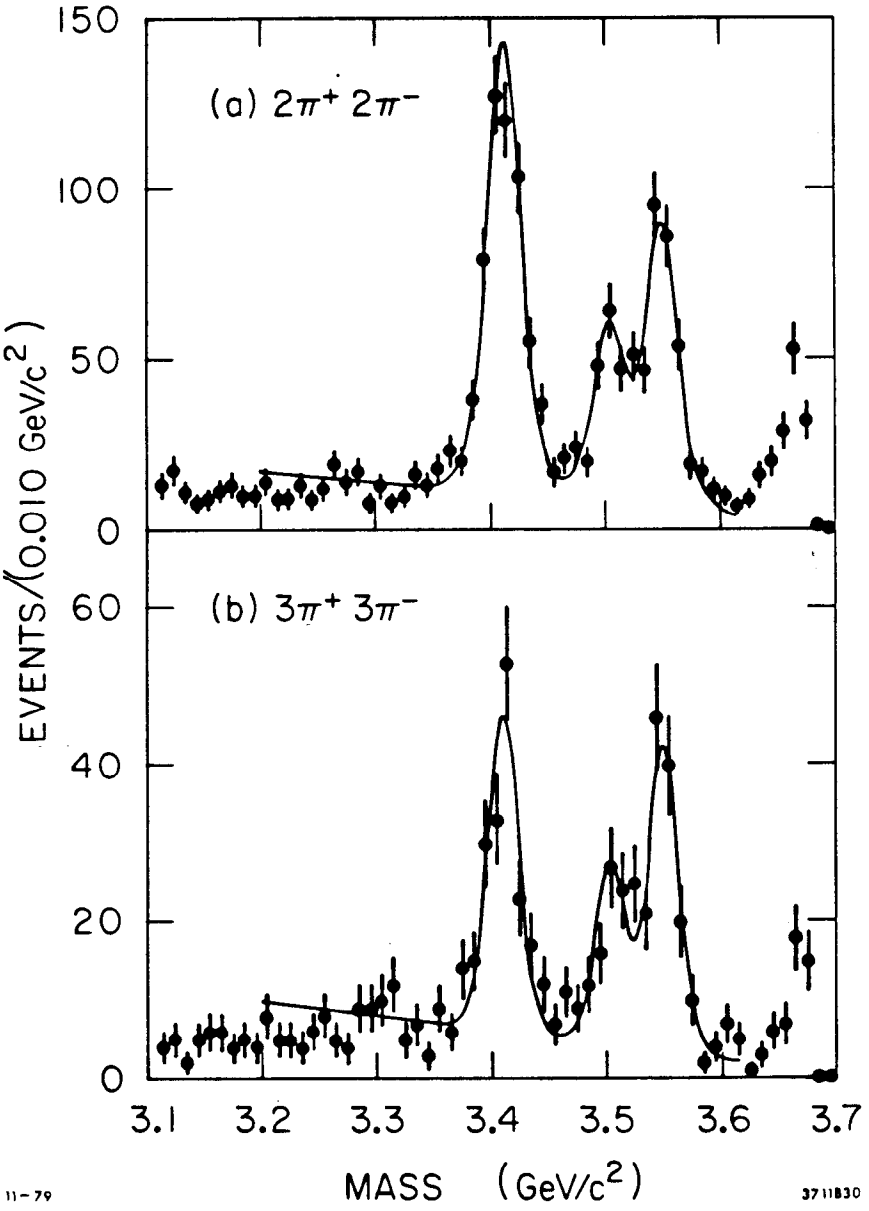

FIG. 12. Example of hadronic decays of P-wave states, from Ref. 106.

transition, if the detector resolution were adequate. The Crystal Ball has recently determined values for these widths, given in Table IV.[13]

Table IV. Widths of P-Wave $c\bar{c}$ States

State	Width (γ) (MeV)	Width $p\bar{p}$ (MeV)
$^3P_2$	≤ 3.8	$2.6^{+1.4}_{-1.0}$
$^3P_1$	$0.8 - 4.9$	≤ 1.3
$^3P_0$	$13.5 \pm 3.3 \pm 4.2$	–

A more precise measurement was recently obtained[14] by performing a formation experiment using $\bar{p}$ in the ISR storage ring, and a hydrogen gas jet target. The center of mass energy spread is small ($\delta E_{cm} \approx^{+0.4}_{-1.4}$ MeV). The $\bar{p}$ momentum is stepped to produce a scan over the P-wave mass (see Fig. 13):

$$p\bar{p} \rightarrow \chi_J \rightarrow \psi + \gamma$$

where χ_J are the common names corresponding to the ^3P_J states. The excitation curve is measured by counting events from $\psi \rightarrow e^+e^-$. The results are shown in Table IV for the narrower χ_J states. In addition, the masses $M_{\chi_1} = 3511.3 \pm 0.4 \pm 0.4$ MeV and $M_{\chi_2} = 3556.9 \pm 0.4 \pm 0.5$ MeV were measured.

The 1^1P_1 (η_c) and 2^1P_1 (η_c') states of the $c\bar{c}$ system have been measured by the inclusive photon technique. These splittings, being less than 100 MeV are a particular experimental challenge. The η_c' has only been observed in one experiment,[15] while the existence of the η_c has been confirmed through its hadronic decays[16] and extensively measured.[17] The η_c and η_c' signal in inclusive photons are shown in Fig. 14 , while Fig. 15 shows typical hadronic decays of the the η_c.

2.4.2 $^1P_1$ and ^3P_J states of $b\bar{b}$.

As indicated in Figure 4, the radiative transitions in the $b\bar{b}$ system are more complex because of the presence of two sets of P-wave states (usually denoted χ_b and χ_b'). A summary of the measurements of the χ_b states from the observation of the photons in the transitions $\Upsilon(2S) \rightarrow \gamma + \chi_b^{j=0,1,2} \rightarrow$ *anything* are shown

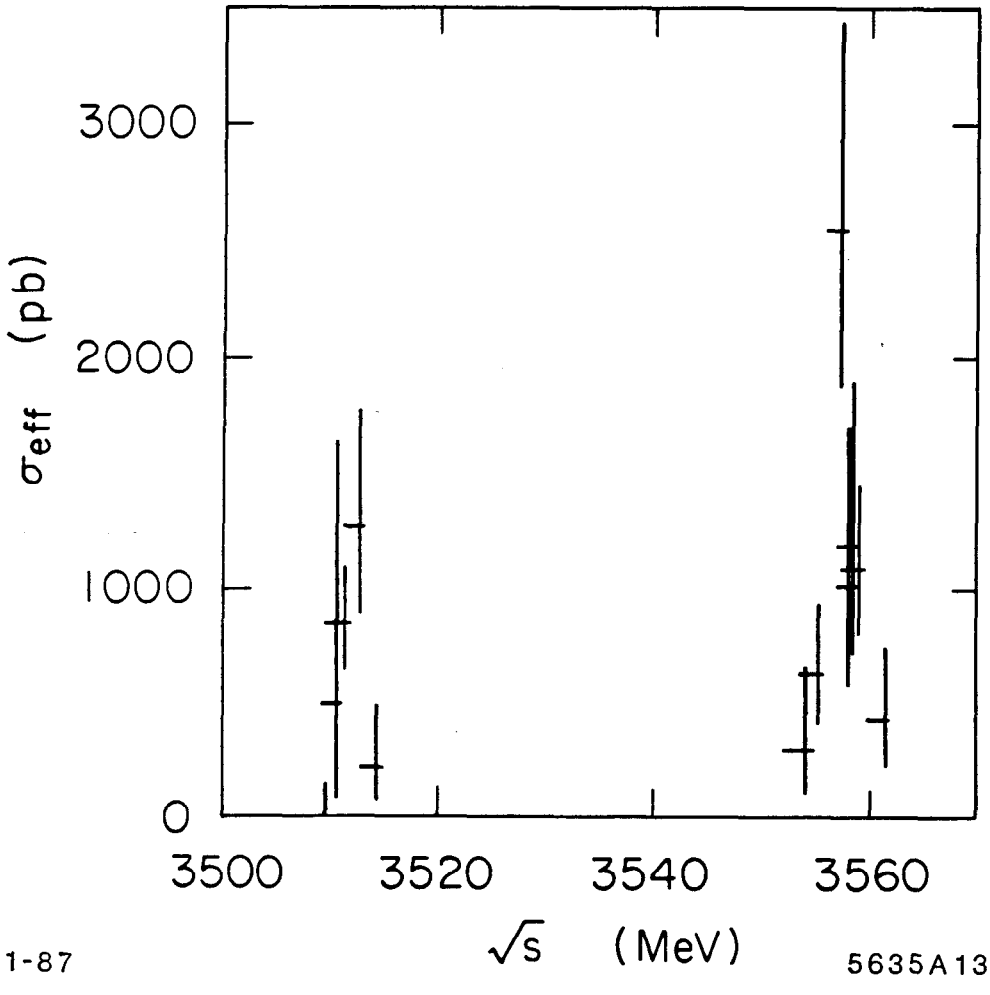

FIG. 13. Formation experiment[14] to measure masses and widths of the χ_c states.

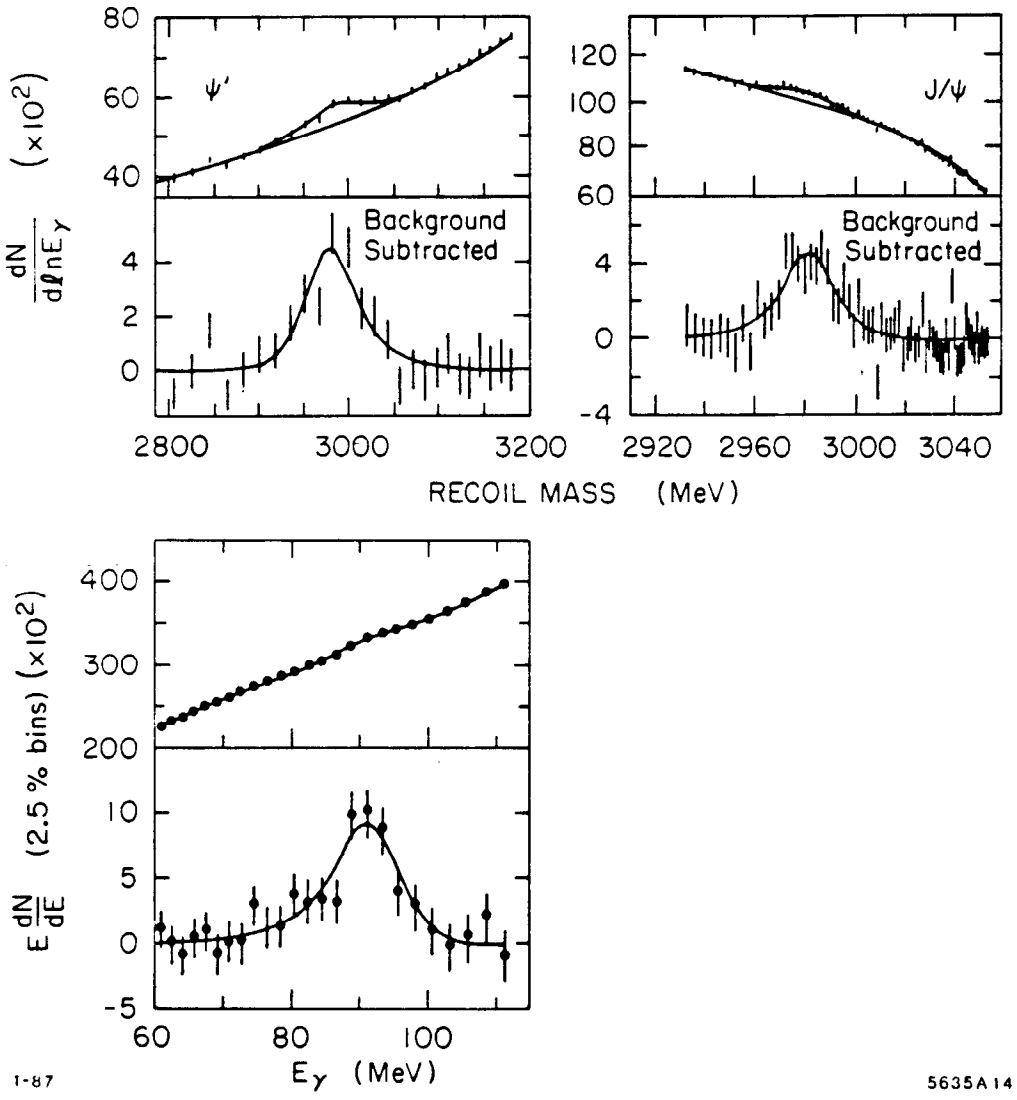

FIG. 14. Inclusive photons from Crystal Ball show signals for both the η_c and the η_c' states.

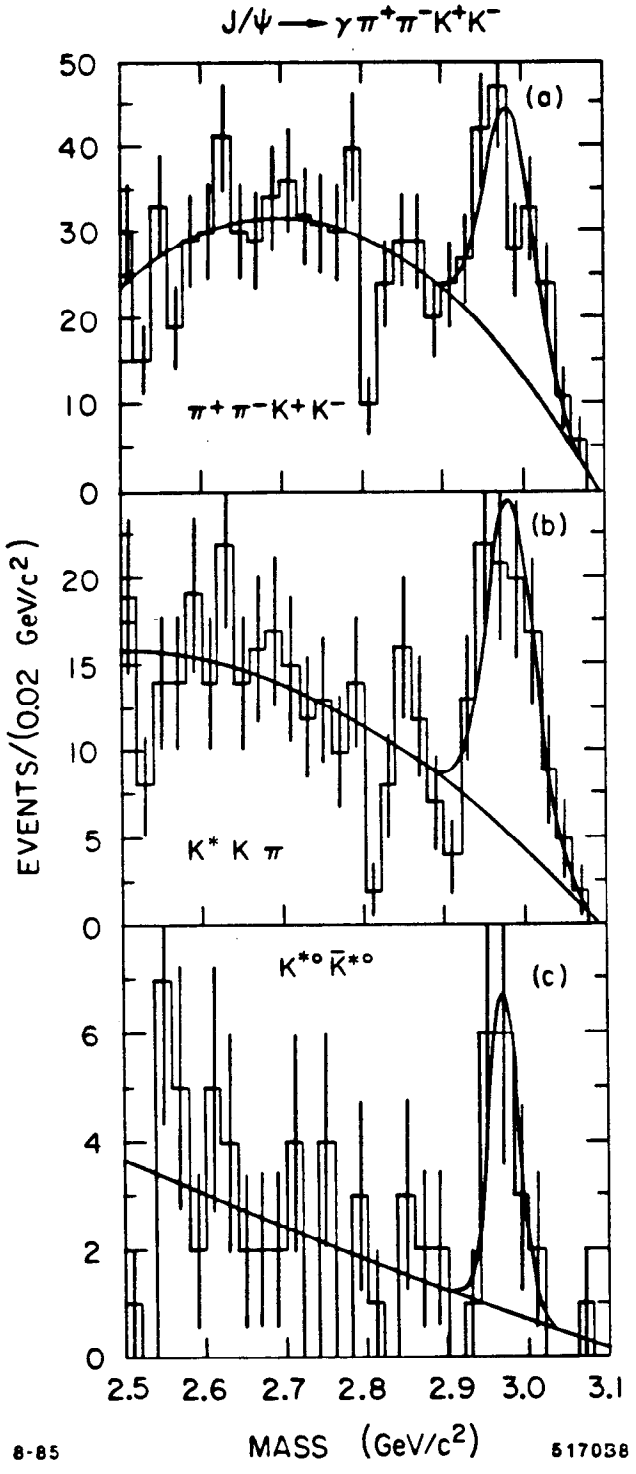

FIG. 15. Hadronic decays of the η_c from Mark III.[107]

in Fig. 16.In these measurements, the 1 MeV resolution of the converted pairs in the ARGUS detector separates the states unequivocably. The transitions to the 2^3P_J multiplet from the reaction $\Upsilon(3S) \rightarrow \gamma + \chi_b'^{j=0,1,2} \rightarrow$ *anything* are less well established. The first inclusive measurements are shown in Fig. 17 , indicating the presence of the multiplet, but not clearly separating the states. The J=2, 1 and 0 states of the χ_b' have fitted lines of 122±5, 100±2 and 84±2 MeV respectively. New data[12][18] using CUSB-II (a BGO augmented device) has improved the resolution of these states.

2.5 Experimental and Theoretical Comparisons

This section summarizes the data on E1, M1 and hadronic transitions in the charmonium and bottomonium systems, comparing the data with theoretical expectations. More details of the models under discussion appear in the parallel lectures of F. Gilman.

2.5.1 Charmonium splittings.

Table V summarizes the average energies and branching fractions of the χ_c states. As was noted, in the absence of a confining term the COG of ^3P_J states would remain degenerate with the 2^3S_1. The spin dependent part of the potential would break the degeneracy of the multiplet, but leave the singlet ($^1P_1$) state unchanged at the COG. The splitting of the ^3P_J provides information on the Lorentz structure of the spin dependent part of the potential. The parameter R, defined :

$$R = \frac{^3P_2 - ^3P_1}{^3P_1 - ^3P_0} \tag{3}$$

is used as a measure of the splitting. In the charmonium system $R = 0.50 \pm 0.02$. A purely Coulombic spin dependent potential would give $R \approx 0.8$. If however there is a scalar contribution, then R is decreased, while a vector contribution would increase it further. The value of 0.5 suggests that these added terms are scalar in their Lorentz structure.

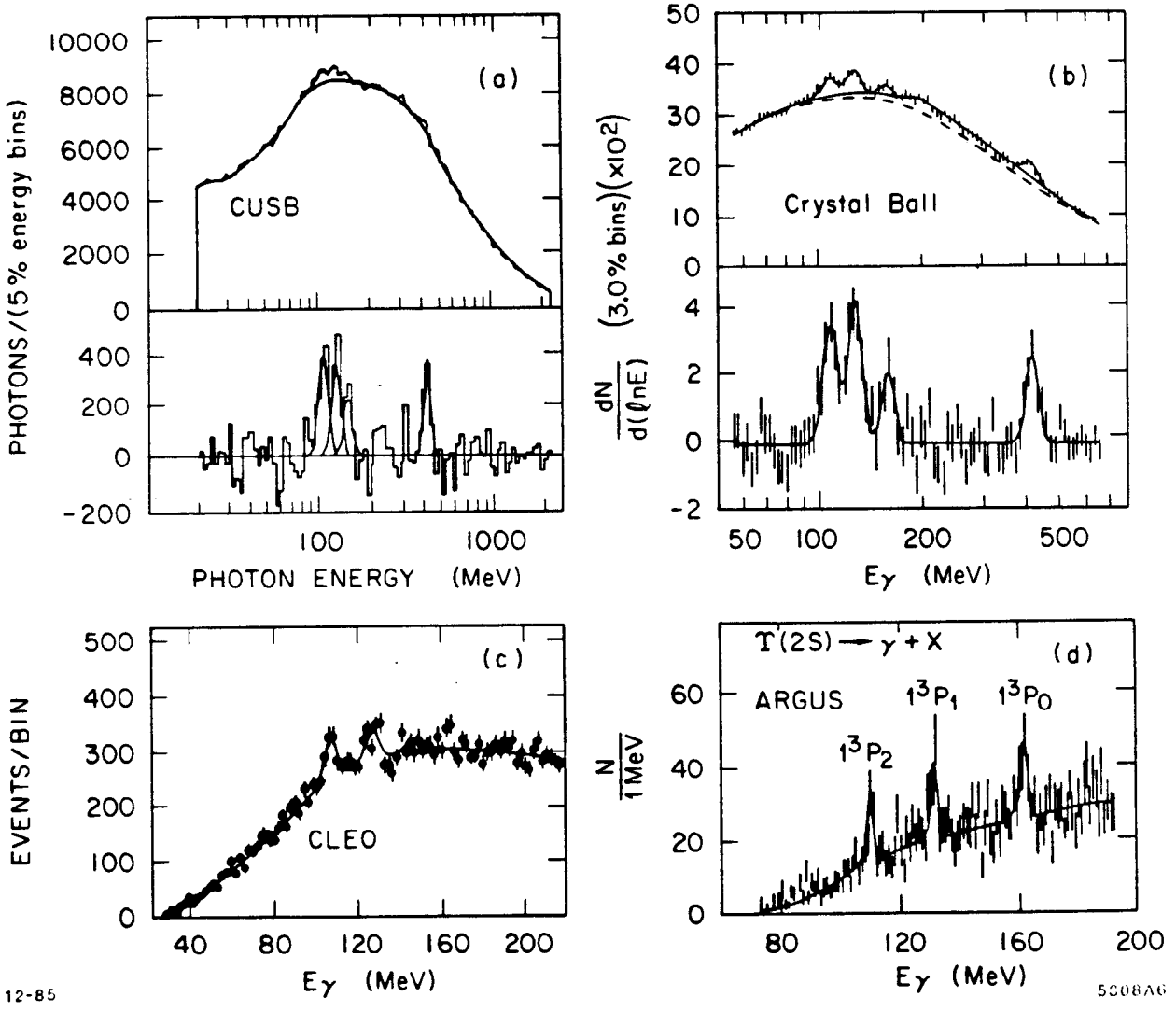

FIG. 16. Recent summary of inclusive photons from the $\Upsilon(2S)$.[108]

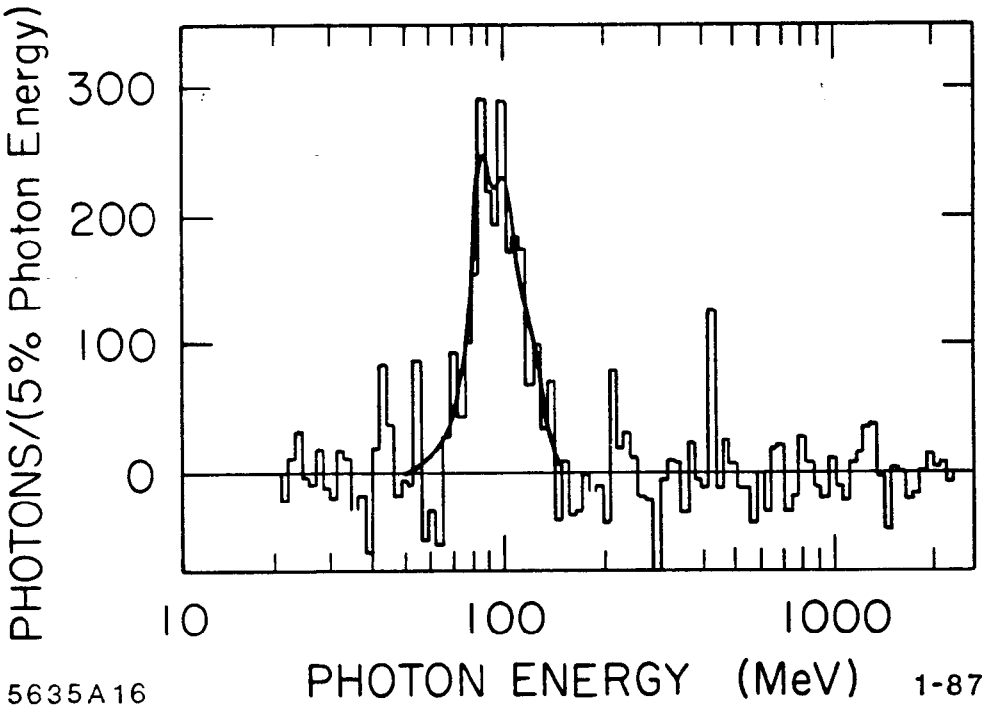

FIG. 17. Early CUSB inclusive photon data on the $\Upsilon(3S)$ showing the narrowly resolved lines of the 2P multiplet.[8]

Table V. Summary of Data on the χ_c Transitions[10]

χ_c	Energy $(2^3S_1 \rightarrow 3P_1)$	$Br(2^3S_1 \rightarrow^3 P_1)$	$Br(^3P_1 \rightarrow^3 P_1)$	Γ_{had} (MeV)
$J=2$	129.7 ± 0.4	$7.83 \pm 0.82\%$	$14.8 \pm 1.7\%$	$2.6^{+1.4}_{-1.0}$
$J=1$	175.3 ± 0.5	8.65 ± 0.81	26 ± 3	< 1.3
$J=0$	271.1 ± 1.1	9.35 ± 0.80	0.7 ± 0.2	$13.5 \pm 3.3 \pm 4.2$

2.5.2 Charmonium E1 and M1 transitions.

The E1 rates are summarized in Table VI, along with the nonrelativistic coupled channel model of Eichten *etal.* The E1 rates for such transitions are given:

$$\Gamma(2^3S_1 \rightarrow 1^3P_J) \propto q^2(2J+1)k^3 < r >^2$$

where k is the photon energy, and $< r >$ is the overlap integral of the dipole operator (r) between the initial and final states. While the transitions $\chi_c \rightarrow \gamma\psi$ are in fairly good agreement, the primary transitions $\psi' \rightarrow \gamma\chi_c$ have predicted E1 rates about a factor of 2 off from the data. McClary and Byers[19] recently looked at relativistic corrections in the charm system. Their explanation is shown schematically in Fig. 18 they point out that the $2S \rightarrow 1P$ transition is sensitive to corrections of $O(\frac{v^2}{c^2})$ which may shift the node of the radial wavefunction of the $2S$ state, right at the peak of the $1P$ wavefunction, thus reducing the transition rate. This is not the case for the $1P \rightarrow 1S$ transition. The corrected numbers for the E1 transitions are shown in Table VI, and are good agreement with the data.

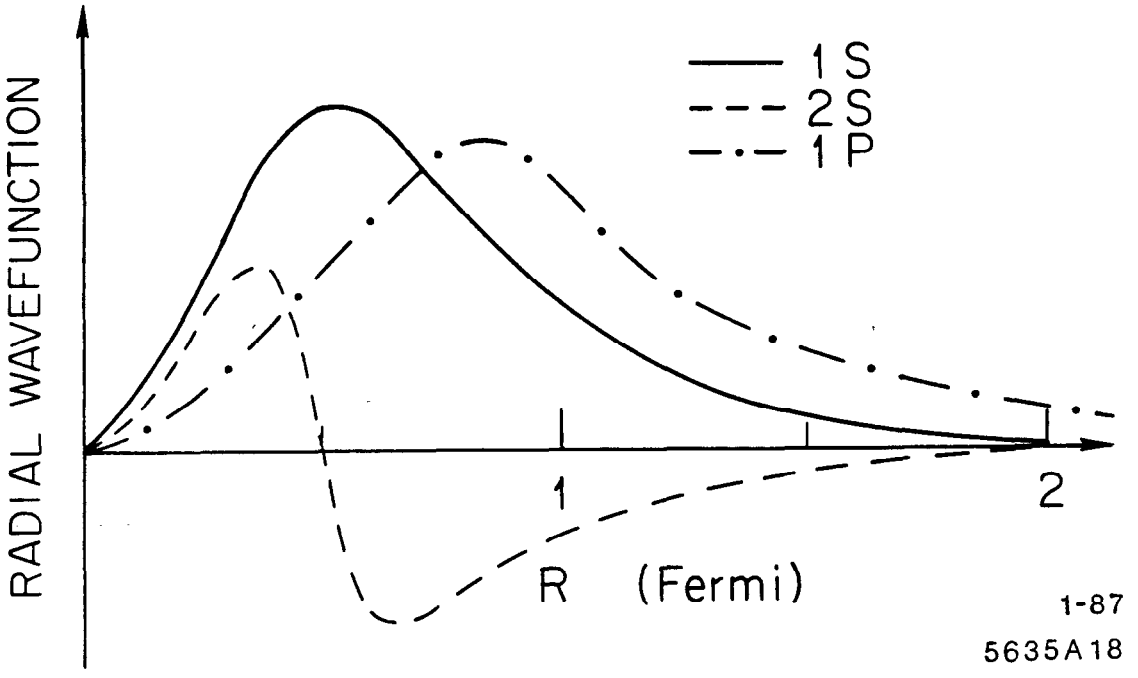

FIG. 18. Schematic showing the relative position of nodes in the S and P wave states, and their effect on transition rates.

Table VI. E1 Transitions in Charmonium[10][19]

Charmonium Transition	Angular Momentum (J)	Nonrelativistic Width (KeV)	Relativised Width (KeV)	Coupled Channel (KeV)	Data (KeV)
$\psi' \rightarrow \gamma\chi_c$	0	45	19	16	20.1 ± 4
	1	40	31	23	18.6 ± 4
	2	27	27	22	16.8 ± 4
$\chi_c \rightarrow \gamma\psi$	0	121	128	117	95 ± 37
	1	250	270	240	≤ 252
	2	362	347	305	429^{+270}_{-169}

Measurements of M1 transitions are considerably poorer as is seen in Table VII where data and theory are compared:

Table VII. M1 Transitions in Charmonium[6][10]

Charmonium Transition	Branching Ratio (%)	Width (KeV)	Model (KeV)
$\psi \rightarrow \gamma\eta_c$	1.27 ± 0.36	0.8 ± 0.24	2
$\psi' \rightarrow \gamma\eta_c'$	0.28 ± 0.06	0.6 ± 0.18	1

There is no evidence of any discrepancy owing to the large errors that remain in the data.

2.5.3 The $^1P_1$ charmonium state.

The $p\bar{p}$ gas jet formation experiment mentioned in Section 2.4.1 has also searched for the singlet-P state. Five candidate events have been found with a mass of $3525.4 \pm 0.8 \pm 0.5$ MeV. This state is seen to be close to the COG of the three ^3P_J states, 3525.38 MeV, confirming the expectation that the hyperfine spin-spin splitting of the P-wave states should effect both the singlet and the COG of the triplet equivalently, creating no net displacement.

2.5.4 Bottomonium COG and splittings.

Table VIII summarizes the average energies and branching fractions of the χ_b and χ_b' states. New data from CUSB-II[12] [18] has been included in the table. The COG of the χ_b and χ_b' are 9900.2 MeV and 10261.6 MeV, respectively. The COG as noted is a sensitive measure of the long range confining term in the potential. Table IX is a comparison between various models[7] [19] [21] [22] [23] [24] [25] [26] [27] [28] [29] which predict the COG of the χ_b states. These models generally use the $\Upsilon(1S)$ mass as input to set the scale. As can be seen, the relativistic potential models do very well in predicting the COG.

Table VIIIa. Bottomonium 1^3P_J Masses and Widths[10]

χ_b	Energy $(2^3S_1 \rightarrow 1^3P_J)$	Br(%) $(2^3S_1 \rightarrow 1^3P_J)$	Br(%) $(1^3P_J \rightarrow 1^3S_1)$
$J=2$	109.5 ± 0.6	6.6 ± 0.9	22 ± 4
$J=1$	130.7 ± 0.7	6.7 ± 0.9	35 ± 8
$J=0$	162.3 ± 1.3	4.3 ± 1.0	< 6

Table VIIIb. Bottomonium 2^3P_J Masses and Widths[10]

χ_b'	Energy $(3^3S_1 \rightarrow 2^3P_J)$	Br(%) $(3^2S_1 - 2^3P_J)$	Br(%) $(3^3P_J - 2^3S_1)$
$J=2$	84.1 ± 1.7	12.7 ± 4.1	-
$J=1$	99.7 ± 1.7	15.6 ± 4.2	-
$J=0$	122.1 ± 5.0	7.6 ± 3.5	-

Table IX. Theoretical Predictions for the COG[7] [19] [21] [22] [24] [25]

Models	$M_{COG}(\chi_b) = 9900.2$ MeV		$M_{COG}(\chi_b') = 10261.6$ MeV
PM	Khare	9871	-
NP	Eichten, Feinberg	9925	10275
B	Buchmuller	9888	10250
RP	Moxhay,Rosner	9906	10262
RP	Gupta *et al*	9900	10258
RP	McClary, Byers	9923	10267
NP	Richardson	9896	10250
P	Martin	9861	10242

PM = PHEN. POT. NP = NON-REL. POT. B = BAG RP = REL. POT.

The parameter R (see Eq. (3)) measuring the multiplet splitting is calculated from Table IX to be:

$$R_{\chi_b} = 0.67 \pm 0.05 \qquad R_{\chi_b'} = 0.70 \pm 0.20 \ .$$

These values are higher than in the charmonium system. Table X summarizes many of the theoretical models which predict R for the $b\bar{b}$ system. Again the relativistic potential models appear to track the data quite well. The large values of R in the $b\bar{b}$ system compared with charmonium's 0.5, are still below the 0.8 value predicted for a purely Coulombic potential, going in the right direction for an additional scalar confinement term. The larger values suggest however that potential is more strongly vector-Coulombic on average over the wavefunction at the shorter distances probed in the heavier $b\bar{b}$ system.

Table X. Summary of ^3P_J (χ_b, χ_b') [24] [21] [7] [27] [19] [28] [25] [23] [27] [29]

Models	Data	$R\chi_b = 0.67 \pm 0.05$ PDG	$R\chi_b' = 0.70 \pm .20$ PDG
PM	Khare	0.50	-
NP	Eichten,Feinberg	0.80	0.80
B	Buchmuller	0.73	0.78
RP	Moxhay,Rosner	0.42	0.42
RP	Gupta *et al*	0.68	0.70
RP	McClary,Byers	0.45	0.48
BR	Baacke	0.73	0.77
RP	Kang	0.52	0.57
RP	Beavis	0.96	1.0

The absolute size of the fine structure splitting is defined:

$$\Delta_{fs} = {}^3P_2 - {}^3P_0.$$

This splitting is sensitive directly to the strong coupling constant (α_s), and is found from Table IX to be:

$$\Delta_{fs}^{\chi_b} = 52.8 \pm 1.4\text{MeV} \quad \Delta_{fs}^{\chi_b'} = 38.0 \pm 5.3\text{MeV} .$$

Table XI compares these values with those of numerous models of the $b\bar{b}$ system. The general trend of a reduction in the absolute splitting is seen to arise in all models, while the absolute magnitude is only close for some of the fully relativised models, and those that treat relativistic effects perturbatively.

Table XI. Theoretical Predictions for the Fine Structure Splittings[7] [21] [23] [26]

Models	Data	$\Delta_{fs}\chi_b \approx 52.8 \pm 1.4$	$\Delta_{fs}\chi'_b = 38.0 \pm 5.3$
NP	Eichten Feinberg	51.0	36.0
B	Buchmuller	38.0	32.0
RP	Moxhay, Rosner	37.0	28.0
RP	Gupta *et al*	42.0	34.0
BR	Baacke	52.0	42.0

2.5.5 Bottomonium E1 transitions.

The E1 rates for the $2S \rightarrow 1P$ transitions are summarized in Table XII, along with the predictions of several models.[8] Because the $E1$ rates scale as k^3, the predictions have been scaled to the correct photon energies, when calculating the total E1 widths in Table XII. New CUSB-II data for the $3S \rightarrow 2P$ transitions are also included in the table. The agreement is generally good, and suggests that the relativistic corrections are less important in this case, than the $c\bar{c}$.

Table XII. E1 Transitions of Bottomonium[7] [24] [29] [22] [8]

Models	2^3P_0	2^3P_1	2^3P_2	$\Sigma_{\text{total}}^{\text{corrected}\dagger}$	$\Sigma\chi'_b$
Khare	0.56	1.06	1.6	3.0	
Buchmuller	1.3	2.4	2.8	5.6	6.4
Kang	1.4	2.8	3.6	4.7	5.3
Moxhay,Rosner	1.0	2.1	2.2	5.4	6.9
EXPT (KeV)	1.3 ± 4	2.0 ± 0.5	2.0 ± 0.5	5.3 ± 0.8	$4.3^{+3.6}_{-1.7}$ ‡

† From reference 8. ‡ CUSB-II data.[18] [12]

There is no data on M1 transitions in the bottomonium system.

2.5.6 Hadronic widths of the χ_b states.

The total width of each χ_b^J state is the sum of its E1 width, $\Gamma_{E1}(2^3P_J \rightarrow 1^3S_1)$, plus its hadronic width, $\Gamma(^3P_J)$. Inclusive photon measurements give the $\mathrm{Br}(2^3S_1 \rightarrow 1^3P_J + \gamma)$. Exclusive measurements of the cascades give the product:

$$Br(2^3S_1 \rightarrow 1^3P_J + \gamma) \cdot Br(^3P_J \rightarrow \gamma 1^3S_1) \cdot Br(1^3S_1 \rightarrow l^+l^-) \ .$$

Hence, dividing by the leptonic branching ratio of the 1^3S_1 and by $Br(2^3S_1 \rightarrow 1^3P_J + \gamma)$ gives $B_J = \frac{\Gamma_{E1}}{\Gamma_{tot}}$. Combining this with the definition of Γ_{tot} gives:

$$\Gamma_{had} = \Gamma_{E1}(\frac{1}{B_J} - 1) \ . \qquad (4)$$

Using theoretical E1 widths for the $1P \rightarrow 1S$ transitions is reasonable in light of the good agreement for the $2S \rightarrow 1P$ rates.[30] The results are shown in Table XIII, in comparison with the theoretical values from Kuang and Yan[31] using the QCD multipole expansion. The agreement is rather good. The ggg and $q\bar{q}g$ decays are seen to be smaller than the gg decays of the J=0,2 states.

Table XIII. Hadronic Widths of the χ_b States[10] [31]

2^3P_J	$J=0$	$J=1$	$J=2$
B_J	<6	35 ± 8	22 ± 4 (%)
$<\Gamma_{E1}>^\dagger$	27 ± 5	33 ± 5	27 ± 5 KeV
Γ_{HAD}	>423	61 ± 29	96 ± 33 KeV
Typ. Theor. Est.	380	30-80	100-200
Had. Decays	gg	$(ggg, q\bar{q}g)$	gg

† from Ref. 30.

2.5.7 Hadronic transitions in $c\bar{c}$ and $b\bar{b}$.

The QCD multipole expansion has been used[31] to scale the hadronic transitions of $\psi' \rightarrow \psi$, to those of the $b\bar{b}$ system. The ratios between $c\bar{c}$ and $b\bar{b}$ are largely determined by the quark masses, the size of the initial states, and the available phase space (PS):

$$\frac{\Gamma(\Upsilon' \to \pi\pi\Upsilon)}{\Gamma(\psi' \to \pi\pi\psi)} = \frac{< r^2_{\Upsilon'} >}{< r^2_{\psi'} >} \approx \frac{1}{16} \text{ , and}$$

$$\frac{\Gamma(\Upsilon' \to \eta\Upsilon)}{\Gamma(\psi' \to \eta\psi)} = (\frac{M_c}{M_b})^4 (\frac{PS(\Upsilon)}{PS(\psi)})^3 \approx \frac{1}{300} \text{ .}$$

Results for ψ transitions are given in Table XIV, along with the expectations and measurements in the Υ system in Table XV. The agreement between data and theory is seen to be quite good.

Table XIV. Hadronic Transitions of Charmonium[10]

Transition	Br(%)
$\psi' \to (\pi\pi)^o\psi$	50.3 ± 4.2
$\psi' \to (\pi^o\pi^o)\psi$	26.7 ± 3.0
$\psi' \to \eta\ \psi$	2.66 ± 0.44
$\psi' \to \pi^o\ \psi$	0.1 ± 0.03

Table XV. Hadronic Transitions of Bottomonium[10]

Transition	Theory(%)	Experiment (%)
$\left\{ \begin{array}{l} \Upsilon \to \pi^+\pi^-\Upsilon \\ \Upsilon' \to \pi^o\pi^o\Upsilon \end{array} \right\}$	25-29	$\left\{ \begin{array}{l} 18.8 \pm 1.0 \\ 8.6 \pm 1.1 \end{array} \right\}$ 27.4 ± 1.5
$\Upsilon' \to \eta\Upsilon$	0.04%	< 0.2 @ 90% C.L.
$\Upsilon'' \to \pi^+\pi^-\Upsilon$	2-5	4.5 ± 0.8
$\Upsilon'' \to \pi^+\pi^-\Upsilon'$	2-3	3.1 ± 2.0

2.5.8 The $^1P_1$ bottomonium state.

As was indicated in section 2.2, the additional phase space in the $b\bar{b}$ system may allow a sizeable rate (about 1%) for $\Upsilon(3S) \to \pi^+\pi^-\Upsilon(^1P_1)$. The $^1P_1$ state should lie at the COG of the χ_b states, at a mass of 9900.5 ± 1.3.[32] The recoil mass from opposite charge pion pairs at the $\Upsilon(3S)$ is shown in Fig. 19 . Evidence[33] for a narrow bump with 335 ± 135 events is seen, at a mass of 9894.8 ± 1.5 MeV. While only a 2.5 σ effect, the peak lies close the COG of the χ_b states, and has a

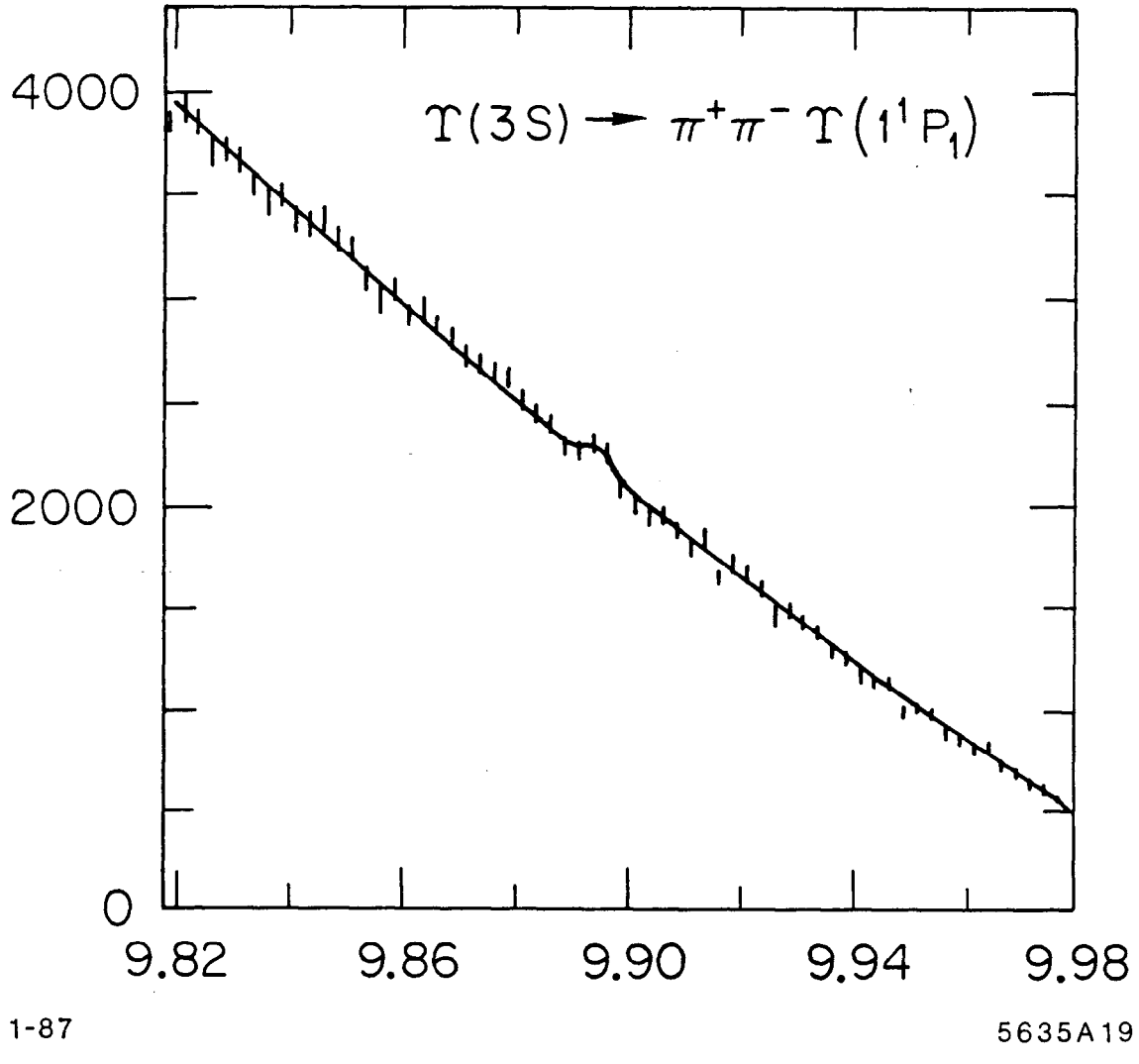

FIG. 19. Recoil mass from $\pi^+\pi^-$ pairs at the $\Upsilon(3S)$ from CLEO.

branching ratio of $0.37 \pm 0.15\%$, thus making it an excellent candidate for the $^1P_1$ state.

3. STATES OF EXCITED CHARM AND BEAUTY

I deal here with the data on the vector and orbitally excited states of charm and beauty mesons. This section lies naturally midway between the spectroscopy of the bound $c\bar{c}$ and $b\bar{b}$ states and the weak decays of the ground state charmed $(c\bar{q})$ and b-mesons $(b\bar{q})$, discussed in the subsequent section.

In the standard parton model, the light u, d, and s quarks are expected to combine with the heavier charmed (c) quark to form the three lowest lying pseudoscalar states: D^0 $(c\bar{u})$, D^+ $(c\bar{d})$ and D_s $(c\bar{s})$.[34] Analogous B meson states also exist, denoted B_u, B_d and B_s. In addition the heavy state B_c should also exist. Spectroscopically, these correspond to the $^1S_0$ states. The D^0 , D^+ and B_d, B_u form isotopic doublets; the D_s ,B_s and B_c are isosinglets. With the exception of the B_c, these states have been isolated in either e^+e^- annihilation, hadroproduction, photoproduction, or ν-scattering experiments. The masses[10] [35] and lifetimes[36] of the groundstates are summarized in Table XVI.

Table XVI. Ground and Excited States of Charmed Mesons[10] [35] [36] [37]

Charmed Meson	Quark Content	Mass GeV/c^2	Width (MeV) (Lifetime $\times 10^{-13}$)	J^P Assignment
D^0	$c\bar{u}$	1864.6 ± 0.6	$(4.43^{+0.19}_{-0.17})$	0^-
D^+	$c\bar{d}$	1869.3 ± 0.6	$(10.29^{+0.54}_{-0.43})$	0^-
D_s^+	$c\bar{s}$	1970.5 ± 2.5	$(3.85^{+0.65}_{-0.48})$	0^-
B_u	$b\bar{u}$	5277.6 ± 0.6	-	0^-
B_d	$b\bar{d}$	5280.4 ± 0.8	-	0^-
D^{*0}	$c\bar{u}$	2007.2 ± 2.1	≤ 5.0	1^-
D^{*+}	$c\bar{d}$	2010.1 ± 0.7	≤ 2.2	1^-
D_s^{*+}	$c\bar{s}$	2110 ± 6	≤ 22	1^-
B^*	$b\bar{q}$	$\Delta M = 0.052 \pm 0.005$	-	1^-
D^{**0}	$c\bar{u}$	2420 ± 6	70 ± 21	$1^+, 2^+$

Each ground state meson is expected to have a vector state ($^3S_1$)corresponding to the parallel alignment of its constituent quark spins. The D^{*0} and D^{*+} are now well established.[38] The excited state of the D_s has only recently been established in e^+e^- annihilation,[39][40] through both its direct decay, and its associated production ($e^+e^- \rightarrow D_s\bar{D}_s^*$) near threshold. The B^* has only been seen indirectly through the gamma ray transition to the B_u or B_d meson.[35]

As in the spectroscopy of light quark mesons, a set of orbitally excited charmed mesons is also expected with the lowest lying states having spectroscopic and quantum number assignments: $^1P_1$ (1^+) or ^3P_j ($0^+, 1^+$ and 2^+), and masses typically 500 MeV/c^2 higher than the ground states.[41]

A typical set of mass splittings expected for bound $c\bar{q}$ states in both non-relativistic and relativistic potential models are indicated in Fig. 20 . The first candidate for an orbitally excited state (D^{**0}) has only recently been observed.[42] The experimental evidence for the state, is shown in Fig. 21 .

The D^0, D^+, and D_s, being the lightest charmed mesons, and the B_u, B_d, B_s, and B_c being the lightest bottom mesons, must decay weakly through a charm-changing charged current. The details of these decays will encompass the greater part of the next lecture. The vector states D^{*0} , D^{*+} , and B^* decay strongly and electromagnetically to the ground states through $\pi^{\pm}$, π^0, and γ emission. Some of these transitions (such as $D^{*0} \rightarrow \pi^- D^+$) are energetically forbidden (see Fig. 22). While all the decays have been measured, there are still discrepancies in the branching fractions, owing to the difficulty of the measurements. The charm-strange D_s^{*+}, being an isosinglet, cannot decay strongly to the D_s^+ via π^0 emission. The γ transition is uninhibited, and is expected to dominate the D_s^{*+} decay. The world average for the mass difference between the D_s^+ and D_s^{*+} is now measured to be $132 \pm 5 \pm 4$ MeV/c^2, forbidding an isospin-violating decay through π emission. The difference in squared masses between vector and pseudoscalar states for both the D, D_s, and B_q lie close to the constant found for all lighter mesons (see Table XVII) to be expected if the meson wavefunction at the origin is determined by the long range confining part of the potential.[43]

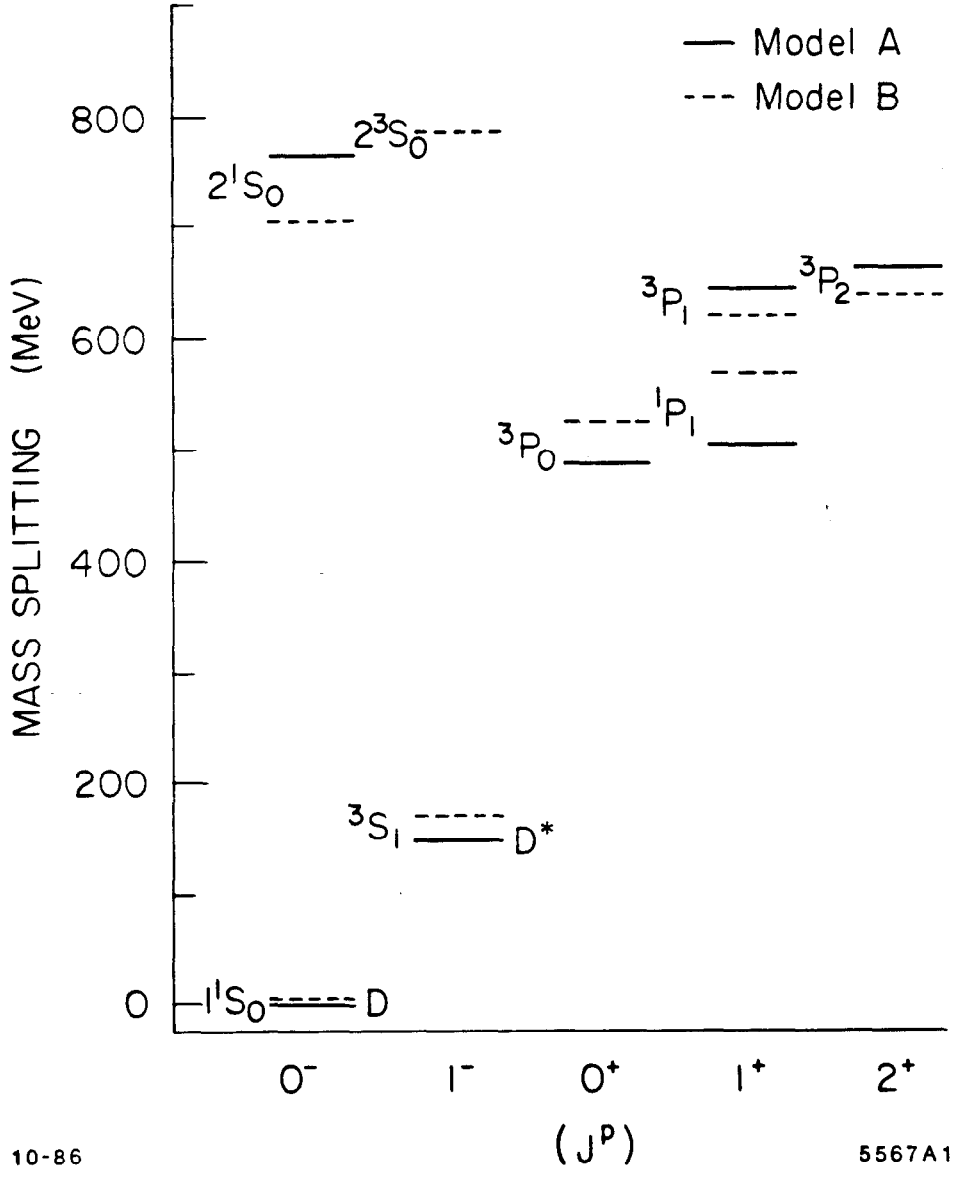

FIG. 20. Expected states for D and D_s mesons. Model A from Eichten *et al.*, Model B from Godfrey and Isgur, Ref [41].

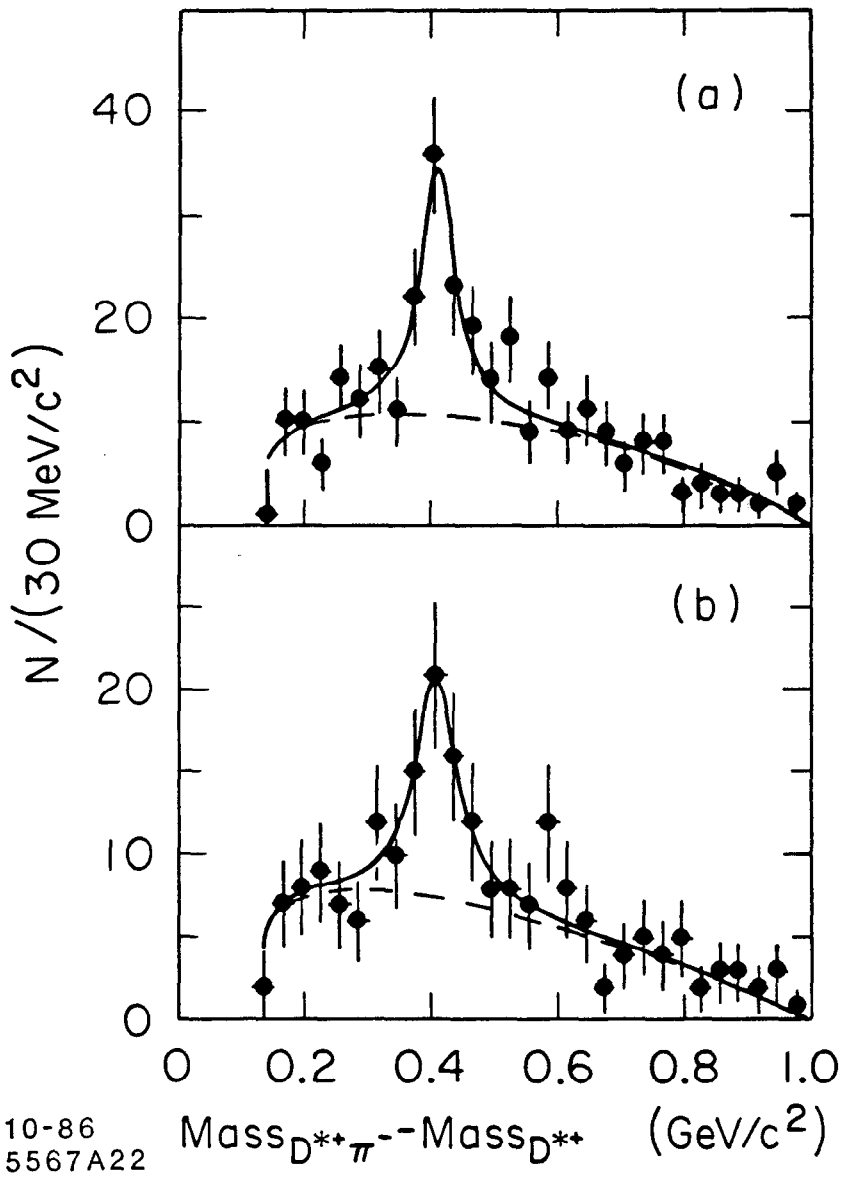

FIG. 21. D^{**0} candidate from Albrecht et al., Ref. [42].

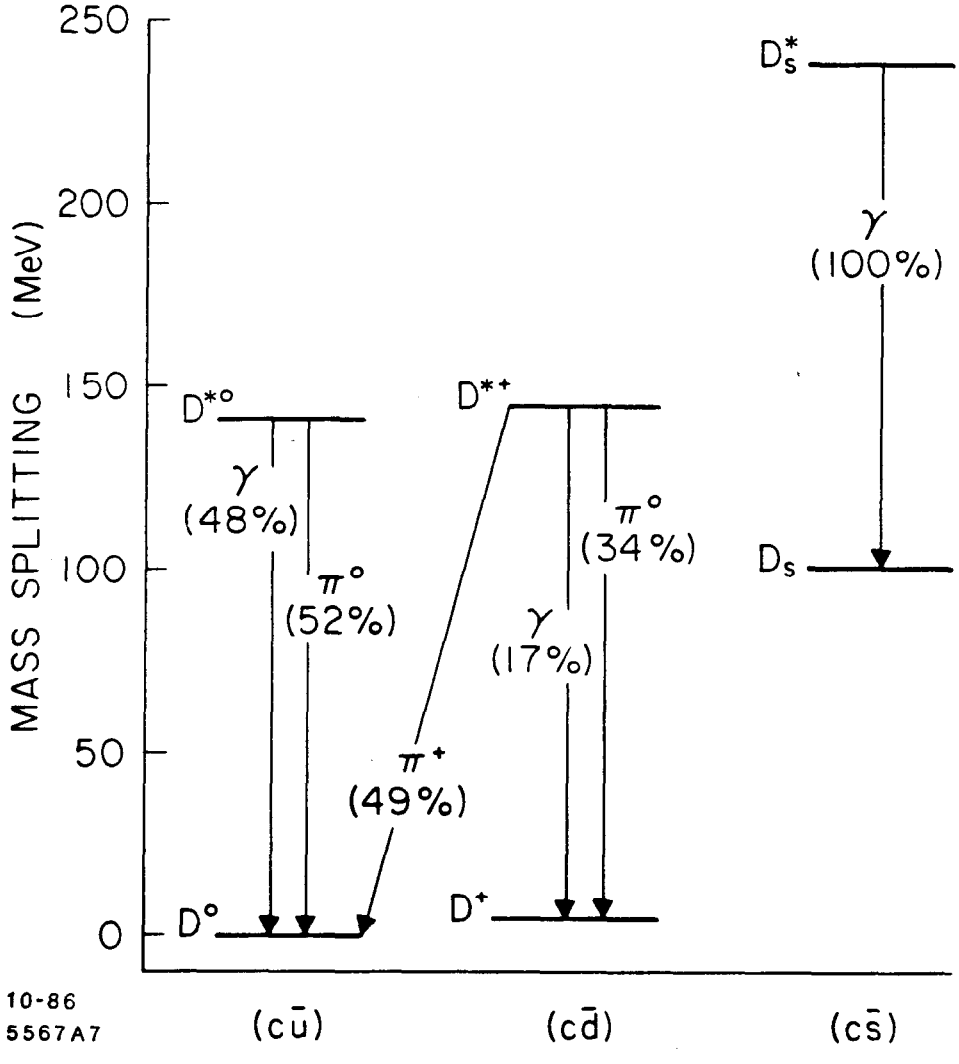

FIG. 22. Transitions of the lowest lying charmed vector mesons.

Table XVII. Difference in $(\text{Mass})^2$ for Pseudoscalar and Vector Mesons.[44]

Mesons	$(\text{Mass})^2$ Difference
$\rho - \pi$	0.574
$K^* - K$	0.556
$D^* - D$	0.546
$D_s^* - D_s$	0.55 ± 0.01
$B^* - B$	0.55 ± 0.05

The lowest-lying charmed orbitally excited states are at sufficiently high masses to allow the possibility of strong π decays to both the ground states and the vector states from the $^1P_1$, $^3P_1$, and $^3P_2$ states. Parity conservation in the strong decay allows the $^3P_0$ to decay only to the ground state, through single π emission. Widths of 50 to 100 MeV/c^2 are expected for all these decays, making it difficult to distinguish the multiplet of states whose mass splitting should be comparable. Mixing between the singlet and triplet J=1 states may further complicate the picture. Multipion and other strong decays are also likely to occur for these states when energetically allowed. At present, the only candidate for one or more of these 1^+ or 2^+ states is the 70 MeV/c^2 wide resonance $D^{**0}(2420)$, decaying to $D^{*+}\pi^-$.[42] This state appears to play a significant role in charm fragmentation at high energies. One might also expect it to be present in B meson decays.

4. WEAK DECAYS OF CHARM AND BEAUTY MESONS

The following sections encompass the second lecture on heavy quark decays. I concentrate here on the issues surrounding weak hadronic and semileptonic decays of charm and beauty mesons. Much of the associated theory and phenomenology is available in these proceedings, in the lectures of F.Gilman, and the article of I.I.Y.Bigi.

4.1 Lifetimes of Charm and Beauty

In the most naive picture of heavy meson decay, all species of charm and beauty mesons have characteristic lifetimes associated with the weak decay of the

heavy quark within the meson:

$$\Gamma_i = \frac{G_F^2 M_Q{}^5}{192\pi^3} \times \frac{Weak\ Mixing}{Angles} \times \frac{QCD}{Factors} \tag{5}$$

$$\Gamma_{tot} = \frac{1}{\tau} = \Sigma\ \Gamma_i\ .$$

Here, the index i refers to any of the final states of the $W^{\pm}$ decay (see Fig. 23), and light quark masses are ignored.

The first evidence for differing lifetimes between charm meson species came from the semileptonic decays. The most recent and precise values available are shown in Table XVIII:

Table XVIII.
Semielectronic Branching Ratios[45]

Meson	$B_l(\%)$
D^0	$7.5 \pm 1.1 \pm 0.4$
D^+	$17.0 \pm 1.9 \pm 0.7$
D_s	unmeasured

If one assumes isospin symmetry for the semileptonic decays and that the Cabibbo suppressed decay widths are small, then a relation between the semileptonic branching ratios and the lifetimes of the charged and neutral mesons exist:

$$\frac{\tau^+}{\tau^0} = \frac{\Gamma_0}{\Gamma_+} = \frac{\Gamma_+^{SL}}{\Gamma_+^{TOT}} \Big/ \frac{\Gamma_0^{SL}}{\Gamma_0^{TOT}} = \frac{Br(D^+ \to l^+ + X)}{Br(D^0 \to l^+ + X)}\ . \tag{6}$$

The experimental results are summarized in Table XIX:

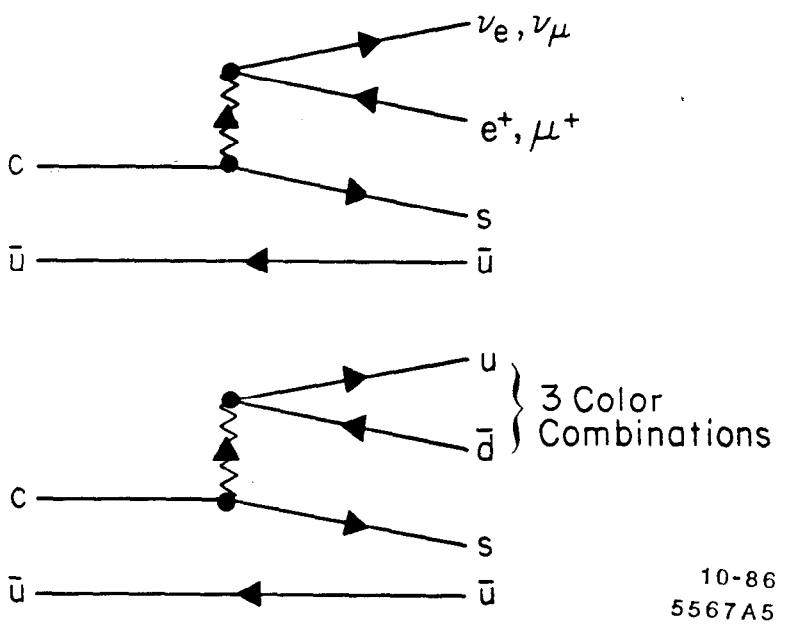

FIG. 23. Spectator model for heavy quark decays.

Table XIX. Lifetime Ratios Through Semileptonic Decays[46] [47] [45] [48]

Quark System	Experiment	Lifetime Ratio $(\frac{\tau^+}{\tau^0})$
Charm	DELCO	≥ 4.3 *at* 90% C.L.
Charm	MARK II	$3.1^{+4.2}_{-1.4}$
Charm	MARKIII	$2.3^{+0.5}_{-0.4} \pm 0.1$
Beauty	CLEO	$2.3 \geq \frac{\tau^+}{\tau^0} \geq 0.49$

The measurements of MARK II and MARK III are *direct*, using events where one charmed particle is *tagged* in a hadronic decay thus separating charged and neutral mesons while the other decays semileptonically. The DELCO and CLEO results are not direct, as they count single and double leptons inclusively, and rely on knowing the fraction of charged and neutral mesons initially produced. Furthermore, as the mass of the quark increases, corrections for complex final states and cascades through lighter flavors and baryons make the semileptonic branching ratio determination more difficult and model dependent, even near the threshold for meson production.

Charmed meson and beauty-hadron lifetimes have also been measured more directly by geometrical techniques relying on the displacement of their decay vertex from the production vertex. In going from momenta of 1 to 10 GeV/c the decay length (λ) for a D meson changes from $\sim$ 170 to 750 μm while for a B meson it goes from $\sim$150 to 360 μm. Two general strategies are in use. The *visual* techniques of bubble chambers, silicon strip detectors, and emulsions, and the primarily *collider*-based precision drift chamber technique. The visual techniques measure the decay length directly, having measurement errors $\delta\lambda << \lambda$. These devices are employable in fixed target experiments, where momenta in the lab are high, making multiple scattering effects less important.

The collider techniques rely on multiple measurements, each with $\delta\lambda >> \lambda$, to achieve a statistical estimate of the decay length. A hybridization of these techniques is now emerging with the proposed use of silicon strip and CCD devices at higher energy colliders where the multiple scattering in these thicker devices poses less of a problem. The collider techniques break down further into two types. The full vertex reconstruction of final state (for example, a D^0 tagged through its

cascade $D^{*+} \rightarrow D^0\pi^+$ with $D^0 \rightarrow K^-\pi^+$), or the statistical measurement of the impact parameter of one of the tagging particles in the decay (for example, the lepton in a semileptonic heavy quark decay). These techniques are described in more detail in other references .[49] An example of the impact parameter technique from CLEO is shown in Fig. 24 . Note the importance of good signal to background. One of the revolutions in such measurements for the charmed mesons has recently occurred with the Fermilab experiment E691 (TPS). This experiment used silicon microstrip detectors just beyond a Be target, and followed by an elaborate spectrometer with good particle identification. The apparatus resided in a 260 GeV/c tagged photon beam, wherein charm production is thought to proceed largely through gamma-gluon fusion. Typical decay lengths are mm to cm, making lifetime measurements rather simple and bias free. The typical mass spectra for charmed meson decays, with their decay length curves, are shown in Fig. 25 . Table XX summarizes the most recent measurements of charm lifetimes.

The averages from this table are largely dominated by E691:

$$\tau_{D^0} = 4.34^{+0.24}_{-0.22} \times 10^{-13}$$

$$\tau_{D^+} = 10.1^{+0.7}_{-0.6} \times 10^{-13}$$

$$\tau_{D_s^+} = 3.5^{+0.8}_{-0.6} \times 10^{-13} \qquad (7)$$

$$\frac{\tau_{D^+}}{\tau_{D^0}} = 2.33 \pm 0.21$$

$$\frac{\tau_{D_s^+}}{\tau_{D^0}} = 0.81 \pm 0.19 \ .$$

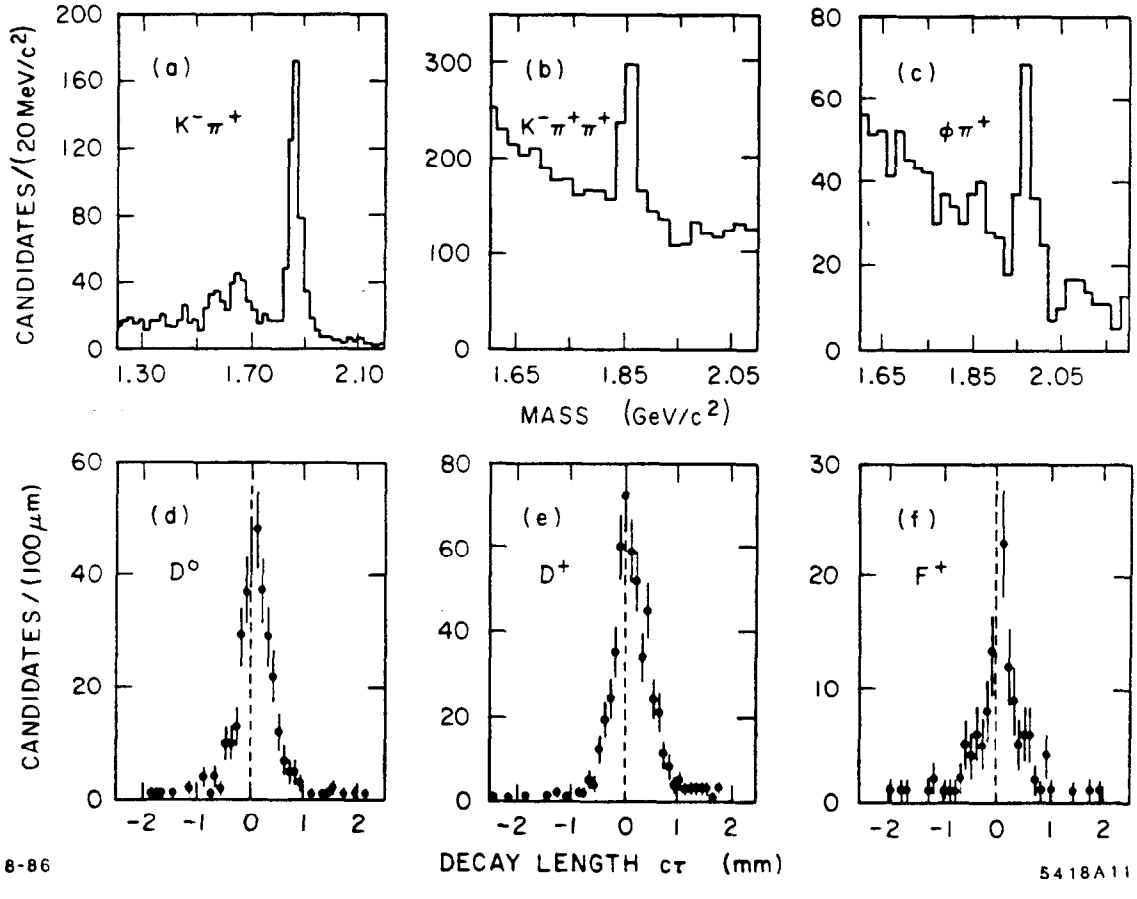

FIG. 24. Impact technique used to measure lifetimes of charmed particles from CLEO.

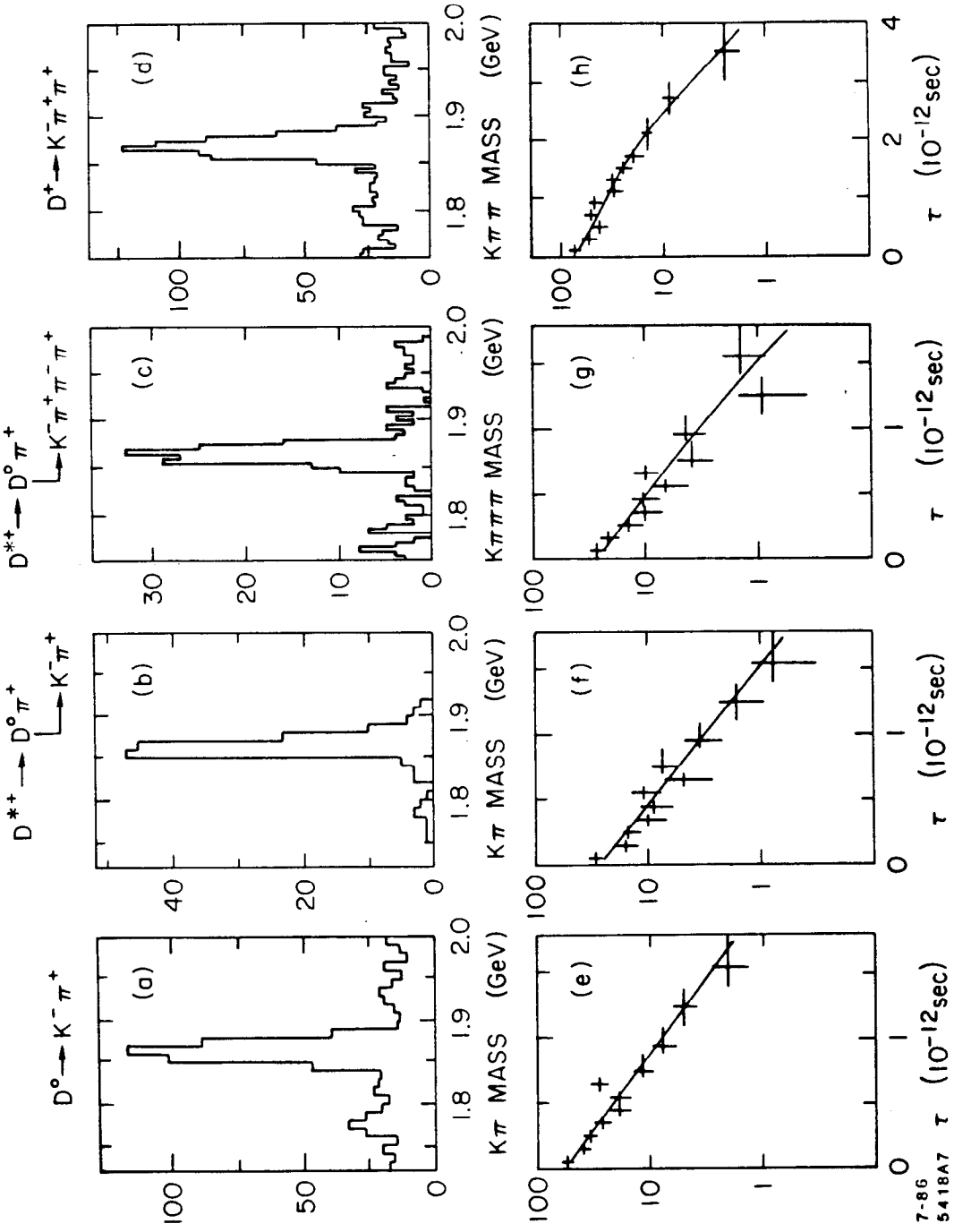

FIG. 25. E691 results for D decays.

Table XX. Summary of Lifetime Measurements†

Expt.	D^0		$D^\pm$		$D_s^\pm$	
E691	672	$4.4 \pm 0.2 \pm 0.2$	480	$10.9 \pm {}^{0.8}_{0.7} \pm 0.6$	35	$4.2 \pm {}^{0.9}_{0.7} \pm 0.6$
CLEO	317	$5.0 \pm 0.7 \pm 0.4$	247	$11.4 \pm 1.6 \pm 1.0$		
DELCO	269	$4.6 \pm 1.5 \pm {}^{0.7}_{0.6}$				
MKII	66	$4.7 \pm {}^{0.9}_{0.8} \pm 0.5$	16	$8.9 \pm {}^{3.8}_{2.7} \pm 1.3$		
E531	58	$4.3 \pm {}^{0.7}_{0.5} \pm {}^{0.1}_{0.2}$	23	$11.1^{+4.4}_{-2.9}$	6	$2.6 \pm {}^{1.6}_{1.1}$
SHF	50	$6.1 \pm 0.9 \pm 0.3$	48	$8.6 \pm 1.3 \pm {}^{0.7}_{0.3}$		
WA58	44	$3.4 \pm {}^{1.2}_{0.8} \pm 0.7$	27	$5.0 \pm {}^{1.5}_{1.0} \pm 1.9$		
NA16	16	$4.1 \pm {}^{1.3}_{0.9}$	15	$8.4 \pm {}^{3.5}_{2.2}$		
NA27	129	$4.2 \pm {}^{0.5}_{0.4}$	147	$10.6 \pm {}^{1.3}_{0.9}$		
NA11	26	$3.7 \pm {}^{1.0}_{0.7} \pm 0.5$	28	$10.6 \pm {}^{3.6}_{2.4} \pm 1.6$	12	$3.1 \pm {}^{1.2}_{0.8}$
TASSO	13	$4.3 \pm {}^{2.0}_{1.4} \pm 0.8$			7	$3.4 \pm {}^{2.9}_{1.6} \pm 0.7$
HRS	53	$4.2 \pm 0.9 \pm 0.6$	114	$8.1 \pm 1.2 \pm 1.6$	13	$3.5 \pm {}^{2.4}_{1.8} \pm 0.9$
NA1	51	$4.3 \pm {}^{1.4}_{0.9}$	98	$9.5 \pm {}^{3.1}_{1.9}$		

† Compiled by V. Lüth, reference 36.

The lifetime ratio evaluated by measuring the individual species is notably close to that obtained by the semileptonic decay ratios of charm in Table XIX, suggesting that the assumptions of Eq. (6) are valid for charmed mesons.

Unlike the D mesons, no individual measurements of B_u or B_d have yet been performed. It is likely[50] that the difference in lifetimes will be less pronounced, owing to the smaller size of the QCD corrections in B-decay. Average measurements of B hadron lifetimes have been made by use of the impact parameter technique on leptons in events that have been topologically selected to be enriched in $b\bar{b}$ quarks. These techniques have been extended to use hadrons from the b-quark fragmentation as well. Table XXI summarizes recent results.[51]

Table XXI. B-Hadron Mean Lifetimes

Experiment	B-hadron Lifetime
JADE	$1.8^{+0.5}_{-0.3} \pm 0.4$
MAC	$1.16^{+0.17}_{-0.17} \pm 0.07$
MKIIa	$0.85^{+0.17}_{-0.17} \pm .21$
MKIIb	$1.25^{+0.26}_{-0.19} \pm .50$
DELCO	$1.17^{+0.27\,+0.17}_{-0.22\,-0.16}$
TASSO	$1.83^{+0.38\,+0.17}_{-0.37\,-0.16}$

The average value is thus $\sim$ 1.2 ps for the B-hadron, a remarkably long lifetime when compared to the naive expectation of Eq. (5), suggesting the severe reduction of the width due to the size of the Kobayashi-Maskawa(KM) parameter. This value along with the average semileptonic branching ratio for B-hadrons can be used to extract limits on the KM matrix elements V_{bu} and V_{bc}.[52] These however rely on the assumptions that B-hadrons all have similar lifetimes and semileptonic branching fractions. The measurements of Table XXI are all at similar energies and thus have similar admixtures of B-hadrons. Measurements of average semileptonic branching ratios have been made both from mixtures of B_u and B_d at the $\Upsilon(4S)$ (determined to $\sim$20%) and from higher energy data containing unknown B-hadron admixtures (where the lifetime measurements were obtained). The results are in rough agreement,[53] and give average semielectronic and semimuonic branching ratios of about $11 \pm 1\%$, thus suggesting that the average lifetime of all species are consistent with one another at this level.

4.2 Patterns of Hadronic and Semileptonic Weak Decays

The remainder of the lecture will concern the hadronic and semileptonic decay measurements of heavy quark systems. Emphasis will be placed on how they can be used to understand the difference in charm lifetimes as well as predict the size of effects in the B meson system.

4.2.1 Contributions to charm and beauty meson widths.

The tree level diagrams thought to contribute to heavy meson decays are summarized in Fig. 26 . Both charm and beauty have principle decays through the

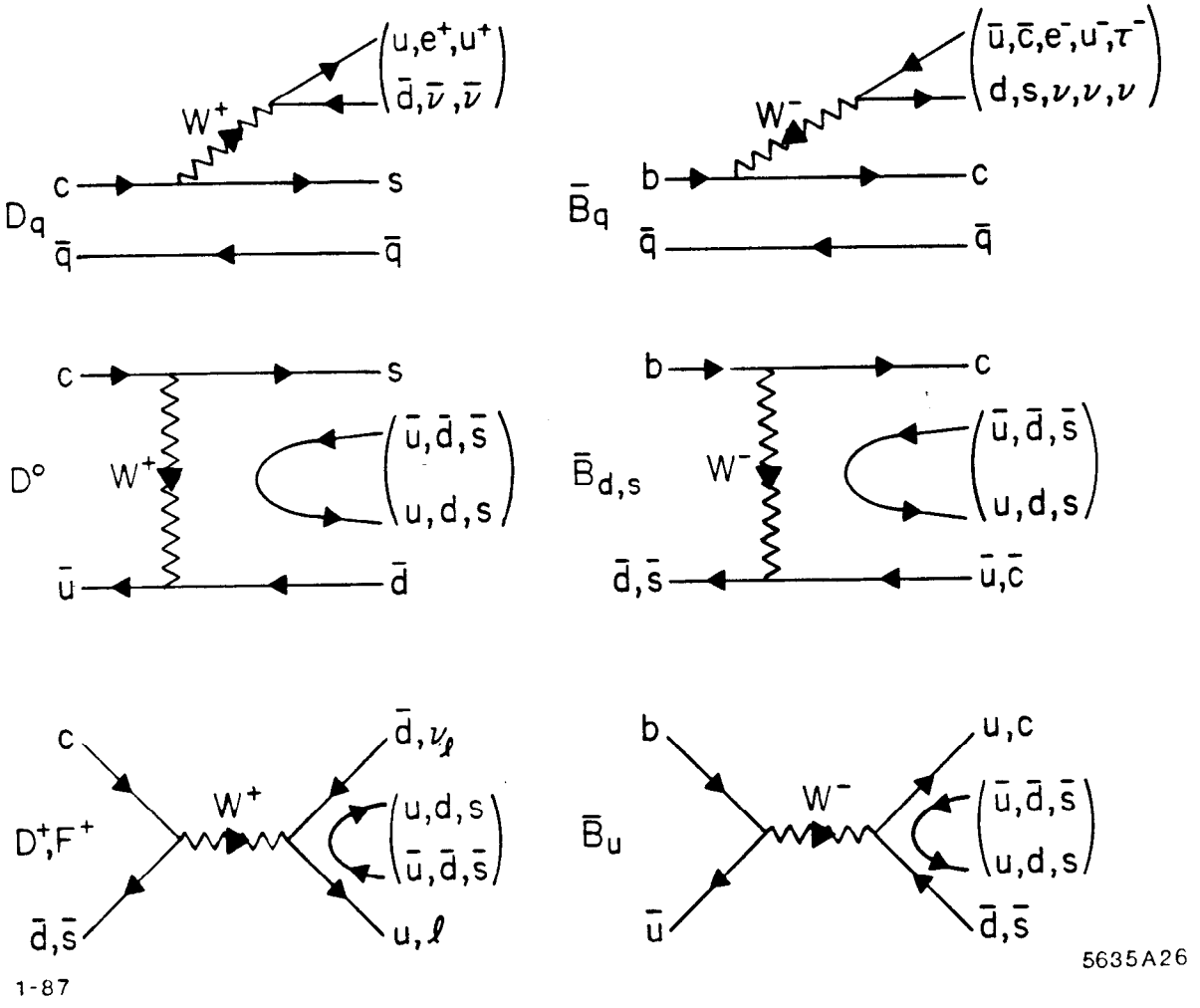

FIG. 26. Principle diagrams leading to charm and beauty meson decays.

so-called spectator graphs. In the spectator diagram, the light quark of the meson is passive. The D meson and B meson decay is similar, except that additional channels for $\bar{B} \rightarrow \tau^- X$ and $\bar{B} \rightarrow c\bar{q}(\bar{c}s)$ are possible. This naive model would predict semileptonic branching fractions of about 20% for charm and 17% for beauty.

The QCD corrections to the non-leptonic decays modify Eq. (5), and account for hard gluon exchanges among the quarks:

$$\Gamma_i = \frac{G_F^2 {M_Q}^5}{192\pi^3} \times \left\{ \begin{matrix} Weak\ Mixing \\ Angles \end{matrix} \right\} \times \frac{2c_+^2 + c_-^2}{3} . \qquad (8)$$

Here, c_+ and c_- are the so called Wilson Coefficients. They are manifestly a function of the strong coupling constant (α_s) and are hence a function of the mass scale of the interaction. The two coefficients are not independent, being related through the expression $c_- = \sqrt{1/c_+}$. The dependence of the coefficients on the mass scale are indicated in Fig. 27 . At infinite masses, or equivalently in the regime of free-quarks, the coefficients go towards unity, recovering Eq. (5). At lower masses, the effect is to enhance the nonleptonic contribution, and thus diminish the semileptonic width. It has been shown that the coefficients, when calculated to next order, continue to move in this direction, although the enhancement appears to diminish (see Fig. 27). For the charm system $c_- \approx 2.3$ while for the beauty system $c_- \approx 1.6$.

The effect of this nonleptonic enhancement on the semileptonic branching fraction (B_l) is shown schematically in Fig. 28 . It is calculated from the simple expression:

$$Br(c \rightarrow e + X) = \frac{1}{2 + 2c_+^2 + c_-^2} \qquad (9)$$

Here, the 2 in the denominator comes from equal contributions from semileptonic muon and electron contributions. At the tree level in B-decay the $b \rightarrow c\tau_-\nu_\tau$ also contributes in the denominator, as do $b \rightarrow c\bar{c}s$ transitions, modifying this slightly. The effect is small because of limited phase space. For charm, the nominal ratio of c_-/c_+ is about 3, while for beauty it is somewhat lower (~2); for top mesons, it would approach unity. These values lead to semileptonic branching fractions being reduced to about 14% for charm, and about 15% for beauty, *without regard to the flavor of the spectator quark.*

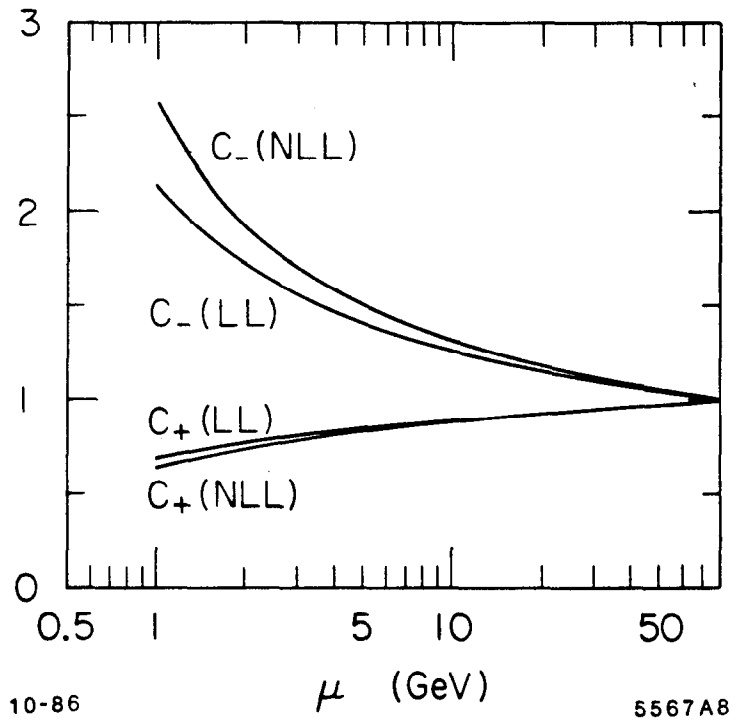

FIG. 27. The Q^2 dependence of the Wilson coefficients in leading and next-to-leading log approximation. The calculation is only up through the charm-flavor.

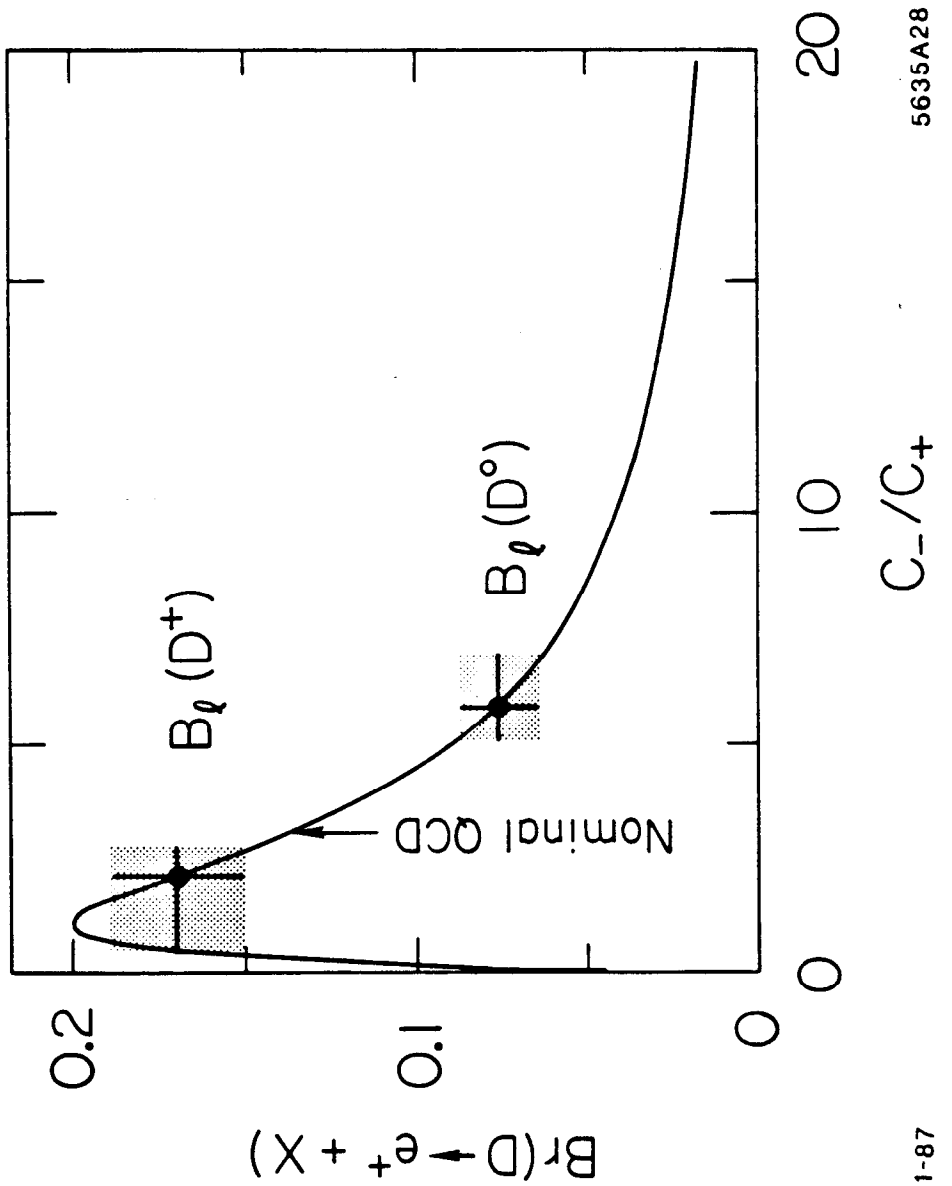

FIG. 28. The semileptonic branching fraction for charm versus the ratio of coefficients c_-/c_+.

These crude estimates when view along with the data are however very enlightening and point to the need for a more sophisticated treatment of the problem. First, they predict average values of B_l which disagree with average values from experiments (about 11% for charm and beauty both). Second, they do not account for the difference between D^0 and D^+ semileptonic branching fractions, nor will they do so when the difference between B_u and B_d is actually measured. To understand the difference, it is necessary to look at differences which might arise in the weak hadronic sector. Two principle mechanisms have been proposed to understand the observed differences in hadronic widths between the D^0 and the D^+ . These are W-exchange or W-annihilation, and Pauli interference, both operative in the charm and beauty system. These mechanisms are depicted in Fig. 29 and Fig. 30 .

4.2.2 Weak flavor annihilation.

The most direct way to enhance the D^0, the D_s , or the B^0 is to add additional diagrams denoted as W-exchange and W-annihilation, respectively.[54] The W-annihilation graph is also present for Cabibbo-suppressed D^+ and B^+ decays. These graphs historically have been ignored because at the quark level they are helicity suppressed ($\propto \frac{M_q^2}{M_c^2}$) and require a large wavefunction overlap of initial state quarks ($\propto \frac{f_D^2}{M_c^2}$, $\propto \frac{f_{D_s}^2}{M_c^2}$ or $\propto \frac{f_B^2}{M_b^2}$):

$$\Gamma_{EXCH}^D = \frac{G_F^2}{8\pi}(m_{q_1}^2 + m_{q_2}^2) M_D f_D^2 \frac{(2c_+ - c_-)^2}{3} ,$$

$$\Gamma_{ANN}^D = \frac{G_F^2}{8\pi}(m_{q_1}^2 + m_{q_2}^2) M_D f_D^2 \frac{(2c_+ + c_-)^2}{3} sin^2(\theta_c) .$$

It has been argued that the helicity suppression may be removed by the presence of gluons in the meson wavefunction,[55] or by the radiation of gluons from the light quark vertex.[56] The former is largely a non-perturbative effect, the latter, perturbative. This leaves the wavefunction overlap factor which is expected to be small owing to the small values ($\sim$ 150 MeV/c) of f_D , f_{D_s} and f_B.[57]

Recent work[58] suggests that a dynamical mechanism such as the presence of a resonance with quantum numbers equal to that of a $\bar{K}$ and mass close to the D^0, could also enhance the annihilation contribution to charm decays. Such a

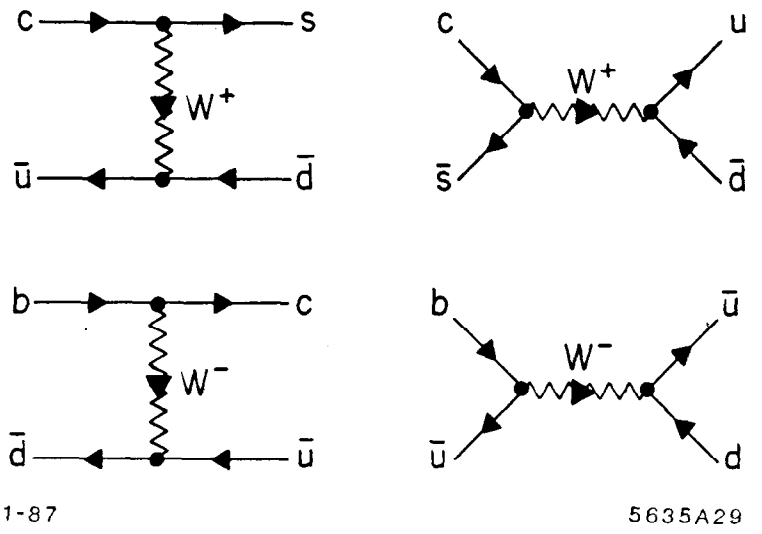

FIG. 29. W-exchange and W-annihilation in D and B decays.

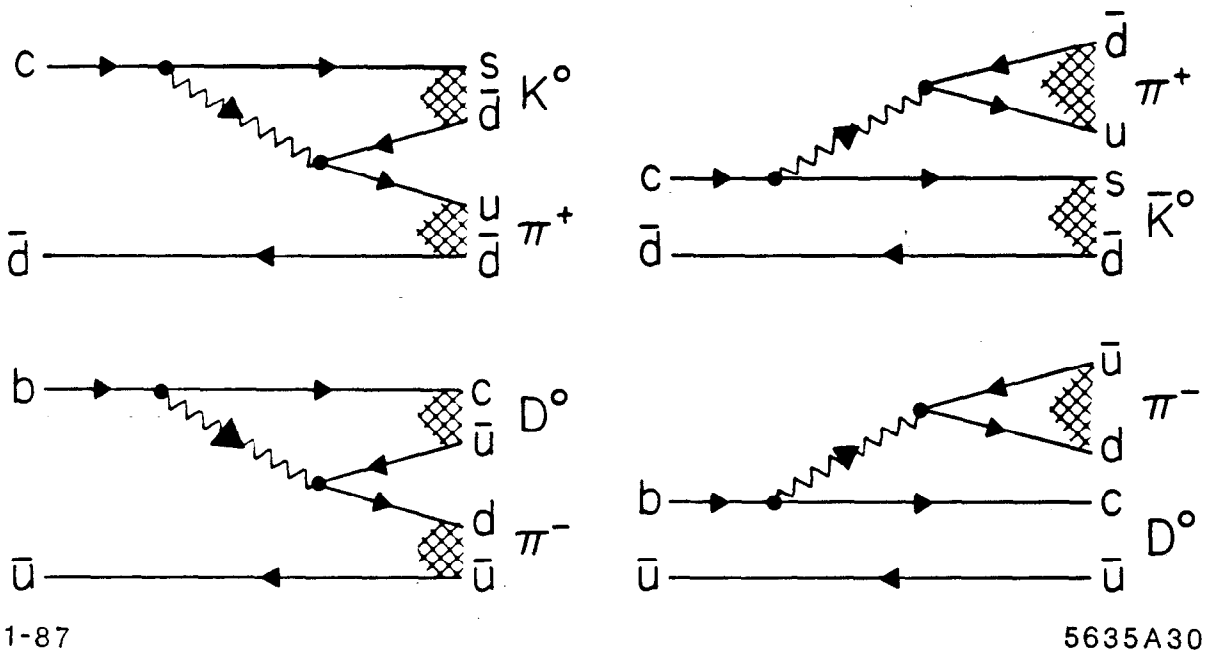

FIG. 30. Pauli interference in B and D decay.

mechanism is unlikely to be present for B mesons, as their higher masses place them out of the light quark resonance region.

Experimentally, certain decays of the D^0, such as $D^0 \rightarrow \bar{K}^0\phi, \bar{K}^0K^0$, and $\bar{K}^0K^{*0}$, should be clear signatures for W-exchange.[59] Here, the $\bar{u}$ quark of the initial state is absent in the final state meson. For the D_s meson, final states with no net strangeness and no $s\bar{s}$ content (such as $\rho\pi$), would be characteristic of W-annihilation. Recent work[60][61] however has suggested that rescattering effects, or non-planar diagrams (see Fig. 31) may lead to final states that mimic the non-spectator decays. Flavor annihilation $\bar{u} \rightarrow \bar{d}$ occurs through the strong interaction, rather than the weak one. The possibility of rescattering being significant is increased when the channels through which rescattering is to occur, are themselves many times larger than the final states in question. The situation will remain unresolved until there is a substantial increase in the world data.[62][63]

4.2.3 Pauli interference.

The D^+ and B_u can receive enhancement in its Cabibbo-suppressed decays through W-annihilation diagrams with the caveats of the previous sections. More importantly, the leading D^+ and B_u Cabibbo-allowed decays may be suppressed by cancellation of final state amplitudes in the presence of strong *color clustering* and QCD sextet enhancement.[64] Figure 30 indicates how color clustering leads to identical final state amplitudes which interfere in the D^+ due to the relative minus sign. To the extent that the coefficient $c_- >> c_+$, a cancellation can occur for pseudoscalar-pseudoscalar decays, while pseudoscalar-vector decays may be enhanced.[65]

The interference can also arise in charm (beauty) decays at the quark level, before hadronization, from the presence of two identical $\bar{d}(u)$ quarks in the final state. In the case of charm, for example, the D^+ width then receives an extra term:[66]

$$\Gamma^{int}(D^+) = -(c_-^2 - 2c_+^2)\frac{12\pi^2}{M_D{}^2} f_D^2 \Gamma_0 \ . \qquad (10)$$

This term is negative for $c_- >> c_+$. More detailed calculations (e.g. potential and bag models) show that the effect of interference in charm decays ranges from a few percent to as large as $\approx 50\%$ and may thus account for much of the D^0 and

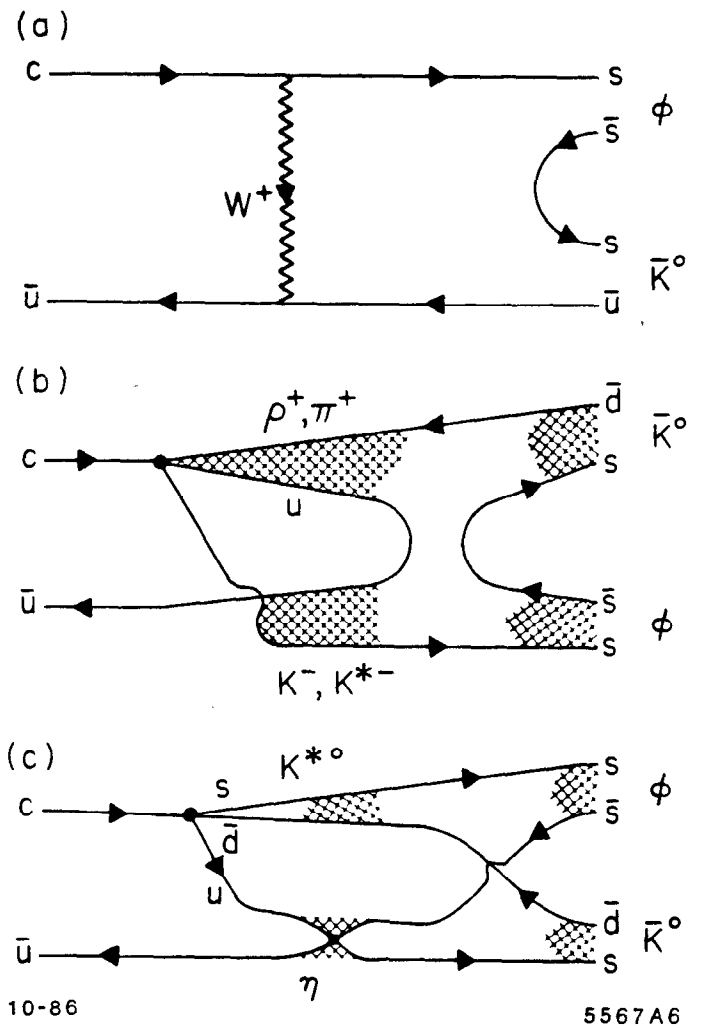

FIG. 31. (a) W-exchange leading to $\bar{K}^0\phi$, and (b)-(c) Non-planar diagrams simulating the same D^0 W-exchange final state.

D^+ lifetime difference.[67] The effect in the B system should be present but smaller owing to the larger mass and slightly smaller value of c_-.

4.2.4 Color suppression and the role of gluons

One final effect that is of theoretical interest, is the role that soft, non-perturbatively treated gluons may play in heavy meson decay. The next-to-leading-log calculation[68] of additional gluons leads to corrections which are small (see Fig. 27). Soft, non-perturbative gluons may however play an important role as pointed out in Section 4.2.2 controlling the degree of W-exchange and W-annihilation as well as the overall level of nonleptonic enhancement. Early attempts to calculate hadronic matrix elements[69] led to predictions which were very sensitive to the QCD corrections. An example of the calculation of the ratio of $\Gamma(D^0 \rightarrow \bar{K}^0\pi^0)\ \Gamma(D^0 \rightarrow K^-\pi^+)$ is shown in Fig. 32 , where a very sharp minimum is seen close to the nominal QCD values for c_-/c_+. This has been frequently referred to as *color suppression*, and would occur in a similar fashion for decays like $D^0 \rightarrow \bar{K}^{*0}\pi^0$, $D^+ \rightarrow \phi\pi^+$ and $B^0 \rightarrow \bar{K}^0\psi$. The origin of the effect is seen in Fig. 33 where the color matching naively reduces amplitude (a) by 3 relative to amplitude (b). Isospin accounts for a factor of $1/\sqrt{(2)}$ and QCD further reduces the relative rate to as little as $\sim 1/40$.

A naive way to reduce color suppression, is to evaluate the Wilson coefficients at a smaller mass scale, such that c_-/c_+ is considerably greater. In essence, this approach can be interpreted as an attempt to increase the non-perturbative contributions beyond the QCD expectation. While this is an ad-hoc approach, it simultaneously reduces the theoretical estimate of the semileptonic branching ratios for D^0 and D^+ , leaving at least the D^0 closer to experiment.

Recent work in calculating hadronic matrix elements has removed the singularities associated with color matching, through the introduction of an additional parameter (ξ) the so-called color screening parameter.[70] This parameter has some phenomenological basis, being related to the QCD 1/N expansion[71] (N is the number of colors). Fitting of data (described in the following sections) yields a value of $\xi \approx 0$ instead of the naive 1/3. This relaxes color suppression in all channels and provides a reasonably good description of the data.[72]

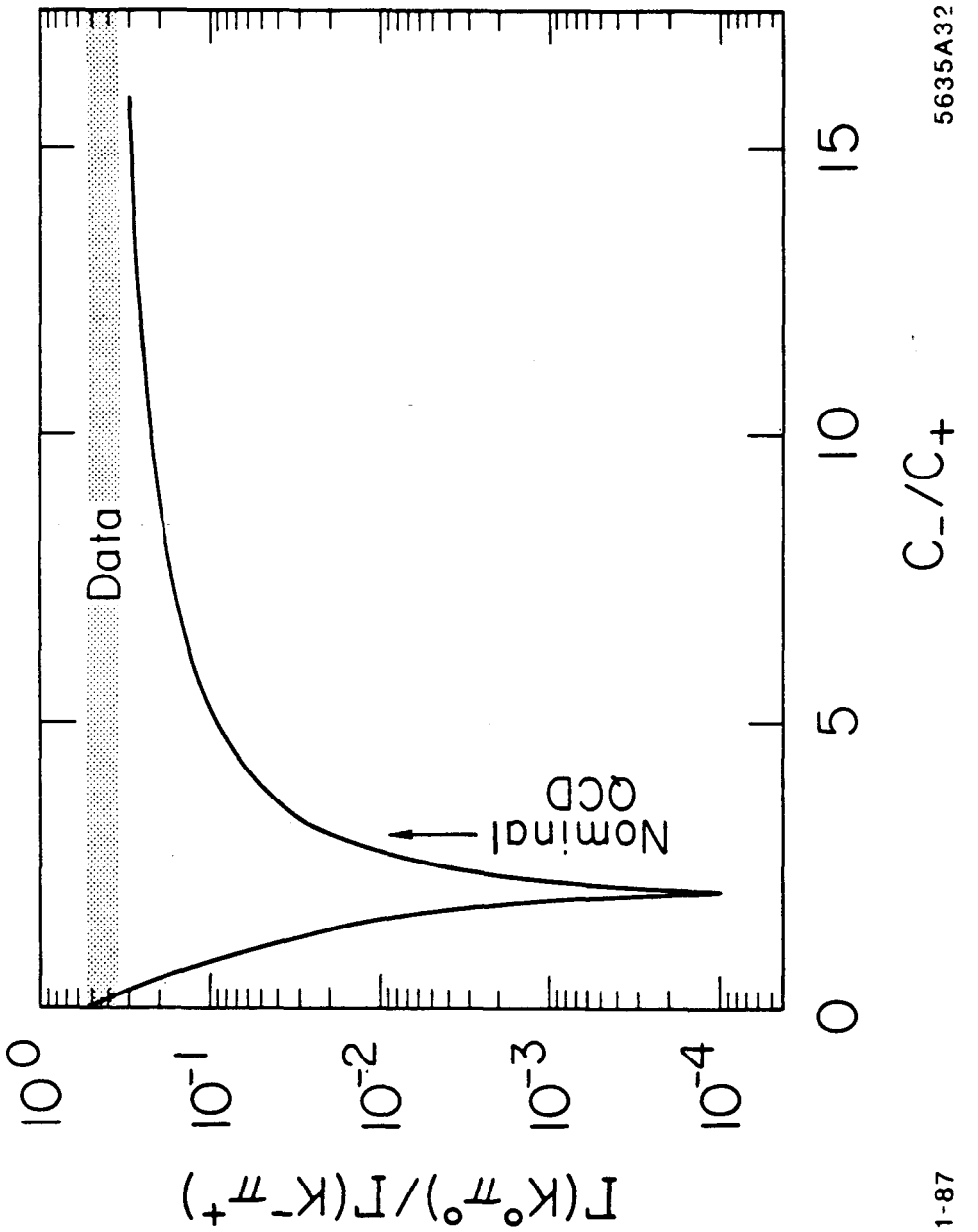

FIG. 32. Prediction for the ratio of $D^0 \to \bar{K}^0\pi^0$ to $D^0 \to K^-\pi^+$.

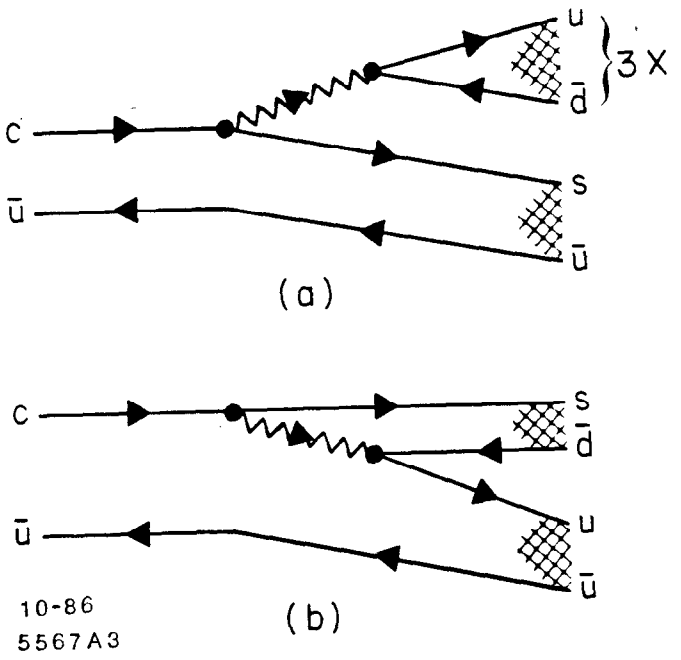

FIG. 33. Origin of color suppression in the spectator model.

4.3 Data on Charmed Meson Decays

A significant fraction of the Cabibbo-allowed and Cabibbo-suppressed decays of D^0 and D^+ have now been measured. The bulk of the information comes from e^+e^- storage ring experiments at the $\psi(3770)$ resonance. Working at slightly higher energies, information on D_s decays has been obtained. Some more recent measurements are coming out high energy machines like CESR, PEP and PETRA, where the extra Lorentz boost improves detection efficiencies.

This was instrumental in the discovery of the D_s and certain rare D^0 decays, and the measurements of the D_s lifetime. Finally, new data is expected in the near future from the photoproduction experiment E691, which may serve to "close the book" on many (but probably not all) the issues of charmed D and D_s decay.

4.3.1 Data on hadronic decays of charmed D^0 ,D^+ and D_s

Let us first summarize the experimental data available now on charmed meson rates.[73] [74] [75] [76] [77] Table XXII summarizes the Cabibbo-allowed decays of the D^0 and D^+ with their production cross section times branching ratio $(\sigma \cdot B)$ at the $\psi(3770)$ from the major experiments.

Table XXII. Cabibbo-Allowed Decays of D Mesons
$\sigma \cdot Br$(nb) at $\sqrt{(s)} = 3.77$ GeV

Decay Channel	MARK III[75,76,77]	MARK II[74]	LGW[73]
$D^0 \to K^-\pi^+$	$0.25 \pm 0.01 \pm 0.01$	0.24 ± 0.02	0.25 ± 0.05
$\bar{K}^0\pi^0$	$0.11 \pm 0.02 \pm 0.01$	0.18 ± 0.08	-
$\bar{K}^0\eta$	$0.09 \pm 0.04 \pm 0.01$	-	-
$\bar{K}^0\omega$	$0.19 \pm 0.07 \pm 0.05$	-	-
$\bar{K}^0\phi$	$0.05^{+0.03+0.02}_{-0.02-0.01}$	-	-
$K^-\pi^+\pi^0$	$0.76 \pm 0.04 \pm 0.08$	0.68 ± 0.23	1.4 ± 0.6
$\bar{K}^0\pi^+\pi^-$	$0.37 \pm 0.03 \pm 0.03$	0.30 ± 0.08	0.46 ± 0.12
$\bar{K}^0K^+K^-$	$0.05^{+0.02+0.01}_{-0.01-0.01}$	-	-
$K^-\pi^+\pi^+\pi^-$	$0.53 \pm 0.03 \pm 0.05$	0.68 ± 0.11	0.36 ± 0.11
$\bar{K}^0\pi^+\pi^-\pi^0$	$0.67 \pm 0.11 \pm 0.15$	-	-
$D^+ \to \bar{K}^0\pi^+$	$0.14 \pm 0.01 \pm 0.01$	0.14 ± 0.03	0.14 ± 0.05
$K^-\pi^+\pi^+$	$0.39 \pm 0.01 \pm 0.03$	0.38 ± 0.05	0.36 ± 0.06
$\bar{K}^0\pi^+\pi^0$	$0.42 \pm 0.08 \pm 0.08$	0.78 ± 0.48	-
$\bar{K}^0\pi^+\pi^+\pi^-$	$0.31 \pm 0.03 \pm 0.03$	0.51 ± 0.18	-
$K^-\pi^+\pi^+\pi^0$	$0.18 \pm 0.04 \pm 0.04$	-	-
$K^-\pi^+\pi^+\pi^-\pi^+$	-	≤ 0.23 at 90% CL	-

Detailed measurements of the psuedoscalar vector decays of the D mesons are summarized in Table XXIII.[76] [78] It is seen from the table the predominence of quasi two-body decays of the D^0 and D^+ .

Table XXIII. Pseudoscalar-Vector Content of the Three-body Cabibbo-Allowed Modes†
$\sigma \cdot Br$(nb) at $\sqrt{(s)} = 3.77$ GeV[78] [76]

Channel	Fraction(%)	σ·Br(nb)
$D^0 \to K^-\pi^+\pi^0$		
$K^-\rho^+$	$74.0 \pm 4.6 \pm 5.0$	$0.56 \pm 0.05 \pm 0.07$
$K^{*-}\pi^+$	$12.9 \pm 2.7 \pm 2.0$	$0.30 \pm 0.06 \pm 0.06$
$\bar{K}^{*0}\pi^0$	$7.6 \pm 3.3 \pm 2.0$	$0.09 \pm 0.04 \pm 0.03$
nonresonant	$5.5 \pm 4.4 \pm 3.0$	$0.04 \pm 0.03 \pm 0.02$
$D^0 \to \bar{K}^0\pi^+\pi^-$		
$\bar{K}^0\rho^0$	$16.8 \pm 5.3 \pm 2.5$	$0.06 \pm 0.02 \pm 0.01$
$K^{*-}\pi^+$	$63.9 \pm 7.6 \pm 4.5$	$0.36 \pm 0.05 \pm 0.04$
nonresonant	$19.3 \pm 8.6 \pm 3.5$	$0.07 \pm 0.03 \pm 0.01$
$D^+ \to \bar{K}^0\pi^+\pi^0$		
$\bar{K}^0\rho^+$	$86.5 \pm 9.1 \pm 5.0$	$0.37 \pm 0.08 \pm 0.07$
$K^{*0}\pi^+$	$7.0 \pm 4.3 \pm 4.0$	$0.09 \pm 0.06 \pm 0.06$
nonresonant	$6.5 \pm 5.5 \pm 4.0$	$0.03 \pm 0.02 \pm 0.02$

† These results are preliminary.

Finally, Table XXIV contains information of the magnitude of many Cabibbo-forbidden decays. The ratios are quoted here to reduce systematic errors and thus allow more precise comparison with theoretical models.

Table XXIV. Cabibbo-Suppressed Decays of D Mesons
Relative Rates and Br(%) [77] [79] [80]

Decay Channel	Ratio
D^0 Decays	
$\frac{\Gamma(\pi^-\pi^+)}{\Gamma(K^-\pi^+)}$	$0.033 \pm 0.010 \pm 0.006$
$\frac{\Gamma(K^-K^+)}{\Gamma(K^-\pi^+)}$	$0.122 \pm 0.018 \pm 0.012$
$\frac{\Gamma(\bar{K}^0K^0)}{\Gamma(K^-\pi^+)}$	≤ 0.11 *at* 90% *C.L.*
$\frac{\Gamma(\bar{K}^{*0}K^0+cc)}{\Gamma(K^{*-}\pi^+)+\Gamma(K^-\rho^+)}$	≤ 0.034 *at* 90% *C.L.*
$\frac{\Gamma(\bar{K}^{*-}K^++cc)}{\Gamma(K^{*-}\pi^+)+\Gamma(K^-\rho^+)}$	0.05 ± 0.03
$\frac{\Gamma(\pi^-\pi^+\pi^0)}{\Gamma(D^0\rightarrow all)}$	$0.011 \pm 0.004 \pm 0.002$
$\frac{\Gamma(\pi^-\pi^+\pi^+\pi^-)}{\Gamma(D^0\rightarrow all)}$	$0.015 \pm 0.006 \pm 0.002$
D^+ Decays	
$\frac{\Gamma(\bar{K}^0K^+)}{\Gamma(\bar{K}^0\pi^+)}$	$0.317 \pm 0.086 \pm 0.048$
$\frac{\Gamma(\pi^+\pi^0)}{\Gamma(\bar{K}^0\pi^+)}$	≤ 0.15 *at* 90%*C.L.*
$\frac{\Gamma(\pi^-\pi^+\pi^+)}{\Gamma(K^-\pi^+\pi^+)}$	$0.042 \pm 0.016 \pm 0.010$
$\frac{\Gamma(K^-K^+\pi^+)}{\Gamma(K^-\pi^+\pi^+)}$	$0.059 \pm 0.026 \pm 0.009$
$\frac{\Gamma(\phi\pi^+)}{\Gamma(K^-\pi^+\pi^+)}$	$0.084 \pm 0.021 \pm 0.011$
$\frac{\Gamma(K^{*0}K^+)}{\Gamma(K^-\pi^+\pi^+)}$	$0.048 \pm 0.021 \pm 0.011$

Very little data on D_s decays is available; In Table XXV are listed the observed decays of the D_s from both hadroproduction and e^+e^- experiments.[81][40][82][83]

Table XXV. Decays of the D_s Mesons[40][81][82][83]
((†) indicates a preliminary result)

Experiment	$\sqrt{(s)}$ (GeV)	Beam	Channel	Mass (MeV/c^2)
CLEO	10	e^+e^-	$\phi\pi^+$	$1970 \pm 5 \pm 5$
TASSO	14-25	e^+e^-	$\phi\pi^+$	$1975 \pm 9 \pm 10$
ARGUS	10	e^+e^-	$\phi\pi^+$	$1973 \pm 3 \pm 3$
ARGUS	10	e^+e^-	$\phi\pi^+\pi^-\pi^+$	$1976 \pm 5 \pm 3$
TPC	29	e^+e^-	$K^-K^+\pi^+$	$1948 \pm 28 \pm 10$
HRS	29	e^+e^-	$\phi\pi^+$	$1963 \pm 3 \pm 3$
ACCMOR	200	$(\pi, N), (K, N)$	$K^-K^+\pi^+$	1975 ± 4
ARGUS	10	e^+e^-	$\bar{K}^{*0}K^+$	*seen*
MARK III	4.14	e^+e^-	$\phi\pi^+$	$1973 \pm 4 \pm 4^\dagger$
MARK III	4.14	e^+e^-	$\bar{K}^{*0}K^+$	*seen*
MARK III	4.14	e^+e^-	$\bar{K}^0K^+$	*seen*
TPS	260	γN	$\phi\pi^+$	*seen*
TPS	260	γN	$\bar{K}^{*0}K^+$	*seen*

4.3.2 Data on semileptonic and pure leptonic D^0 and D^+ decays

In a previous section we have discussed the inclusive semileptonic decays of charm. Recently, a number of new measurements have been made on the pure leptonic and exclusive semileptonic decays of D mesons. First, by use of tagging, it is possible to look at the exclusive decay modes of semileptonic D-decay. These are expected to be dominated by $D \to Kl^+\nu_l$ and $D \to K^*l^+\nu_l$.[84] Table XXVI summarizes these measurements:

Table XXVI. Exclusive Semileptonic Decays

Decay Mode	Events Sig. (Bkd.)	Branching Ratio (%)
$D^0 \to K^- e^+ \nu_e$	47 (2.1)	$3.9^{+0.6}_{-0.6} \pm 0.6$
$D^0 \to K^- \pi^0 e^+ \nu_e$	7 (1.1)	$1.7^{+0.9}_{-0.7} \pm 0.6$
$D^0 \to \bar{K}^0 \pi^- e^+ \nu_e$	9 (0.7)	$2.2^{+0.9}_{-0.7} \pm 0.4$
$D^0 \to \pi^- e^+ \nu_e$	3 (0.9)	$0.4^{+0.4}_{-0.3} \pm 0.1$
$D^0 \to K^- \mu^+ \nu_\mu$	56 (9.4)	$4.1^{+0.7}_{-0.7} \pm 1.2$
$D^0 \to \bar{K}^0 \pi^- \mu^+ \nu_\mu$	20 (8.5)	$2.7^{+1.1}_{-1.0} \pm 1.6$
$D^+ \to \bar{K}^0 e^+ \nu_e$	15 (1.1)	$6.3^{+2.0}_{-1.6} \pm 1.1$
$D^+ \to K^- \pi^+ e^+ \nu_e$	24 (1.2)	$3.9^{+0.9}_{-0.8} \pm 0.7$
$D^+ \to \bar{K}^0 \mu^+ \nu_\mu$	37 (8.9)	$10.2^{+2.2}_{-2.1} \pm 3.6$

One interesting feature of this data is that the D_{l4} decays appear only partially consistent with pure K^*; there being some room in the fit for a non-resonant component. This has been estimated to be about 45% of all $K\pi l\nu_l$,[85] although it is based on a small number of events beyond the K^*, as shown in Fig. 34 .

Another recent (preliminary) measurement is the $Br(D^+ \to \mu^+\nu_\mu)$. This pure leptonic decay is expected at a rate governed by the decay constant f_D. The decay constant may thus be unambiguously measured by observing this decay:

$$\Gamma_{D^+ \to \mu^+\nu} = \frac{{G_F}^2}{8\pi} {f_D}^2 m_D m_\mu^2 |\, V_{cd}\,|^2 (1. - (m_\mu/m_D)^2)^2 \ .$$

The data[86] gives a 90% C.L. upper limit on the branching ratio of 8.4×10^{-4}. Using a D^+ lifetime of $(10.1\ ^{+0.7}_{-0.6}) \times 10^{-13} s$,[87] and $|\, V_{cd}\,|^2 = 0.0506 \pm .0065$,[88]

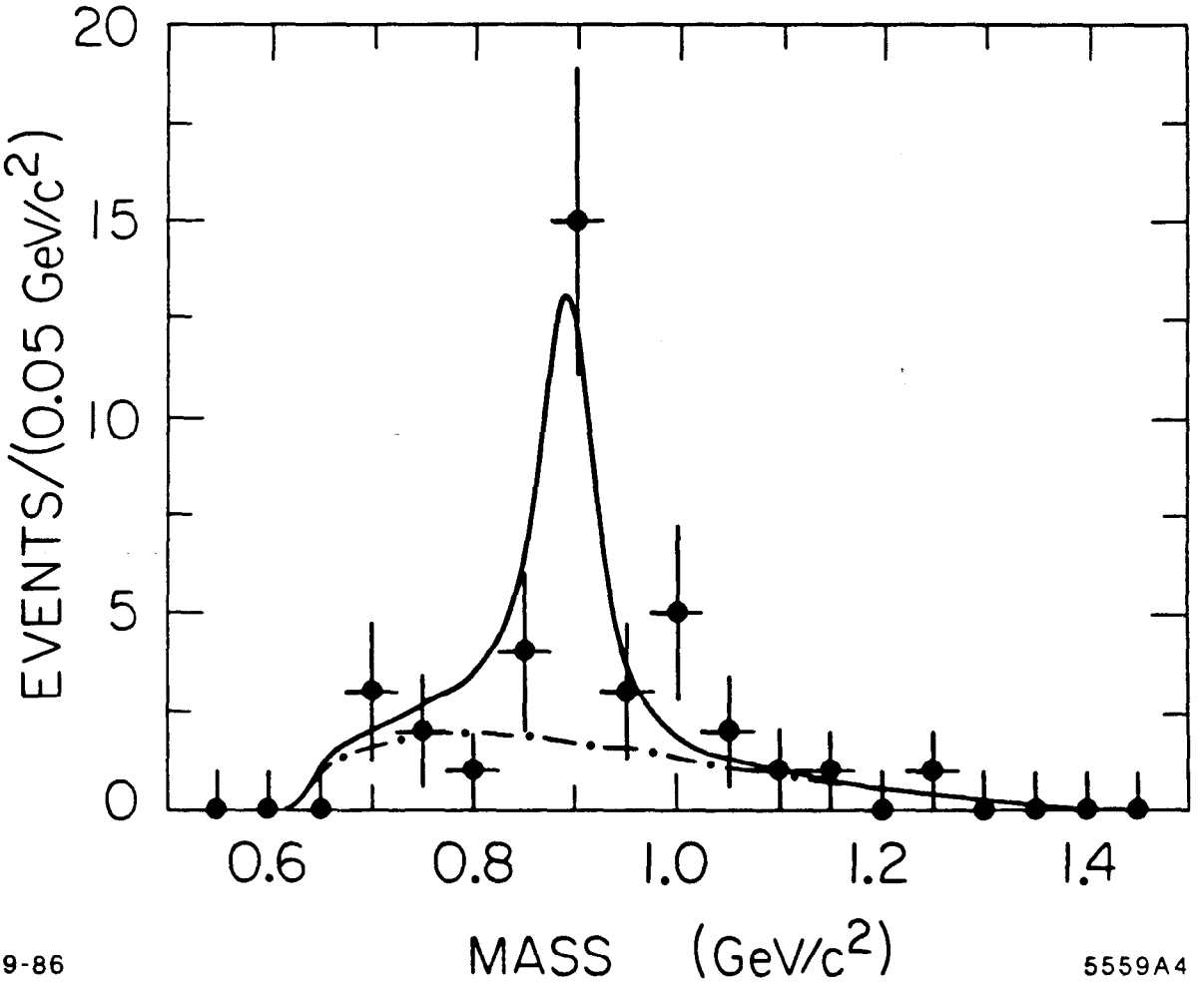

FIG. 34. Fit to $K\pi$ system in D_{e4} decays,[85] indicating the possibility of both K^* and non-resonant contribution ns.

then the 90 % C.L. branching ratio limit corresponds to $f_D = 310$ MeV/c^2. When the errors on τ_{D^+} and $|V_{cd}|^2$ are included, a 90 % C.L. upper limit on f_D of 340 MeV/c^2 is obtained (see Fig. 35).

4.4 Interpretation of the Charm Meson Data

The data on exclusive charm decays is seen to be rather rich, allowing us to address many of the theoretical questions posed in Section 4.2.

4.4.1 Color-suppression.

First we see that color-suppression or color-matching expected from the simplest QCD calculation of hadronic matrix elements appears to be largely absent in both D and D_s decay. From the previous tables we can extract:

$$\frac{\Gamma(D^0 \to \bar{K}^0\pi^0)}{\Gamma(D^0 \to K^-\pi^+)} = 0.45 \pm 0.08 \pm 0.05$$

$$\frac{\Gamma(D^0 \to \bar{K}^{*0}\pi^0)}{\Gamma(D^0 \to K^{*-}\pi^+)} = 0.29 \pm 0.14 \pm 0.09$$

$$\frac{\Gamma(D^0 \to \bar{K}^0\rho^0)}{\Gamma(D^0 \to K^-\rho^+)} = 0.11 \pm 0.04 \pm 0.02$$

$$\frac{\Gamma(D^+ \to \phi\pi^+)}{\Gamma(D^+ \to K^-\pi^+\pi^+)} = 0.08 \pm 0.02 \pm 0.01$$

$$\frac{\Gamma(D_s^+ \to \bar{K}_s^0 K^+)}{\Gamma(D_s^+ \to \phi\pi^+)} = 0.44 \pm 0.12 \pm 0.21$$

In no instance is a significant suppression observed for color mismatched decays. It may be argued that final state interactions may play a significant role in D decays.[89] However, in *all* cases, the suppression expected from the naive spectator model is not present. In particular, since this appears to be true for *both* D^0, D^+, and D_s decays one must seek a common explanation for the effect. It seems unlikely that a conspiracy of final state interactions produces the effect. As noted earlier, the ad-hoc approach of increasing c_-/c_+ would also largely remove

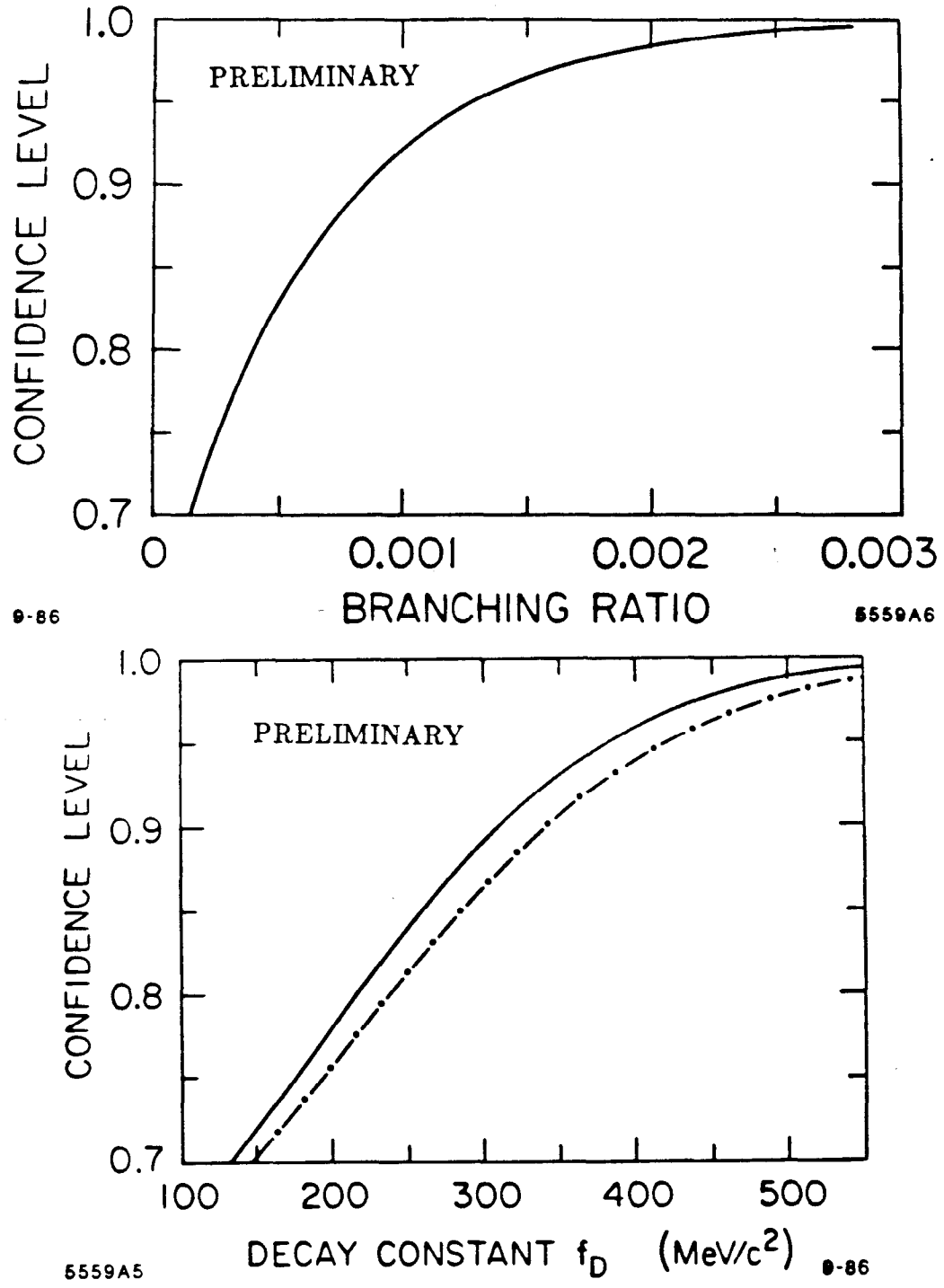

FIG. 35. Shown is the confidence level (C.L.) for the result as a function of (a) $B(D^+ \to \mu^+\nu_\mu)$, and (b) f_D. The limit calculation is described in Ref. [40]. The dashed curve in (b) includes the effects of lowering the values of τ_{D^+} and $|V_{cd}|^2$ by their errors.

cancellations, however it is clear from the data which have reasonable statistics, that this alone cannot - even asymptotically- reproduce the measurements. The most naive interpretation would attribute the lifting of the precise color-matching required by the perturbative calculations to the presence of soft (non-perturbative) gluons in the meson wavefunction. As noted earlier, one attempt to quantitatively introduce the effect is by the *screening factor*(ξ) discussed in Section 4.2.4; taking $\xi \approx 0$ largely removes these cancellations. It should be noted once again that the need to introduce the parameter $\xi \approx 0$ to get the weak hadronic decays correct also reduces B_l for the D^0 :[71]

$$B_l(D^0) = \frac{1}{2 + \frac{3}{2}(c_+^2 + c_-^2) + \frac{3\xi}{2}(c_+^2 - c_-^2)} \cdot \tag{11}$$

Using the nominal values of $c_\pm(q^2)$ and $\xi = 0$ a value of $\sim 11.5\%$ is obtained for B_l, in better agreement with the data than what is obtained using $\xi = \frac{1}{3}$ (for N=3 colors) and the expression in Eq. (8) for B_l. The value for $B_l(D^+)$ requires an additional term discussed in Section 4.4.4.

4.4.2 Non-spectator processes.

The search for direct evidence for W-exchange graphs in D^0 decays can be summarized by the following results:

$$Br(D^0 \to \bar{K}^0\phi) \approx 1.5\%$$

$$\frac{\Gamma(D^0 \to \bar{K}^0 K^0)}{\Gamma(D^0 \to K^-\pi^+)} \leq 0.11 \text{ at } 90\% C.L.$$

$$\frac{\Gamma(\bar{K}^{*0}K^0 + cc)}{\Gamma(K^{*-}\pi^+) + \Gamma(K^-\rho^+)} \leq 0.034 \text{ at } 90\%\ C.L.$$

The first channel, $D^0 \to \bar{K}^0\phi$, is clearly seen (see Fig. 36) by three experiments,[90][77] between experiments due to their assumptions of the backgrounds. The channel is Cabibbo-allowed and occurs at a rate which is surprisingly large, in that it is consistent with that for *ordinary* pseudoscalar-vector decays after a reduction for the limited phase-space and a factor for the removal of an $s\bar{s}$

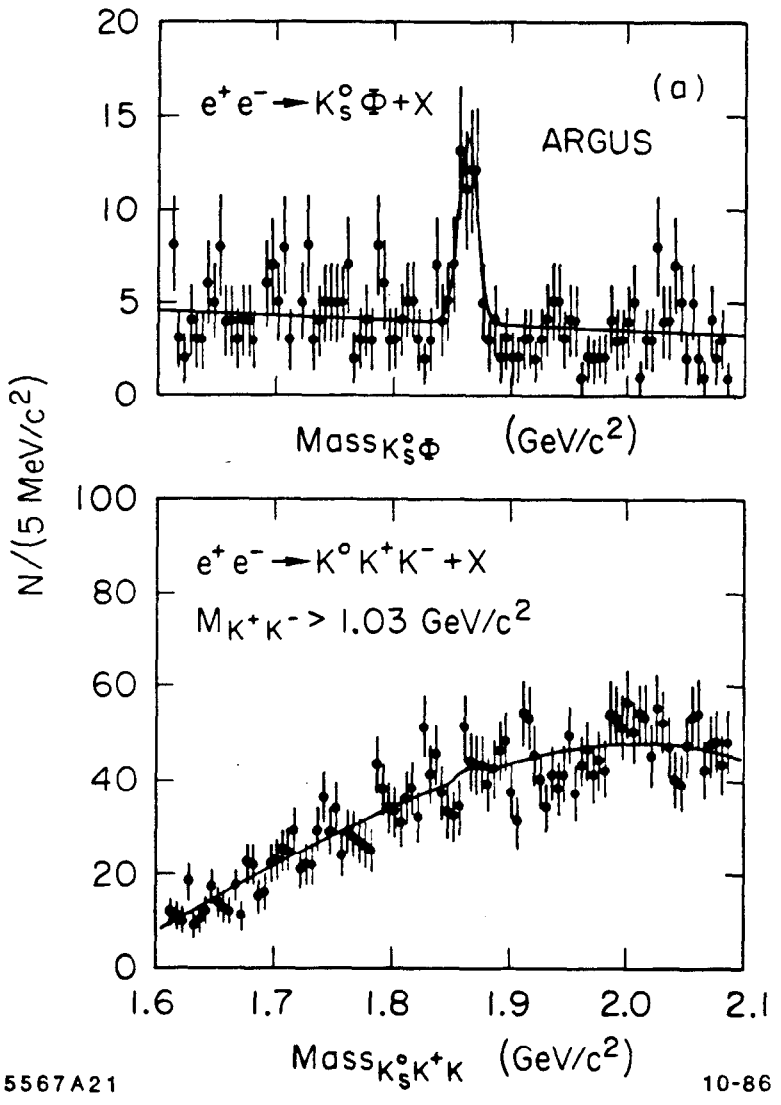

FIG. 36. $D^0 \to \bar{K}^0\phi$ in e^+e^- annihilation.

pair from the vacuum is taken into account.[59] This would suggest that if W-exchange is present, it proceeds at a rate which is largely uninhibited. The same non-perturbative gluon effects suspected for the absence of color cancellations, may also lift the helicity suppression of these channels. Because of the surprisingly large value for the branching ratio, alternate explanations have been proposed, as discussed in Section 4.2.2. This decay may arise for example from *small* rescattering out of the very *large* $K^-\rho^+$ channel, as opposed to the W-exchange mechanism itself. The second decay ($D^0 \to \bar{K}^0 K^0$) is Cabibbo-suppressed and is suppressed in exact SU(3). The limit is already below the value measured for the K^+K^- decay (see Table XXIV), but it is not stringent enough to give additional information. The third channel ($D^0 \to \bar{K}^{*0} K^0$) is Cabibbo-suppressed but not SU(3)-suppressed. While the value of the limit is preliminary,[80] it is *intriguingly* small considering the size of $\mathrm{Br}(D^0 \to \bar{K}^0\phi)$.

The current D_s measurements given in Table XXV do not provide unique information on the presence of W-annihilation graphs; they all may arise from spectator amplitudes as well. Only measurements such as $D_s \to \rho\pi, \omega\pi ....$, will answer the question of W-exchange and W-annihilation, as would inclusive measurements of D_s decays opposite *tagged* D_s .

4.4.3 Interference effects in D^+ decays.

Evidence for interference as discussed in section 4.2.3, in exclusive decays is derived from the following ratios:

$$\frac{\Gamma(D^+ \to \bar{K}^0 K^+)}{\Gamma(D^0 \to \bar{K}^0 \pi^+)} = 0.32 \pm 0.09 \pm 0.05 \qquad (12)$$

$$\frac{\Gamma(D^+ \to \pi^+ \pi^0)}{\Gamma(D^0 \to \bar{K}^0 \pi^+)} \leq 0.15 \text{ at } 90\% \; C.L. \qquad (13)$$

$$\frac{\Gamma(D^+ \to \bar{K}^{*0} K^+)}{\Gamma(D^0 \to \bar{K}^{*0} \pi^+)} = 0.21 \pm 0.17 \pm 0.15 \; . \qquad (14)$$

As can be seen from Figure 30, interference effects are expected for both $\pi^+\pi^0$ and $\bar{K}^0\pi^+$, but not for $\bar{K}^0 K^+$ or $\bar{K}^{*0} K^+$. Thus, since each of the numerators in (12) to (14) are Cabibbo-suppressed, one expects values close to $tan^2(\theta_c) \approx 0.055$

for the ratios. Expression (13) however, is expected[91] to be given by $\frac{1}{2}tan^2(\theta_c)$ although as pointed out earlier, SU(3)-breaking and final-state interactions may alter the value.[63] The deviation from equality in partial widths expected under exact SU(3) for the well measured Cabibbo-suppressed decays $D^0 \rightarrow \pi^+\pi^-$ and $D^0 \rightarrow K^+K^-$ (see Table XXIV) sets the scale for the size of these effects in charm decay.[92] While (13) is clearly consistent with expectations, (12) and (14) are considerably larger, even including the possibility of large SU(3)-violations or final-state interactions. This is then entirely consistent with the pattern expected for interference among D^+ final state amplitudes, which may lead to a longer D^+ lifetime.

If interference is prevalent exclusively, then it leads to a decrease in the width and lengthening of the lifetimes of the D^+ and D_s states. One would introduce into Eq. (11), a term as in Eq.(10), to estimate the effect inclusively for the D^+ . That most charm decays appear to be quasi-two-body, with only a small nonresonant component, strengthens the argument that interference is a major effect in determining the total widths.

4.4.4 The pure leptonic decays and the total widths.

The decay constant f_D is a direct measure of the overlap of the wavefunctions of the heavy and light quarks in the D meson.[57] It thus plays a fundamental role in setting the scale for processes such as weak flavor-annihilation and Pauli interference invoked to account for the differences in D^+ and D^0 lifetimes.[45] A measurement of f_D also provides a stringent test of potential model[57] and QCD sum rule[93] calculations. In addition, it allows reliable estimates of other heavy meson decay constants (f_F, f_B, etc.), which are difficult to obtain due to the large theoretical uncertainties in extrapolating from f_π and f_K to the nonrelativistic heavy quark mesons. The decay constant also is essential in evaluating the magnitude of operators leading to $D^0\bar{D}^0$ and $B^0\bar{B}^0$ mixing.[94] Calculations of the pseudoscalar decay constants obtain values which either increase (QCD sum rule method[93]) or decrease (both relativistic and non-relativistic potential[57] and bag model methods[95]) with the meson mass. While our result does not probe the small values of f_D suggested by the bag model or QCD sum rule calculations (150 $\rightarrow$ 280 MeV/c), it restricts the range of values predicted by recent potential model calculations (208 $\rightarrow$ 450 MeV/c). One important point to make is that the

limit obtained excludes the very high values of f_D which have been suggested[96] as an explanation for the large observed ratio of $\tau(D^+)/\tau(D^0)$. The latter estimate is of a perturbative nature, and is used to break the helicity suppression that would otherwise reduce the contribution of the non-spectator processes to charm decay. The value of f_D cannot be used to eliminate the non-perturbative techniques of reducing helicity suppression, such as the addition of gluons to the meson wavefunction.[55]

4.5 Data on Hadronic Weak Decays of Beauty Mesons

As indicated in Section 4.2.1, the decays of B mesons arise largely from the $b \to c$ transition yielding final states containing D^0 and D^+ and D_s mesons, and their vector partners. The D_s fraction is expected to be small, requiring either a Cabibbo-suppressed decay, or the fluctuation of the vacuum to an $s\bar{s}$ state. There is also the possibility of decays through the heavier D^{**} orbitally excited mesons. The additional features of B decay allow however for the $b \to c\bar{c}s$ transitions providing the possibility of $c\bar{c}$ final states (ψ, ψ', χ_c, etc...). As indicated in Fig. 37, B decays to baryons are also expected to be present at a small level. One final interesting decay would be that of the heaviest B_c meson where the single quark decay of the b and the c would compete favorably owing to the relative sizes of the KM matrix elements.

Table XXVII summarizes the measurements of hadronic B decays. These results all come from data taken at the $\Upsilon(4S)$, and thus correspond exclusively to the decays of B_u and B_d mesons. No data on the heavier states exists, except in the inclusive analyses at PEP and PETRA energies, where such states presumably contaminate the B_u and B_d sample.

Table XXVII also contains the published values[97] for the ratio of $(b \to u)/(b \to c)$. The theoretical uncertainty in evaluating this quantity now sheds doubt on the validity of the measurement. These questions are addressed more thoroughly in the lectures of B.Winstein in these proceedings.

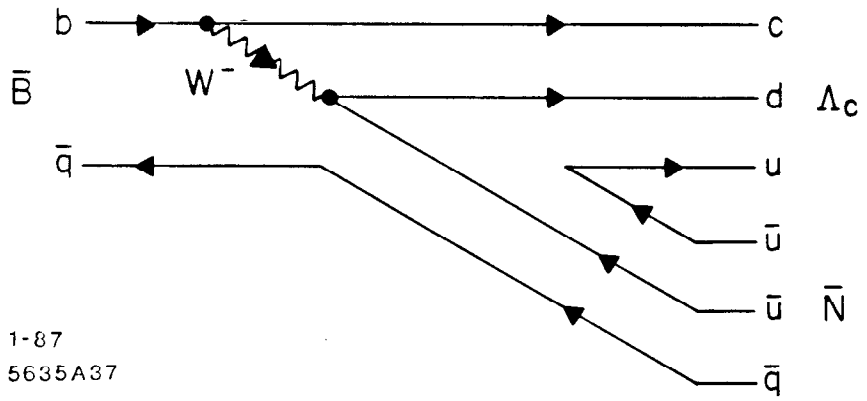

FIG. 37. Diagrams leading to B meson decays containing baryons.

Table XXVII. B Meson Branching Ratios(%) [48] [98] [99] [100] [101]

Decay Modes	CLEO	ARGUS	CUSB
$\bar{B}^0 \to D^+\pi^-$	$0.14 \pm 0.19 \pm 0.05$		
$\bar{B}^0 \to D^0\pi^+\pi^-$	$1.6 \pm 0.9 \pm 0.6$ $(7 \pm 5)^\dagger$		
$\bar{B}^0 \to D^{*+}\pi^-$	$0.35 \pm 0.14 \pm 0.11$ $(1.7 \pm 0.5 \pm 0.5)^\dagger$	$0.25 \pm 0.15 \pm 0.15$ $0.40 \pm 0.20 \pm 0.20$	
$\bar{B}^0 \to D^{*+}\pi^-\pi^0$		$1.1 \pm 0.6 \pm 0.6$	
$\bar{B}^0 \to D^{*+}\pi^-\pi^-\pi^+$		$2.4 \pm 0.7 \pm 1.1$	
$B^- \to D^0\pi^-$	$0.4 \pm 0.1 \pm 0.1$ $(1.1 \pm 0.6)^\dagger$		
$B^- \to D^+\pi^-\pi^-$	$0.9 \pm 0.5 \pm 0.3$		
$B^- \to D^{*+}\pi^-\pi^-$	$0.3 \pm 0.2 \pm 0.1$ $(2.7 \pm 1.7)^\dagger$	$0.4 \pm 0.2 \pm 0.2$	
$B^- \to D^{*+}\pi^-\pi^-\pi^0$		$3.5 \pm 1.1 \pm 2.1$	
$B^- \to D^{*+}\rho^-$	$8.1 \pm 2.9^{+5.9}_{-2.4}$		
$B^0 \to \psi X$	$1.1 \pm .2 \pm .2$	$1.2 \pm .2 \pm .2$	
$B \to \psi' X$		0.50 ± 0.23	
$B \to \psi_{\text{direct}} X$		0.90 ± 0.30	
$B \to \psi K^-$	$0.09 \pm 0.06 \pm 0.02$	< 0.20	
$B \to \psi K^{*0}$	$0.41 \pm 0.19 \pm 0.03$	0.44 ± 0.27	
$B \to \psi X$	$2.3 \pm 0.6 \pm 0.6$		
$B \to pXX$	≥ 3.6 at 90% C.L.		
$B \to \Lambda X$	≥ 2.2 at 90% C.L.		
$B \to uX$	10.8 ± 1.2		11.2 ± 1.3
$B \to eX$	12.0 ± 0.9		13.2 ± 1.6
$B \to D^0 X$	$39 \pm 5 \pm 4$	$50 \pm 7 \pm 8$	
$B \to D^+ X$	$17 \pm 4 \pm 4$	$23 \pm 8 \pm 5$	
$B \to D^* X$	$23 \pm 3^{+7}_{-4}$		
$(B \to D_s X)(D_s \to \phi\pi)$	0.004 ± 0.001	$0.002 \pm 0.001 \pm 0.001$	
$b \to u / b \to c$	≤ 4.0 at 90% C.L.‡		≤ 5.5 at 90% C.L.‡

† Previously published values. ‡ See Ref. 97.

4.6 Interpretation of the B Meson Data

While the B system is expected to behave closer to the naive spectator picture, the detailed measurements of specific, exclusive decay modes do not yet exist to prove this assertion. Under these circumstances, and almost without exception, it has been experimentally necessary to resort to inclusive measurements at the $\Upsilon(4S)$ to establish the pattern of decays. The results and conclusions are discussed in the following sections.

Because these measurements are inclusive, one should keep in mind that they are normalized to the height of the $\Upsilon(4S)$ resonance, which is assumed to decay entirely to $B\bar{B}$ pairs. This assertion has been tested by CLEO,[48] and the limit on non-$B\bar{B}$ decays of the $\Upsilon(4S)$ is found to be $\leq 3.8\%$ at 90% C.L. This is analogous to the case at the $\psi(3770)$. A major uncertainty remains however in the assignment of the relative production $B_u\bar{B}_u$:$B_d\bar{B}_d$, because of the proximity to threshold. For example, a mass difference of 2 MeV produces a ratio $\frac{N^+}{N^0} = 1.2$ while a mass difference of 4 MeV produces a ratio $\frac{N^+}{N^0} = 1.5$. Using the same mass scale for the $\Upsilon(4S)$ of 10579.8 MeV, the mass difference of B_u and B_d are given:[48]

$$M(B_d) - M(B_u) = 3.1 \pm 1.4(CLEO)$$

$$M(B_d) - M(B_u) = 2.4 \pm 1.6(ARGUS) \ .$$

This implies that an uncertainty in the relative fractions of B_u and B_d produced at the $\Upsilon(4S)$ remains.

4.6.1 Color suppression in B decays.

As was seen in charm decays, no evidence for a suppression resulting from color mismatch appears to be evident in the data. In B decay, the analogous effects would be present in comparisons of $\bar{B}_d \to D^0\pi^0$ to $\bar{B}_d \to D^-\pi^+$, (and analogous vector-pseudoscalar channels) although the size of the suppression should be smaller.[102] Neither of these channels are well measured.

A cleaner and better measured system is that of the B decays containing bound $c\bar{c}$. The total B meson branching fraction to a final state with a charmed and anti-charmed quark is expected to be 10% to 15% based on the spectator model. In some fraction of these, the final state will contain a $c\bar{c}$ meson. These are seen in

Fig. 38 to have the same *color matching* topology as in the D meson case. The theoretical estimates[103] of the size of this component range from ~ 0.4 to $\sim 3.0\%$ for the inclusive ratio $\Gamma(b \to \psi)/\Gamma(b \to all)$. The higher values have ignored color matching, the middle values of $\sim 2\%$ assume some color-suppression, and the smallest values $\sim 0.5\%$ include the full QCD correction. Theoretical uncertainties arise from phase space effects and hadronization of the $c\bar{c}$ system into detectable ψ mesons. The next section discusses this question. As can be seen in Table XXVII, the experimental values are about $1.1 \pm 0.3\%$, consistent with the lack of a full suppression just as was seen in charm decays.

4.6.2 Charm in beauty decay.

Since the branching ratios of the charmonium states are well known, the absolute branching ratios for $B \to \psi$ are determinable and are seen from Table XXVII to be within range of expectations.

The rate for D_s production in B decay can only be estimated, since the absolute branching ratio for D_s into $\phi\pi^+$ (the only channel observed) is not known. From Table XXVII, one sees that the ARGUS and CLEO results are in poor agreement. Taking the CLEO value and assuming the branching ratio of say 3% for $D_s \to \phi\pi^+$, one obtains a rate for $B \to D_s + X \approx 13\%$ which is consistent with expectations[104] of about 9% for D_s production from both $b \to c(\bar{u}d)$ and $b \to c(\bar{c}s)$ combined.

The previous section discussed the issue of color-suppression signatures in B meson decay. One sidelight is the hadronization process in beauty decays. In charm decays, it was seen that a large fraction of the decays appear to be quasi-two body. It is of course interesting to see if this is the case in B decay, as it results in a calculational simplification. To this end, in the absence of good exclusive reconstruction efficiency, it is necessary to look inclusively at the *first* daughters of B meson decay, namely D_s and ψ mesons.

The Z distributions from CLEO and ARGUS for the D_s and ψ mesons in B decay are shown in Fig. 39 . If the CLEO data are correct, 65% of the D_s arise from quasi two-body production, presumably, in conjunction with a similarly hard D^0 or D^+ . The production through W-exchange or internal (D_s -K) decay appear to be largely absent.

The data from ARGUS indicate that ψ production is qualitatively softer, with a significant fraction of ψ coming from ψ'. A large fraction of the spectrum does

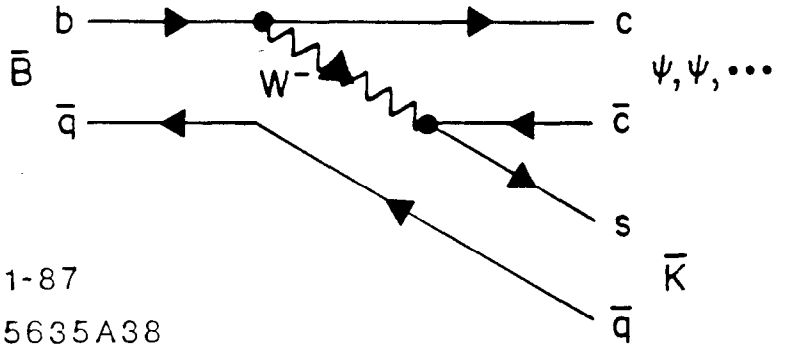

FIG. 38. Diagrams leading to bound charm in B meson decay.

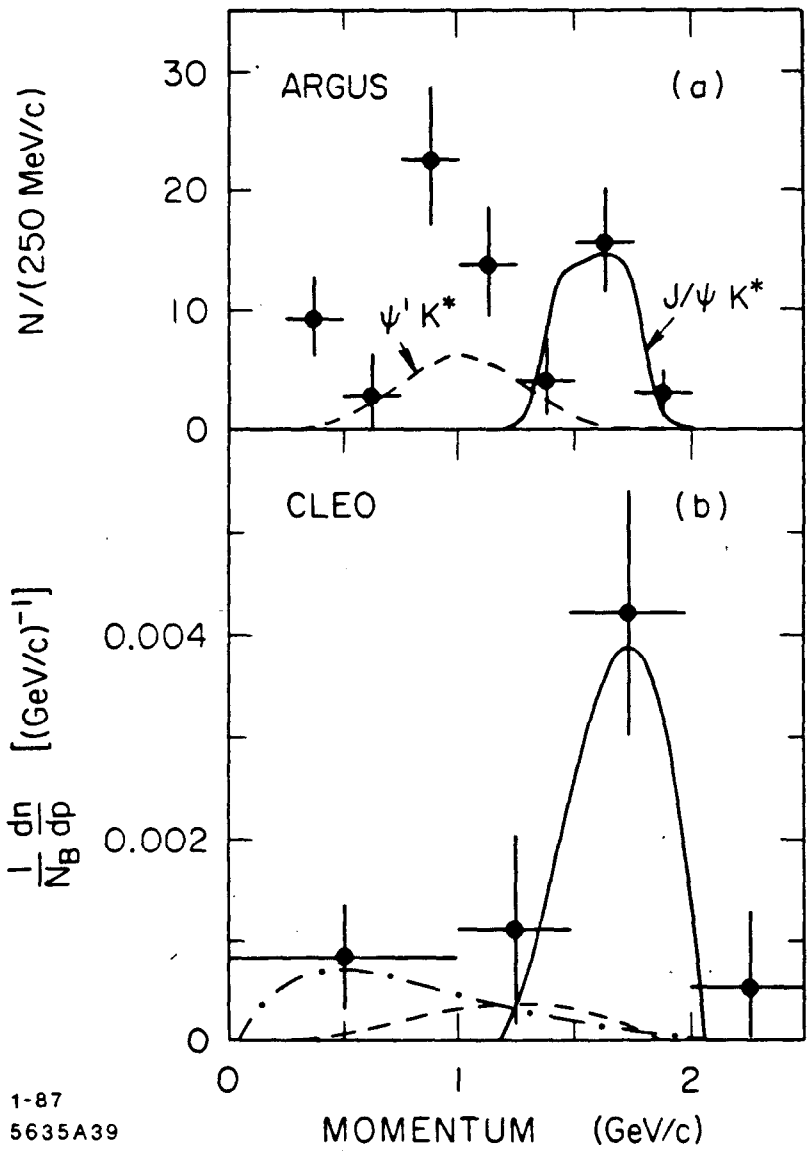

FIG. 39. (a)Z distribution for D_s in B decays. (b)Z distribution for ψ in B decays.

appear to be quasi two-body, with channels such as ψK, ψK^* and $\psi' K^*$ being large.

4.6.3 Baryons in B decay.

While D^0 and D^+ mesons are too light to decay through baryonic channels, the B mesons may have a sizeable rate. Estimates have been made based on the assumption that the quarks in the B decay can pair into diquarks, and pick up a $q\bar{q}$ pair from vacuum fluctuations to make pairs of baryons. These were pictured in Figure 37. The rates estimated in Ref. 105 are given:

$$\frac{Br(\bar{B} \to \Lambda_c \bar{N})}{\bar{B} \to (c\bar{q})(d\bar{u})} = 2 \to 15\%$$

$$\frac{Br(\bar{B} \to N\bar{N})}{\bar{B} \to (u\bar{q})(d\bar{u})} = 1 \to 2\%$$

$$\frac{Br(\bar{B} \to A_c \bar{\Lambda}_c)}{\bar{B} \to (c\bar{q})(s\bar{c})} = 5 \to 24\%$$

$$\frac{Br(\bar{B} \to \Lambda \bar{\Lambda}_c)}{\bar{B} \to (u\bar{q})(s\bar{c})} = 1 \to 7\% \, .$$

The rate for baryon-antibaryon production from B mesons is 4 to 26% overall.[105] The data, from CLEO[99] is consistent with this range, being posed in lower limits for p and Λ inclusive production in Table XXVII.

4.6 Conclusions On the Decays of Open Charm and Beauty

The extensive exclusive measurements of D^0 and D^+ mesons provide a reasonably firm basis for understanding the charm meson width. The decays of D^0 and D^+ appear to have a large quasi two-body component. There is evidence for color-suppressed decays, decays in which interference is occurring, and decays where flavor-annihilation appears to be present. Studies of the semileptonic decays point to hadronic matrix elements that are relatively simple, being dominated by form factors that are well modelled by simple poles. Detailed information on the D_s meson is still lacking. The latter would provide the most direct means of

checking the current ideas on interference, flavor-annihilation and the apparent dominance of quasi two-body decays of charm. An alternative is to measure the factors (such as the KM angles and the weak decay constants) that make up the theoretical estimate of the rate for each of these processes. While $D_s \to \tau\nu$ should provide an experimentally accessible measurement of the weak decay constant f_{D_s}, stringent limits on f_D from $D \to \mu\nu$ *already* provide information on the size of perturbative effects that may allow flavor-annihilation to proceed at a measurable rate. Current models favor a small amount of weak flavor-annihilation using decays (such as $D^0 \to \bar{K}^0\phi$) as evidence. Such decays are however under suspicion as possible arising from flavor mixing or rescattering at the strong interaction level.

The decays of light B mesons (B_u and B_d) appears to be dominated as expected by the $b \to c$ transition. The determination of the $b \to u$ fraction has been clouded both by theoretical uncertainties and by experimental difficulty. The lack of a global picture for B hadronic decay has also been hampered by the lack of data on exclusive channels. Inclusive studies of $B \to D_s, \psi$, and D project a spectator-like picture. The smallness of the semileptonic branching ratio however leads one to believe that *the nonleptonic sector of B decay may yet hold some surprises.* The key to understanding B decay will be in the ability to separate the species B_u and B_d and to systematically study the exclusive decays. The heavy B mesons B_s and B_c will also be interesting, the latter providing the possibility of a significant fraction of single quark decays, which otherwise won't be seen until the t-quark is discovered.

References

1. Beauty and bottom will be used interchangeably throughout the text.
2. E.Eichten *et al.*, Phys.Rev.Lett. 34, 369 (1975),
   Also see reference 6 for more details.
3. F.Gilman, Proceedings of the XIVth SLAC Summer Institute on Particle Physics, Stanford, CA. July 28-August 8 (1986).
4. The only available data is from J.Feller LBL-9017-MC May (1979). It gives 1.09 ± 0.20 for the fraction of ψ'' decaying into $D\bar{D}$ pairs.
5. J.Siegrist, SLAC-REPORT-225 October (1979).
6. E.Eichten *et al.*, Phys.Rev D17, 3090 (1978),
   E.Eichten *et al.*, Phys.Rev D21, 203 (1980).
7. W.Buchmuller and S.H.H.Tye Phys.Rev D24, 132 (1981).
8. G.Eigen, Ph.D. Thesis, MPI-PAE/Exp. E1.145 (1984).
9. D. M. J. Lovelock *et al.*, Phys.Rev.Lett. 54, 377(1985),
   D.Besson *et al.*, Phys.Rev.Lett. 54, 381(1985).
10. M.Aguilar-Benitez, *et al.*, Phys. Lett. 170B, 1 (1986).
11. ARGUS Collaboration, Proceedings of the XXIII International Conference on High Energy Physics, Berkeley, California, July 16-23 (1986).
12. J.Lee-Franzini, Proceedings of the XXIII International Conference on High Energy Physics, Berkeley, California, July 16-23 (1986).
13. J.E.Gaiser *et al.*, Phys.Rev. D34,711 (1986).
14. C.Baglin *et al.*, Phys.Lett. B172,455 (1986).
15. C.Edwards *et al.*, Phys.Rev.Lett. 48, 70 (1982).
16. T.Himel *et al.*, Phys.Rev.Lett. 45, 1146 (1980).
17. R.M.Baltrusaitus *et al.*, Phys.Rev. D33, 1842, (1985).
18. P.M.Tuts, Proceedings of the XIVth SLAC Summer Institute, Stanford, CA. July 28-August 8 (1986).
19. R.McClary and N.Byers , Phys.Rev. D28, 1692 (1983).
20. The COG is calculated using the mass averages from Ref. 10 for the χ_c states.
21. E.Eichten and F.Feinberg, Phys.Rev. D23, 2724(1981).

22. P.Moxhay and J.Rosner, Phys.Rev. D28, 1132 (1983).

23. S.Gupta *et al.*, Phys.Rev. D26, 3305 (1982).

24. A.Khare, Phys.Lett. 98B, 385 (1981).

25. A.Martin, Phys.Lett. 103B, 55 (1981).

26. J.Baake *et al.*, Dortmund-Report DO-TH81/10 (1981).

27. D.Beavis *et al.*, Phys.Rev. D20, 2345 (1981).

28. J.L.Richardson, Phys.Lett. 82B, 272 (1979).

29. J.S.Kang, International Symposium on Lepton and Photon Physics, Cornell (1983), Submitted paper C-199.

30. S.Cooper, Proceedings of the International Europhysics Conference on High Energy Physics, Bari, July 18-24 (1985).

31. Y.P.Kuang and T.M.Yan, Phys.Rev. D24, 2874 (1981).

32. The mass scale of CLEO has been used here.

33. CLEO Collaboration, paper presented at the XXIII International Conference on High Energy Physics, Berkeley, CA., July 16-23 (1986).

34. M.Gaillard, B.Lee, and J.Rosner, Rev. Mod. Phys. 47, 277 (1975).

35. K.Han *et al.*, Phys. Rev. Lett. 55, 36 (1986).

36. V.Lüth, Proceedings of the International Symposium on Production and Decay of Heavy Flavors, Heidelberg, May 20-23 (1986).

37. S.Abachi *et al.*, Preprint ANL-HEP-CP-86-50 June (1986).

38. G.Goldhaber *et al.*, Phys. Lett. 69B, 503 (1977),
G.Feldman *et al.*, Phys. Rev. Lett. 38, 1313 (1977).

39. H.Aihara *et al.*, Phys. Rev. Lett. 53, 2465 (1984),
H.Albrecht *et al.*, Phys. Lett. 146B, 111 (1984),
A.E.Asratyan *et al.*, Phys. Lett. 156B, 441 (1985).

40. R.H.Schindler, Proceedings of the XXIII International Conference on High Energy Physics, Berkeley, California, July 16-23 (1986). SLAC-PUB-4055.

41. See for example: A. De Rujula *et al.*, Phys. Rev. D12, 143 (1975).
A. De Rujula *et al.*, Phys. Rev. Lett. 37, 398 (1976).
E.Eichten *et al.*, Phys. Rev. D21, 203 (1980).
S.Godfrey and N.Isgur, Phys. Rev. D32, 189 (1985).

42. H.Albrecht *et al.*, Phys. Rev. Lett. 56, 549 (1986),
Evidence also appears in G.Goldhaber *et al.*, Phys. Lett. 69B, 503 (1977).

43. M.Frank and P.O'Donnell, Phys. Lett. 159B, 174 (1985),
K.Igi, and S.Ono, Phys. Rev. D32, 232 (1985).

44. The B^* mass is from K.Han *et al.*, Ref. 35, and assuming an average B mass of 5277 ± 4 MeV/c^2.

45. R.M.Baltrusaitis *et al.*, Phys. Rev. Lett. 54, 1976 (1985).

46. R.H.Schindler *et al.*, Phys.Rev. D24, 78 (1981).

47. W.Bacino *et al.*, Phys.Rev.Lett. 45, 329 (1980).

48. M.Gilchriese, Proceedings of the XXIII International Conference on High Energy Physics, Berkeley, California, July 16-23 (1986).

49. For an excellent review of the current techniques, see Ref.36, and references therein.

50. See R.Rückl, for a discussion of relative effects leading to differences in total meson widths.

51. D.M.Ritson, Proceedings of the XXIII International Conference on High Energy Physics, Berkeley, California, July 16-23, 1986. SLAC-PUB-4102.

52. For an excellent review, see S.Stone, 6th International Conf. on Physics in Collision, Chicago, Illinois, Sept 3-5 (1986).

53. The only result which deviates markedly is from DELCO, where $14.9 \pm 2.2 \pm 1.9\%$ is observed from T.Pal *et al.*, CALT-68-1283 (1986).

54. S.P.Rosen, Phys. Rev. Lett. 44, 4 (1980).

55. H.Fritzsch and P.Minkowski, Phys. Lett. 90B, 455 (1980).

56. M.Bander, D.Silverman and A.Soni, Phys. Rev. Lett. 44, 7 (1980).

57. See for example: V.A.Novikov *et al.*, Phys. Rev. Lett. 38, 626 (1977).
H.Krasemann, Phys. Lett. 96B, 397 (1980),

L.Maiani, Proceedings of the XXI International Conference on High Energy Physics, (Editions de Physique, Le Ulis, France, 1982), pp. 631-657,
V.S.Mathur, and M.T.Yamawaki, Phys. Rev. D29, 2057 (1984),
S.N.Sinha, U. of Alberta Preprint Thy-3-86 (1986),
P.J.O'Donnell. CERN-TH-4419/86 (1986)
Also see, S.Godfrey, Phys.Rev. D33, 1391 (1986), for an excellent comparison of potential model calculations, as well as new calculations using a relativised model.

58. M.Lusignoli, and A.Pugliese, INFN Roma Preprint-515 July (1986).
F.Hussain and A.N.Kamal, U. of Alberta Preprint Thy-17-86 (1986).

59. I.I.Y. Bigi and M.Fukugita, Phys. Lett. 91B, 121 (1980).

60. J.F.Donoghue, U. of Mass., Amherst, Preprint UMHEP-241(1986),
F.Hussain, and A.N.Kamal, U. of Alberta Preprint Thy-1-86,(1986).

61. B.Stech, "Perspectives in Electroweak Interactions and Unified Theories," XXI Moriond Conference, ed. J.Tran Thanh Van, (1986).

62. A.N.Kamal, Phys. Rev. D33, 1344 (1986).

63. I.I.Y.Bigi, Proceedings of the XIVth SLAC Summer Institute on Particle Physics, Stanford CA., July 28-August 5 (1986). SLAC-PUB-4067.

64. Interference in the charm system was first proposed by B.Guberina, R.Peccei, and R.Rückl Phys. Lett. 89B, 111 (1979).

65. Y.Koide , Phys.Rev. D20, 1739 (1979),
I.I.Y.Bigi, Z.Phys. C6, 83 (1980).

66. T.Kobayashi, and Y.Yamazaki, Prog. Theor. Phys. 65, 775 (1981).

67. G.Altarelli, and L.Maiani, Phys. Lett. 118B, 414 (1982),
N.Bilic, B.Guberina, and J.Trampetic, Nucl. Phys. B248, 261 (1984).

68. G.Altarelli *et al.*, Phys.Lett. 99B, 141 (1981).

69. J.Ellis, M.K.Gaillard, and D.V.Nanopoulos, Nucl.Phys. B100, 313 (1976),
N.Cabibbo and L.Maiani, Phys. Lett. 73B, 418 (1978),
D.Fakirov and B.Stech, Nucl. Phys. B133, 315 (1978).

70. M.Bauer and B.Stech, Phys.Lett. 152B, 380 (1985),
B.Stech, "Flavor Mixing and CP Violation," 5th Moriond Workshop, ed. J. Tran Thanh Van, p151 (1985).

71. A.J.Buras, J.M.Gérard, R.Rückl, Nuclear Phys. B268, 16 (1986).
M.A.Shifman, M.B.Voloshin, Preprint ITEP-62 (1984).

72. M.Bauer, B.Stech, and M. Wirbel, Heidelberg Preprint HD-THEP-86-19 (1986).

73. I.Peruzzi *et al.*, Phys. Rev. Lett. 39, 1301 (1977),
D.Scharre *et al.*, Phys. Rev. Lett. 40, 74 (1978).

74. R.H.Schindler *et al.*, Phys. Rev. D24, 78 (1981).

75. A.J.Hauser, PhD Thesis, California Institute of Technology, unpublished, (1984).

76. R.M.Baltrusaitis *et al.*, Phys. Rev. Lett. 56, 2140 (1986).

77. R.M. Baltrusaitis *et al.*, Phys. Rev. Lett., 56, 2136 (1986).

78. See for example R.H.Schindler, Proceedings of the 13th SLAC Summer Institute of Particle Physics, Stanford, CA., July (1985). These results are still preliminary in nature.

79. R.M.Baltrusaitus *et al.*, Phys.Rev.Lett. 55, 150 (1985).

80. R.M.Baltrusaitis *et al.*, SLAC-PUB-3858, December (1985).

81. P.Karchin, Proceedings of the XXIII International Conference on High Energy Physics, Berkeley, California, July 16-23 (1986).

82. C.Chen *et al.*, Phys. Rev. Lett. 51, 634 (1983),
H.Aihara *et al.*, Phys. Rev. Lett. 53, 2465 (1984),
H.Althoff *et al.*, Phys. Lett. 136B, 130 (1984),
R.Bailey *et al.*, Phys. Lett. 139B, 320 (1984),
H.Albrecht *et al.*, Phys. Lett. 153B, 343 (1985),
M.Derrick *et al.*, Phys. Rev. Lett. 54, 2568 (1985).

83. W.Toki, Talk presented at the XIVth SLAC Summer Institute on Particle Physics, Stanford, CA. July 28-August 8 (1986). These results are preliminary.

84. B.Grinstein, M.B.Wise, and N.Isgur, CALT-68-1311 (1985),
M.Wirbel, B.Stech, and M.Bauer, Z.Phys. C29, 637 (1985),
A.Ali, T.C.Yang, Phys.Lett. 65B, 275 (1976),
M.Suzuki, Phys.Lett. 155B, 112 (1985),

S.C. Chao, G.Kramer,W.F.Palmer,and S.S.Pinsky, Phys.Rev. D30,1916 (1984).

85. For details, see D.Coffman, PhD Thesis, unpublished, CALT-68-1415 (Dec. 1986).

86. R.H.Schindler, Proceedings of the XXIII International Conference on High Energy Physics, Berkeley, CA., July 16-23 (1986). SLAC-PUB-4055.

87. The lifetime used is shorter than that now determined in Ref. 36.

88. M. Aguilar-Benitez *et al.*, Rev. Mod. Phys. 56, S43 (1984).

89. H.Lipkin, Phys. Rev. Lett. 44, 710 (1980).

90. H.Albrecht *et al.*, Phys. Lett. 158B, 525 (1985),
C.Bebek *et al.*, Phys. Rev. Lett. 56, 1983 (1986).

91. L.L-Chao, Physics Reports 95, 1 (1983).

92. See A.N.Kamal and R.C.Verma, U. of Alberta Preprint Thy-13-86 (1986), for a recent discussion of SU(3)-symmetry and final-state interactions in charm decays.

93. V.S.Mathur and M.T.Yamawaki, Phys.Rev. D29, 2057 (1984),
V.A.Novikov *et al.*, Phys. Rev. Lett. 38, 626 (1977).

94. I.I.Bigi, G.Köpp, and P.M.Zerwas, Phys. Lett. 166B, 238 (1986),
J.F.Donoghue *et al.*, , Phys. Rev. D33, 197 (1986).

95. E. Golowich, Phys. Lett. 91B, 271 (1980),
M. Claudson, HUTP-81/A016 (1982).

96. M. Bander, D. Silverman, A. Soni, Phys. Rev. Lett. 44, 7 (1980).

97. A.Chen *et al.*, Phys.Rev.Lett. 52, 1084 (1984).
C.Klopfenstein *et al.*, Phys.Lett. 130B, 444 (1983).

98. S.Behrends *et al.*, Phys.Rev. Lett. 50, 881,(1983).

99. M.S.Alam *et al.*, Phys.Rev. Lett. 51, 1143, (1983).

100. R.T.Giles *et al.*, Phys.Rev. D30, 2279, (1984).

101. A.Chen *et al.*, Phys.Rev. D31, 2386, (1985).

102. H.Fritzsch Phys. Lett. 86B, 164 (1979).

103. J.Kühn *et al.*, Z. Phys. C5, 117, (1980),
M.Wise, Phys. Lett.89B, 229 (1980),
J.Kühn and R.Rückl, Phys. Lett. 135B, 477 (1984),
P.H.Cox *et al.*, Phys.Rev. D32, 1157 (1985).

104. M.Suzuki, Phys.Rev. D31, 1158 (1985).

105. I.I.Y.Bigi, Phys. Lett. 106B, 510 (1981).